

WIND-TUNNEL RESEARCH  
FOR IAP SAND STUDY PROJECT

by

J. E. Cermak  
H. W. Shen  
J. A. Peterka  
L. F. Janin

Final Report

September 1982

Project  
No. 5-3-5684

Fluid Mechanics and Wind Engineering Program  
Colorado State University  
Fort Collins, Colorado

CER82-83JEC-HWS-JAP-LFJ24

## TABLE OF CONTENTS

| <u>Section</u> | <u>Page</u>  |
|----------------|--|
| I              | INTRODUCTION . . . . . 1   |
|                | A. Authorization . . . . . 1   |
|                | B. Scope and Specific Tasks of the Study . . . . . 1                                       |
|                | C. Organization of this Report . . . . . 2   |
| II             | FLOW AND SAND MOVEMENTS WITHOUT OBSTRUCTIONS . . . . . 3                                   |
|                | A. Brief Description of Previous Studies . . . . . 3                                       |
|                | B. Experimental Facilities and Results . . . . . 6   |
| III            | SAND TRAP SAMPLERS . . . . . 17  |
|                | A. Horizontal Trap Samplers . . . . . 17   |
|                | B. Vertical Trap Samplers . . . . . 23   |
|                | C. Conclusions . . . . . 31  |
| IV             | ROADWAY MODELS . . . . . 31  |
|                | A. Roadway Models Tested and Sequence of Testing . . 31                                    |
|                | B. Testing Results . . . . . 34  |
|                | C. Summary and Conclusions . . . . . 47  |
| V              | SINGLE ROW OF SAND FENCES . . . . . 48   |
|                | A. Introduction . . . . . 48   |
|                | B. Review of Literature and Analysis . . . . . 48  |
|                | C. Accumulation of Sand Particles around the Fence . 59                                    |
|                | D. Testing Program . . . . . 62  |
|                | E. Experimental Results . . . . . 76   |
|                | F. Sand Accumulation around Each Type of Fence . . . 76                                    |
|                | G. Conclusions . . . . . 110   |
| VI             | MULTIPLE ROWS OF FENCES . . . . . 111  |
|                | A. Brief Description of Previous Studies . . . . . 111                                     |
|                | B. Testing Program . . . . . 114   |
|                | C. Experimental Results . . . . . 115  |
|                | D. Analysis and Conclusions . . . . . 116  |
| VII            | APPLICATION OF WIND-TUNNEL TEST RESULTS TO THE<br>PROTECTION OF THE AIRFIELD . . . . . 118 |
| VIII           | FUTURE RESEARCH NEEDS . . . . . 120  |
|                | A. Roadway . . . . . 120   |
|                | B. Fences . . . . . 122  |
|                | C. Vegetated Strips . . . . . 123  |
|                | D. Aeolian Sand Deposition and Deflation near<br>Building Groups . . . . . 123             |
|                | REFERENCES . . . . . 124   |
|                | APPENDIX A--WIND-TUNNEL FACILITY AND TEST<br>CONFIGURATIONS . . . . . 126                  |
|                | APPENDIX B--INSTRUMENTATION . . . . . 132  |

## LIST OF FIGURES

| <u>Figure</u> |   | <u>Page</u> |
|---------------|---|-------------|
| 1             | Vertical Flow Velocity Distribution . . . . .   | 4           |
| 2             | Relationship between $U_{100}$ Velocity at 100 cm<br>above Bed and Shear Velocity . . . . .                 | 7           |
| 3             | Comparison of Several Formulas ( $d_{max} = 0.20$ mm)<br>of Sand Transport as a Function of $u_*$ . . . . . | 8           |
| 4             | Vertical Distribution of Sand Drift . . . . .   | 9           |
| 5             | Vertical Flow Velocity Distribution from CSU . . . . .  | 11          |
| 6             | Flow Characteristics at 1 m Upstream of the<br>Fence Location but without the Fence . . . . .               | 12          |
| 7             | Sand Size Distribution . . . . .  | 15          |
| 8             | Vertical Sand Transport Rate Distribution<br>Measured by Aspirator . . . . .                                | 16          |
| 9             | Photograph of Horizontal Traps with inside<br>Diameters of 12 mm, 16.5 mm and 34 mm . . . . .               | 18          |
| 10a           | Sand Collection in Horizontal Traps at Ground Level . .   | 19          |
| 10b           | Trap Efficiency for 34 mm inside Diameter Sand Trap<br>Set at Ground Level . . . . .                        | 21          |
| 10c           | Vertical Distribution of Sand Trapped by Horizontal<br>Sand Traps . . . . .                                 | 25          |
| 10d           | Comparison of Horizontal Sand Trap Samplers with<br>Aspirator . . . . .                                     | 26          |
| 11a           | Photograph of Vertical Sand Traps Developed by<br>Horikawa and Shen . . . . .                               | 27          |
| 11b           | Schematic Diagram of Vertical Sand Traps Developed<br>by Horikawa and Shen . . . . .                        | 28          |
| 12            | Amount of Sand Trapped by Vertical Sand Traps . . . . .   | 29          |
| 13            | Roadway Cross Sections and Alternater Embankments<br>for Wind-Tunnel Testing . . . . .                      | 32          |
| 14a-g         | Sand Accumulation for Various Fence Configurations .  | 37-43       |
| 15a           | Side View of Sand Deposition at the Upstream Slope<br>of Roadway Model Configuration No. 5 . . . . .        | 45          |

| <u>Figure</u> |  | <u>Page</u> |
|---------------|--|-------------|
| 15b           | Upstream View of Sand Deposition near the Roadway,<br>Configuration No. 5 . . . . .                                      | 46          |
| 15c           | Side View Showing Migration of Sand Particles over<br>Roadway Model Configuration No. 3 . . . . .                        | 46          |
| 16            | The Flow Zones of a Boundary Layer Disturbed by Fence .  | 48          |
| 17a           | Mean Flow Velocity Profile after Chang (1966) . . . . .  | 50          |
| 17b           | Turbulence Characteristics after Chang (1966) . . . . .  | 50          |
| 17c           | Pressure Distribution behind Solid Fence<br>after Chang (1966) . . . . .   | 51          |
| 18            | Experimental Verification of Equation (6)<br>after Chang (1966) . . . . .  | 52          |
| 19            | Determination of $\sigma$ after Plate (1971) . . . . .   | 52          |
| 20            | Flow Fields around Porous Fence with Height of h<br>after Plate (1971) . . . . .   | 53          |
| 21a           | Velocity Distribution across a Fence of Porosity<br>$\beta = 0.182$ after I. P. Castro (1971) . . . . .                  | 54          |
| 21b           | Velocity Distribution across a Fence of Porosity<br>$\beta = 0.425$ after I. P. Castro (1971) . . . . .                  | 54          |
| 22a           | Turbulence Downstream from a Fence of Porosity<br>$\beta = 0.182$ after I. P. Castro (1971) . . . . .                    | 55          |
| 22b           | Turbulence Downstream from a Fence of Porosity<br>$\beta = 0.425$ after I. P. Castro (1971) . . . . .                    | 55          |
| 23a           | Isotachs Downstream from Fences of Different<br>Permeabilities after J. K. Raine and D. C.<br>Stevenson (1977) . . . . . | 57          |
| 23b           | Isoturbs Downstream from Fences of Different<br>Permeabilities after J. K. Raine and D. C.<br>Stevenson (1977) . . . . . | 58          |
| 24            | Different Sand Accumulations after Al Ain International<br>Airport Preliminary Design Report (1980) . . . . .            | 61          |
| 25a           | Different Fence Configurations - horizontal slat,<br>1/16 inch slats, 1/16 inch gaps, 50% porosity . . . . .             | 64          |
| 25b           | Different Fence Configurations - horizontal slat,<br>1/8 inch slats, 1/4 inch gaps, 66% porosity . . . . .               | 65          |

| <u>Figure</u> |  | <u>Page</u> |
|---------------|--|-------------|
| 25c           | Different Fence Configgrations - horizontal slat,<br>1/8 inch slat, 1/16 inch gaps, 33% porosity . . . . .                           | 66          |
| 26a           | Different Fence Configurations - horizontal slat,<br>with 20% bottom gap, 1/8 inch slats, 1/8 inch<br>gaps, 50% porosity . . . . .   | 67          |
| 26b           | Different Fence Configurations - horizontal slat,<br>with 20% bottom gap, 1/16 inch slats, 1/16 inch<br>gaps, 50% porosity . . . . . | 68          |
| 27a           | Different Fence Configurations - vertical slat,<br>1/8 inch slats, 1/8 inch gaps, 50% porosity . . . . .                             | 69          |
| 27b           | Different Fence Configurations - vertical slat,<br>1/16 inch slats, 1/16 inch gaps, 50% porosity . . . . .                           | 70          |
| 27c           | Different Fence Configurations - 1/8 inch vertical<br>slat fence with 60% porosity . . . . .   | 71          |
| 28            | Different Fence Configurations - solid panel fence<br>with 0% porosity . . . . .   | 72          |
| 29            | Different Fence Configurations - vertical spires I,<br>80% porosity . . . . .  | 73          |
| 30            | Different Fence Configurations - vertical spires II,<br>50% porosity . . . . .   | 74          |
| 31a           | Schematic Diagram, Top View, for a 30-degree<br>Inclined Fence . . . . .   | 75          |
| 31b           | Schematic Diagram, Top View, for a 60-degree<br>Inclined Fence . . . . .   | 75          |
| 32a           | Flow Characteristics Downstream from Horizontal<br>Slat Fence with 50% Uniform Porosity (Run 1) . . . . .                            | 77          |
| 32b           | Flow Characteristics Downstream from Horizontal<br>Slat Fence of 50% Uniform Porosity and 20% Bottom<br>Gap (Run 2) . . . . .        | 78          |
| 33            | Sand Accumulation Profiles for 1/16 inch Horizontal<br>Slat Fence with 50% Uniform Porosity (Run 1) . . . . .                        | 79          |
| 34            | Sand Accumulation Profiles for 1/8 inch Horizontal<br>Slat Fence with 50% Porosity and 20% Opening at<br>Bottom (Run 2) . . . . .    | 80          |
| 35            | Sand Accumulation Profiles for 1/16 inch Horizontal<br>Slat Fence with 50% Porosity and 20% Opening at<br>Bottom (Run 3) . . . . .   | 81          |

| <u>Figure</u> |   | <u>Page</u> |
|---------------|---|-------------|
| 36            | Sand Accumulation Profiles for 1/8 inch Horizontal Salt Fence with 50% Porosity, 20% Opening at Bottom and a Subsurface Barrier Installed (Run 4) . . . . . | 82          |
| 37            | Sand Accumulation Profiles for 1/8 inch Vertical Slat Fence with 50% Uniform Porosity (Run 5) . . . . .   | 83          |
| 38            | Sand Accumulation Profiles for 1/8 inch Vertical Slat Fence with 50% Uniform Porosity and a Subsurface Barrier Installed (Run 5A) . . . . .                 | 84          |
| 39            | Sand Accumulation Profiles for a Solid Panel Fence (0% porosity) with a Subsurface Barrier Installed (Run 6) . . . . .                                      | 85          |
| 40            | Sand Accumulation Profiles for a 1/16 inch Vertical Slat Fence with 50% Uniform Porosity (Run 7) . . . . .  | 86          |
| 41            | Sand Accumulation Profiles for a 1/8 inch Horizontal Slat Fence with 66% Uniform Porosity (Run 8) . . . . .   | 87          |
| 42            | Sand Accumulation Profiles for Special Spire Fence with 80% Porosity and a Subsurface Barrier Installed (Run 9)   | 88          |
| 43            | Sand Accumulation Profiles for 1/8 inch Horizontal Slat Fence with 33% Uniform Porosity (Run 10) . . . . .  | 89          |
| 44            | Sand Accumulation Profiles for 1/8 inch Horizontal Slat Fence with 33% Uniform Porosity and a Subsurface Barrier Installed (Run 11) . . . . .               | 90          |
| 45            | Sand Accumulation Profiles for 1/8 inch Vertical Slat Fence with 60% Uniform Porosity and a Subsurface Barrier Installed (Run 12) . . . . .                 | 91          |
| 46            | A Sand Fence was Installed at the Top of a Dune which was 10.16 cm Downstream from the First Fence . .  | 92          |
| 47            | Vertical Spires II with 60% Uniform Porosity with Subsurface Barrier (Run 14) . . . . .   | 93          |
| 48            | Sand Accumulation Profile with 60% Uniform Porosity and a Subsurface Barrier Installed (Run 15)(30° fence) . .  | 94          |
| 49            | Sand Accumulation Profile with 60% Uniform Porosity and a Subsurface Barrier Installed (Run 16)(60° fence) . .  | 95          |
| 50            | Sand Accumulation Reaching Top of Fence . . . . .   | 96          |
| 51            | Scour Hole Downstream from Fence in Run 2 . . . . .   | 97          |

| <u>Figure</u> |   | <u>Page</u> |
|---------------|---|-------------|
| 52            | Comparison of Sand Accumulation Profiles to Determine Effect of Opening between the Fence and Surface (Runs 1, 3, 6 at 16 hours) . . . . .                                    | 98          |
| 53            | Comparison of Sand Accumulation Profiles to Determine Effect of Subsurface Barrier on a Horizontal Slat Fence with 20% Opening at Bottom (Runs 2 and 4 at 14 hours) . . . . . | 99          |
| 54            | Comparison of Sand Accumulation Profiles to Determine Effect of Subsurface Barrier on a Vertical Slat Fence with 50% Uniform Porosity (Runs 5 and 5A at 16 hours) . . . . .   | 101         |
| 55            | Comparison of Profiles to Illustrate the Effect of the Slat Width on Sand Accumulation (Runs 5 and 7 at 16 hours) . . . . .   | 102         |
| 56a           | Run 7 after 2 Hours . . . . .   | 103         |
| 56b           | Run 7 after 16 Hours . . . . .  | 103         |
| 57            | Comparison of Profiles to Illustrate the Effect of Porosity on Sand Accumulation (Runs 8 and 11 at 12 hours) . . . . .  | 104         |
| 58            | Run 9 with Vertical Spires . . . . .  | 105         |
| 59a           | Scour Developed Underneath Fence . . . . .  | 106         |
| 59b           | Sand Accumulation around Fence with Subsurface Barrier to Reduce Scour . . . . .  | 106         |
| 59c           | Comparison of Sand Accumulation Profiles to Determine the Effect of a Subsurface Barrier (Runs 10 and 11 at 10 hours) . . . . .   | 107         |
| 60            | Typical Sand Accumulation Profiles, Double Fence Section, 25-foot Spacing . . . . .   | 113         |
| 61            | Typical Sand Accumulation Profiles, Double Fence Section, 50-foot Spacing . . . . .   | 113         |
| 62            | Sand Accumulation for Two Fences, Acting as Two Individual Rows . . . . .   | 114         |
| 63            | Sand Accumulation for Two Rows of Fences Acting Together . . . . .  | 114         |
| 64            | Schematic Diagram for Top View of Staggered Fence . . .   | 115         |

| <u>Figure</u> |  | <u>Page</u> |
|---------------|--|-------------|
| A-1           | Meteorological Wind Tunnel, Fluid Dynamics and Diffusion Laboratory, Colorado State University . . . . | 127         |
| A-2           | Plan View of Entrance to MWT Test Section . . . . .  | 128         |
| A-3           | Elevation View of Downwind Portion of MWT Test Section . . . . .                                       | 129         |
| B-1           | Isokinetic Sand-Sampling Aspirator . . . . .   | 135         |

LIST OF TABLES

| <u>Table</u> |  | <u>Page</u> |
|--------------|--|-------------|
| 1            | Characteristics of Vertical Flow Velocity Profiles . . . .   | 5           |
| 2            | Comparison of Sand Transport for Different Velocities . .  | 14          |
| 3            | Horizontal Sand Traps at Ground Level . . . . .  | 20          |
| 4            | Comparison of Horizontal Sand Trap Set at Ground<br>Level with Theoretical Values . . . . .  | 22          |
| 5            | Characteristics of Horizontal Sand Traps for 8 m/sec . . .   | 24          |
| 6            | Trap Efficiency for Vertical Sand Trap as Developed<br>by Horikawa and Shen . . . . .  | 30          |
| 7            | Roadway Models Tested . . . . .  | 35          |
| 8            | Volumes of Sand Collected by Sand Fences on Core Banks<br>from Installation to July 1961 (single fence sections) . .                               | 59          |
| 9            | Experimental Runs for Different Configurations for<br>Single Row of Fences . . . . .   | 63          |
| 10           | Volume of Sand Deposition in $\text{cm}^{-3}$ along Centerline<br>per Unit Centimeter for 9 meters/sec Freestream<br>Flow Velocity . . . . .       | 109         |
| 11           | Sand Accumulation around Fences, Multiple Rows,<br>after Savage (1963) . . . . .   | 112         |
| 12           | Sand Accumulation for Different Fence Spacings in<br>Cubic Centimeters per Unit Width along Centerline<br>of Wind Tunnel (multiple rows) . . . . . | 117         |
| A-1          | Location of Multiple/Special Fences in MWT . . . . .   | 131         |

## I. INTRODUCTION

### A. Authorization and Purpose of This Final Report

According to the October 17, 1981 telex from Dr. Danilo Anton, Research Institute, University of Petroleum and Minerals, Dhahran, Saudi Arabia to Dr. J. E. Cermak, Colorado State University was authorized to immediately begin a one-year Wind-Tunnel Research for IAP Sand Study.

The purpose of this report is to present all our results from this study. The specific tasks of the study are described in the next section.

### B. Scope and Specific Tasks of the Study

The major scope of this study was to conduct a series of wind tunnel tests on sand movements with respect to fences, roadways, and sand traps. This study was limited to experimental design, laboratory data acquisition, and data analysis of wind induced sand movement realized in the meteorological wind tunnel at the Fluid Dynamics and Diffusion Laboratory at Colorado State University.

The specific tasks were:

1). For sand fence studies - investigation of the optimum i) porosity, ii) geometry, and iii) spacings between multiple rows of fences, for the trapping of sand and the protection of airfield. One fence height was tested with one sand size under a neutral, stability condition. Fences with four different porosity geometries were tested. According to an agreement between Mr. Al Hinai of the Research Institute, University of Petroleum and Minerals, Dhahran, Saudi Arabia and Dr. J. E. Cermak of Colorado State University, the other fence geometries as proposed in the original proposal were not tested so that sand movements over different roadway configurations, as described in the next section, could be tested.

2). For sand movements over roadways - As requested by Mr. Al Hinai, six roadway configurations were used. Configuration 6 was not tested because after the testing of other configurations, it was determined that the behavior of sand movements across configuration 6 could be derived from the results from other configurations.

3). For sand traps - Horizontal sand traps similar in geometry to the circular trap used in the field measurements were studied to determine the ratio between the actual sand movement at different heights of each trap and the amount of sand trapped in each horizontal sand trap at these respective heights. In addition to these horizontal sand traps, a vertical sand sampler as developed by Horikawa and Shen (1962) was tested in the wind tunnel. This was not included in the original proposal.

4). Exploratory study of chemical and vegetative sand stabilization methods - Since the wind tunnel tests for fences, roadways, and samplers far exceeded the original proposed wind tunnel time, no test was made for this item. As stated in the original proposal, "In so far as wind-tunnel time and funds permit, several chemical and vegetative stabilization methods will be evaluated. The specific details of the methods and the experimental techniques for evaluation will be developed in close cooperation with the sponsor...." However, no instructions were received from the sponsor on this item.

#### C. Organization of This Report

In section II, the vertical flow velocity and sand distribution measurements for this study are presented, and these data are compared with data collected from previous studies by other investigators. The relationship between flow and the amount of sand movement is established. The wind-tunnel facility and test configurations for the fences, roadways and sand traps are described in Appendix A. Measuring instrumentation is described in Appendix B.

Section III describes the testing results of the experiments with the horizontal sand traps. These sand traps were provided to us by Mr. Al Hinai of the Research Institute, University of Petroleum and Minerals, Saudi Arabia. A series of tests were also conducted for a vertical sand trap as developed by Horikawa and Shen (1962).

Section IV describes the tests for sand movements over roadways. Sections V and VI describe our tests for sand movements through a single row of fences and multiple rows of fences, respectively.

Section VII discusses the application of wind tunnel test results in the actual field situation, and the last Section VIII presents future research needs.

## II. FLOW AND SAND MOVEMENTS WITHOUT OBSTRUCTIONS

### A. Brief Description of Previous Studies

Once sand particles begin to be moved by the fluid flow, the flow velocity profile will be altered by the movements of sand particles. Bagnold (1941); Zingg (1953); Horikawa and Shen (1960); Chepil and Woodruff (1963); and Willets and Phillips (1978) all found that the flow velocity profiles were modified by the sand movements.

As shown in Figure 1, before the sand moves, all flow profiles varied logarithmically with height above the ground. As soon as the sand particles were moved, all flow velocity profiles met at a focal point  $Z_0$  above the ground surface for each set of data. For each flow velocity profile, the flow velocities varied logarithmically with height above  $Z_0$  and below  $Z_0$ , respectively, with two different slopes. Table 1 gives a summary of some of the characteristics of flow velocity profiles. However, the relationship between  $Z_0$  and sand size is not clear.

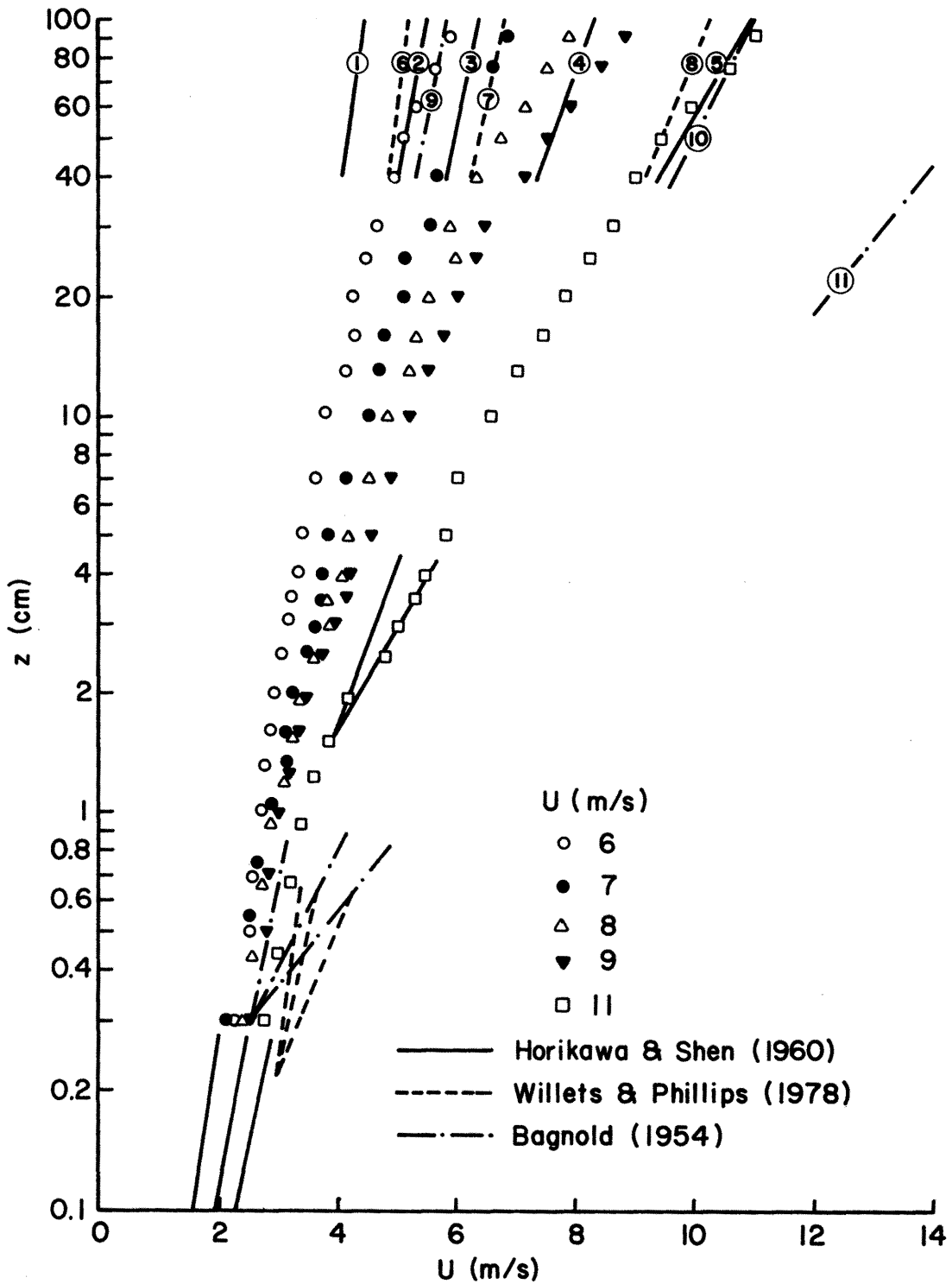


Figure 1. Vertical Flow Velocity Distribution

Table 1. Characteristics of Vertical Flow Velocity Profiles

| Source                          | Curve | $u_{*b}$ bottom<br>(cm/s) | $u_{*u}$ upper<br>(cm/s) | Symbol | Sand diameter<br>(mm) | $z_o$ |
|---------------------------------|-------|---------------------------|--------------------------|--------|-----------------------|-------|
| C.S.U.                          |       | 13.7                      | 38.3                     | ◦      | 0.145                 |       |
|                                 |       | 19.4                      | 41.7                     | ●      | 0.145                 |       |
|                                 |       | 20.2                      | 48.7                     | Δ      | 0.145                 |       |
|                                 |       | 24.5                      | 57.4                     | ▼      | 0.145                 |       |
|                                 |       | 25.9                      | 68.3                     | □      | 0.145                 |       |
| Horikawa<br>&<br>Shen (1959)    | 1     |                           | 15.7                     | —      | 0.2                   |       |
|                                 | 2     |                           | 20.9                     | —      | 0.2                   |       |
|                                 | 3     |                           | 24.0                     | —      | 0.2                   |       |
|                                 | 4     |                           | 41.7                     | —      | 0.2                   | 1.5   |
|                                 | 5     |                           | 64.3                     | —      | 0.2                   | 1.5   |
| Willets<br>&<br>Phillips (1978) | 6     |                           | 18.0                     | ----   | 0.25                  | 0.22  |
|                                 | 7     |                           | 30.0                     | ----   | 0.25                  | 0.22  |
|                                 | 8     |                           | 50.0                     | ----   | 0.25                  | 0.22  |
| Bagnold<br>(1954)               | 9     |                           | 19.0                     | -·-·-  | 0.25                  | 0.3   |
|                                 | 10    |                           | 62.0                     | -·-·-  | 0.25                  | 0.3   |
|                                 | 11    |                           | 88.9                     | -·-·-  | 0.25                  | 0.3   |

Figure 2 shows the relationship between  $U_{100}$ , the flow velocity measured at 100 centimeters above the ground, and the shear velocity  $U_*$ . The solid lines represent calculations by Horikawa and Shen (1960) for assumed logarithmic velocity profiles and different  $k$  values, where  $k$  is the von Karman's universal constant as shown in the following equation:

$$\frac{U}{U_*} = \frac{1}{k} \ln_e \frac{Z}{Z_0} + U' \quad (1)$$

where  $Z_0$  and  $U'$  are the focal point height above the ground and the flow velocity there, respectively.

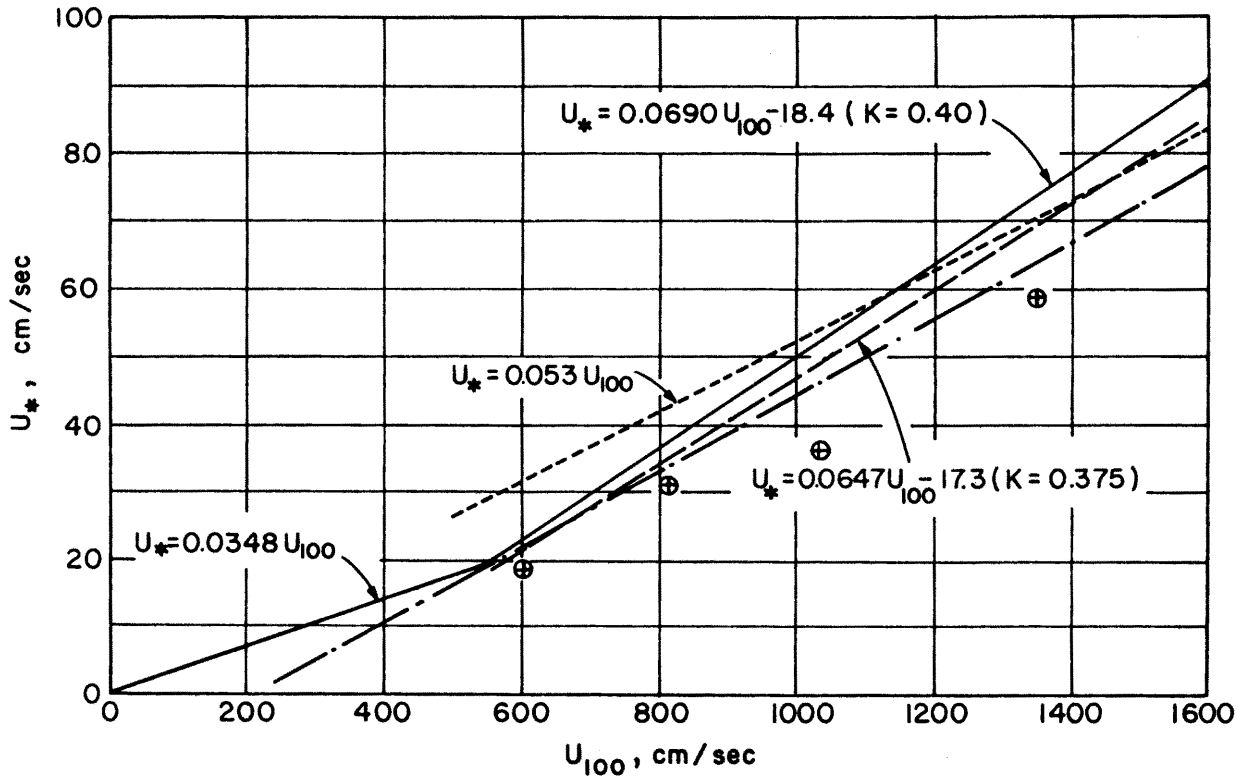
Figure 3 shows the relationship between the shear velocity  $U_*$  and the total sand transport rate. The values of  $U_*$  are based on the flow velocity profile above the focal point  $Z_0$ . The total sand transport  $q$  varied approximately with the third power of the shear velocity as shown by the following equation:

$$q = f(U_*^3) \quad (2)$$

Figures 4a and 4b show the vertical sand distribution based on data collected by Kawamura (1951) and Ishihara and Iwagaki (1950), respectively. Figure 4c illustrates the ratio between  $q_s$ , surface creep, and  $q$ , total sand transport as presented by Horikawa and Shen (1960). In general, this ratio of  $q_s/q$  remained at a constant value of 20 percent.

#### B. Experimental Facility and Results

In making velocity measurements in the environment with sand drifts, a compromise was necessary in selecting a sensor that was rugged enough to withstand the particle impact and dust adhesion without significantly changing its response characteristics and that had a small enough thermal mass to provide



Legend:

- $\oplus$  CSU data from current study. (-----)
- Kawata (1948).
- Modifications by Horikawa and Shen (1960) with different K values. (K is von Karman's universal constant.)

Figure 2. Relationship between  $U_{100}$  Velocity at 100 cm above Bed and Shear Velocity

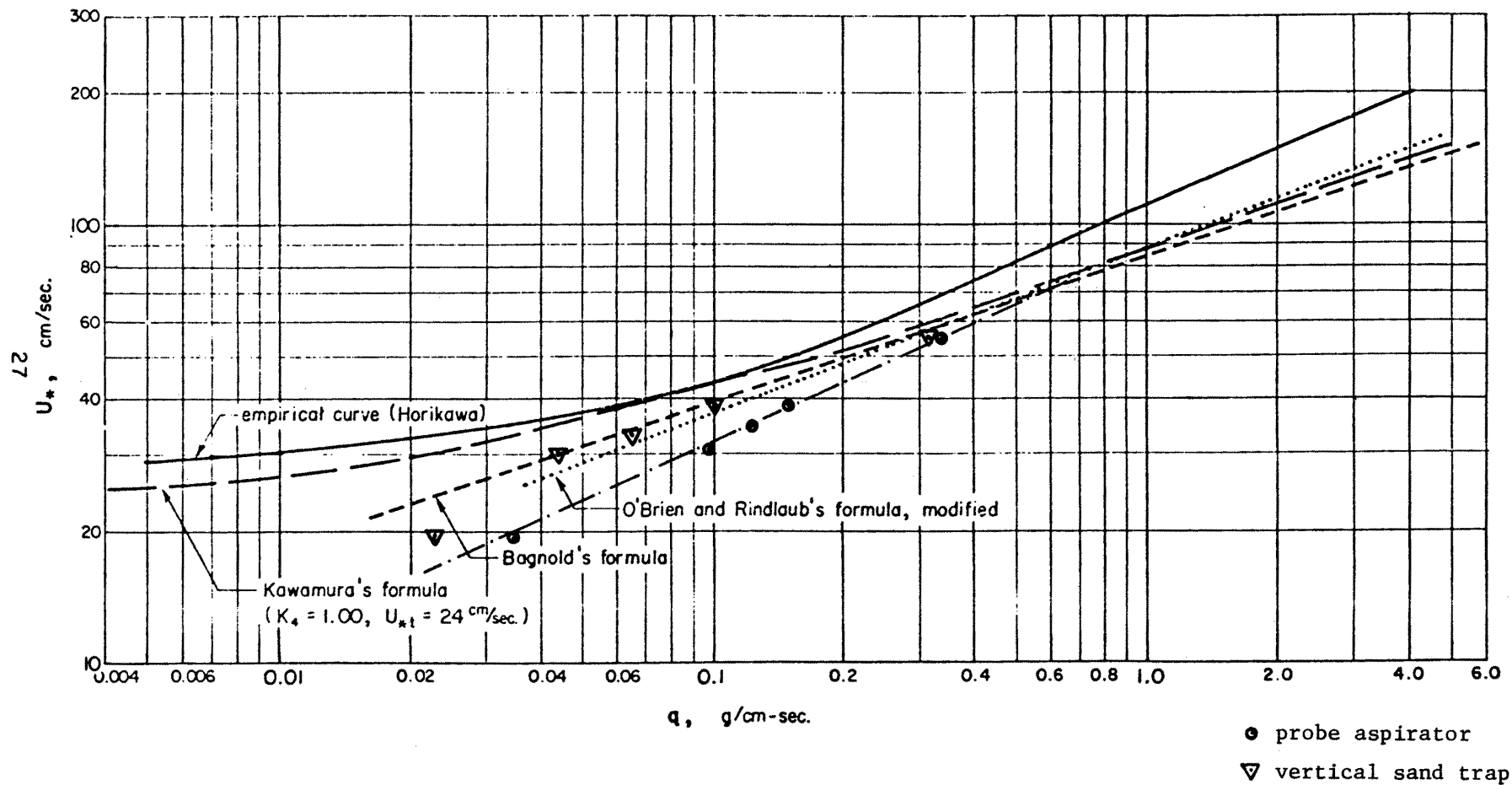
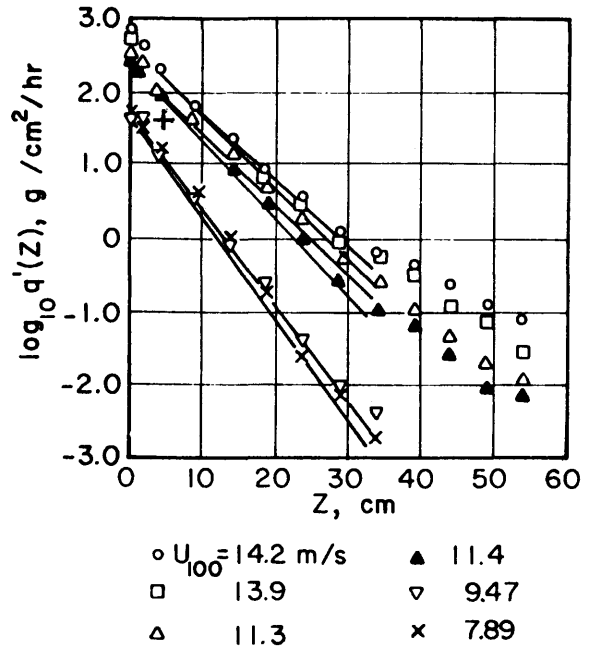
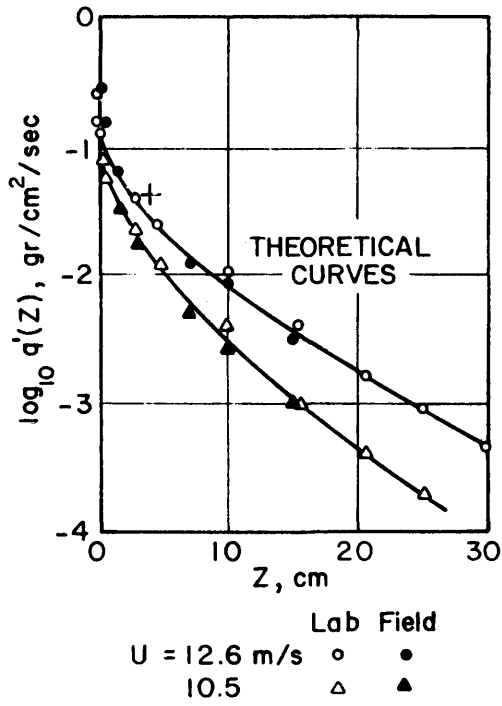
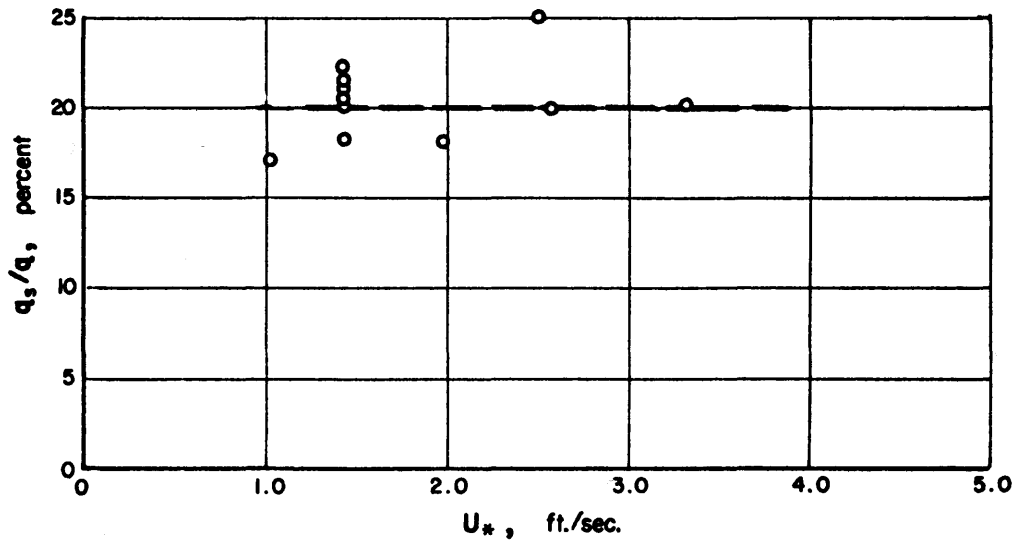


Figure 3. Comparison of Several Formulas ( $d_{max} = 0.20$  mm) of Sand Transport as a Function of  $u_*$ .



(a) After Kawamura (1951)

(b) After Ishihara and Iwagaki (1952)



(c) After Horikawa and Shen (1960)

Figure 4. Vertical Distribution of Sand Drift

a good frequency for making turbulence measurements. Two shielded sensors were used; detailed descriptions are given in Appendix B of this report.

The concentrations of airborne sand were sampled with an aspirating probe set at variable heights above the sand bed; detailed discussion of the probe is also provided in Appendix A.

1). Vertical Flow Velocity Distributions:

Figures 5 and 1 give the vertical flow distributions for various free stream velocities using the flow velocity distribution in the lower 10 centimeters (sand particles were concentrated within 3 cm from bed). It was determined that the corresponding shear velocities were 0.186 meter/sec, 0.307 meter/sec, 0.351 meter/sec, and 0.596 meter/sec for free stream flow velocities of 5.74 meters/sec, 7.90 meters/sec, 10 meters/sec and 13.13 meters/sec.

As shown in Figure 1, the vertical velocity distributions from this study agree reasonably well with all other previous studies; however, for our studies, all velocity distribution curves did not meet clearly at a single focal point which is about 10 sand diameters above the bed, as was found by earlier researchers. Figure 2 also shows the comparison of our shear velocity values with previous studies. The agreement is reasonably good.

2). Turbulent Characteristics:

Figure 6 shows the mean flow and turbulent characteristics measured at 1 meter upstream from the fence location but without the fence. It must be pointed out that these measurements, as described in Appendix B, are rather preliminary, but these results are encouraging. These data have demonstrated that more reliable data are obtainable. The maximum turbulence level (ratio of root mean square of flow velocity fluctuated and the mean flow velocity) reached about 22 percent.

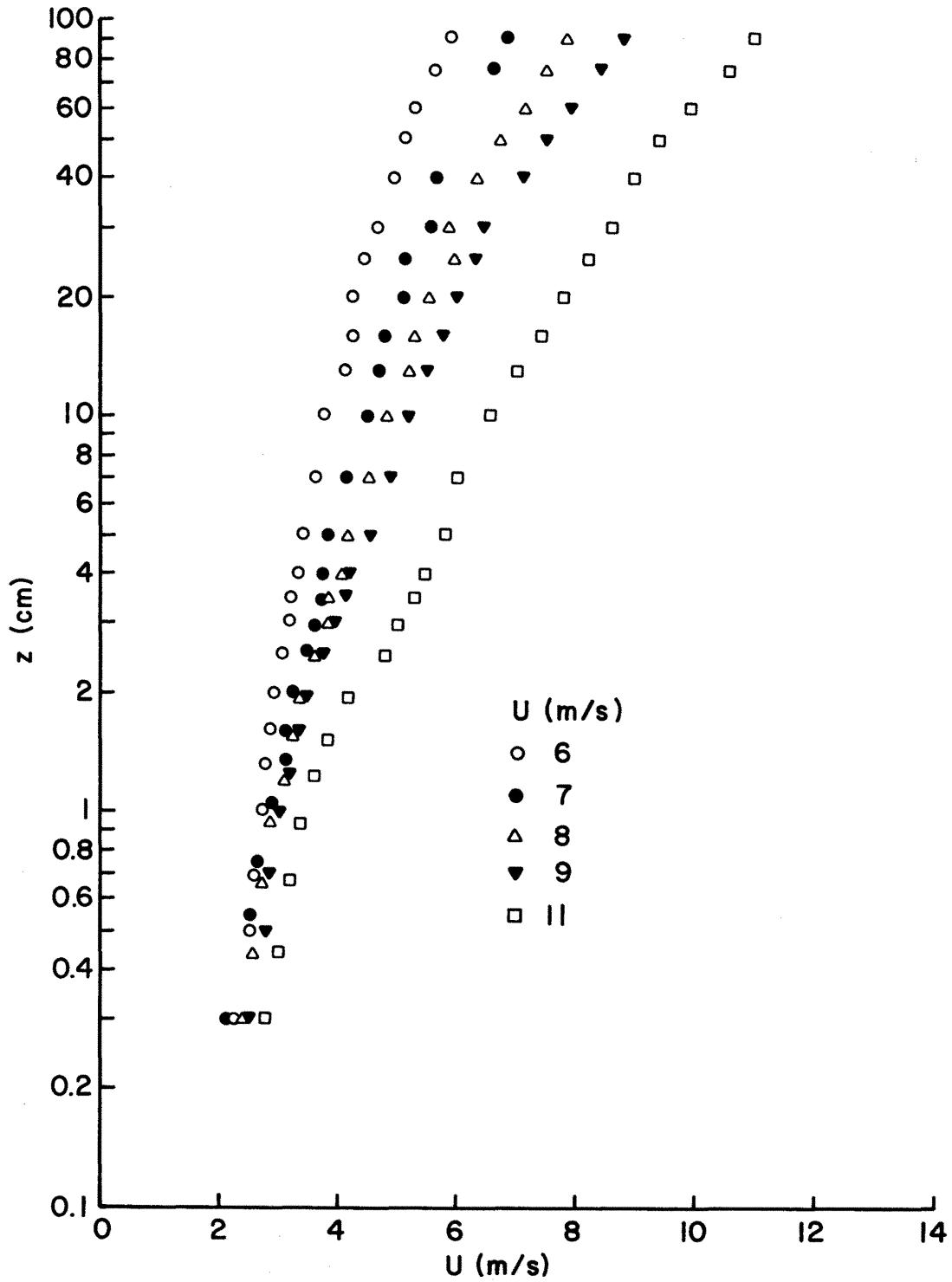
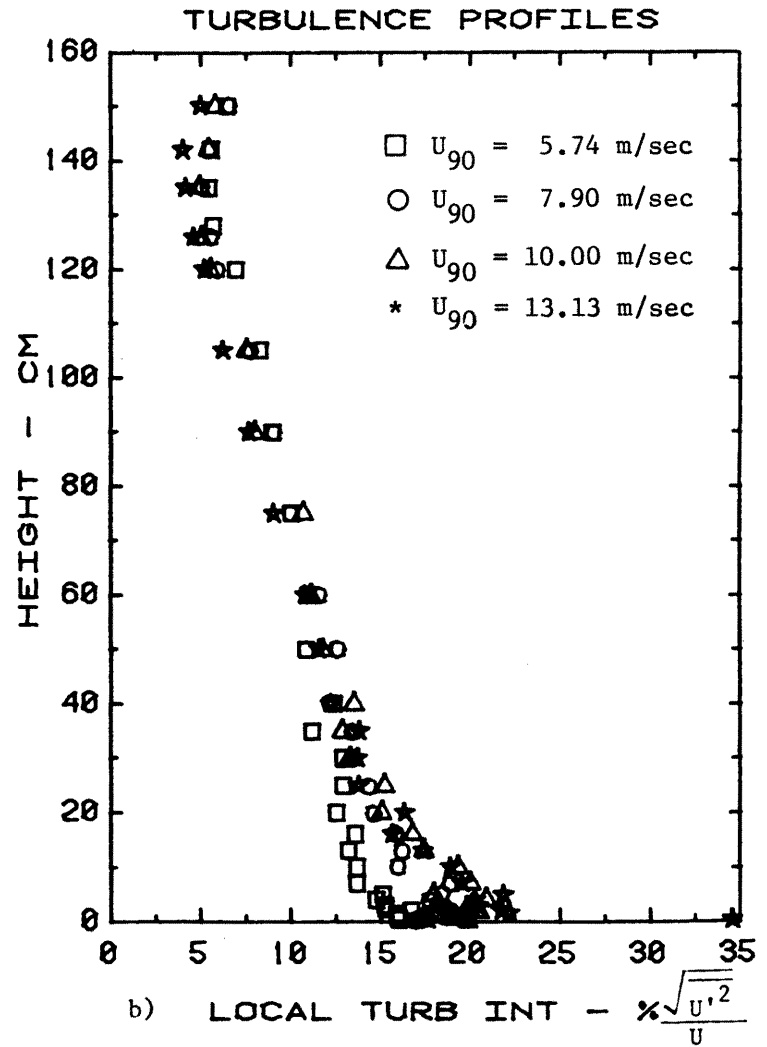
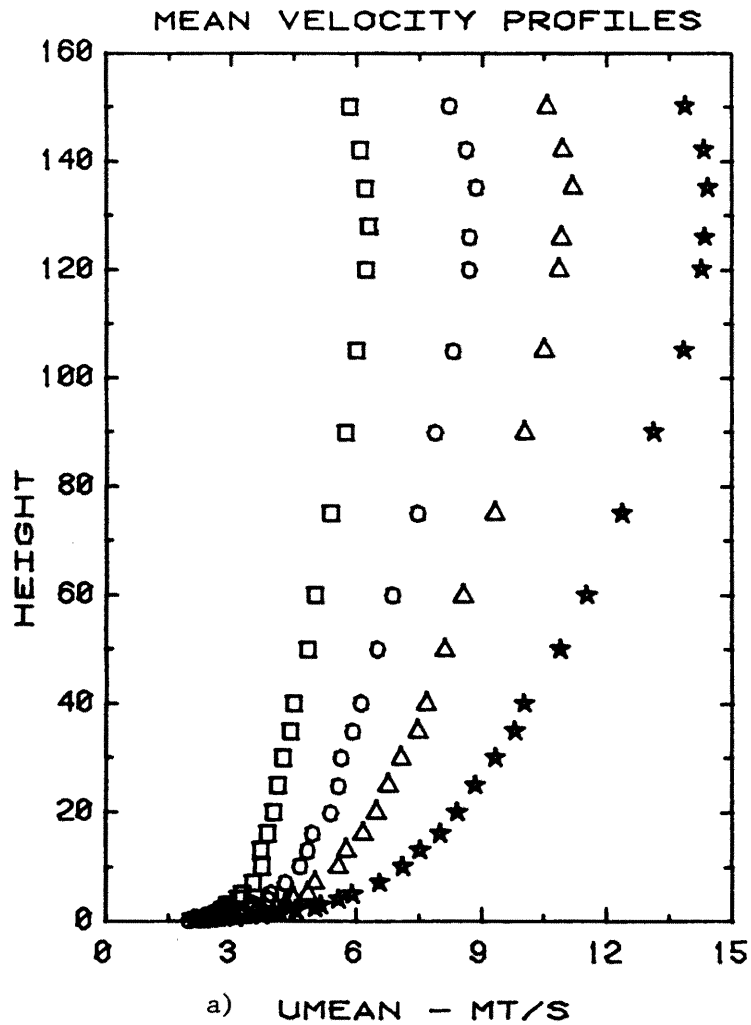


Figure 5. Vertical Flow Velocity Distribution from CSU



$U_{90}$  is the mean flow velocity at 90 cm above the bed.

Figure 6. Flow Characteristics at 1 m Upstream of the Fence Location but without the Fence

### 3). Variation of Sediment Transport Rate with Height:

Figure 7 shows the sand size distribution used for our studies. The size distribution is rather uniform. A horizontal tube, 6.35 millimeters in diameter, was used to collect sediment transport rates at different locations. A detailed discussion of this instrument is given in Appendix B. Since this tube is rather large compared with the moving layer of sediment above the bed, an integration method was used to correct the weighted center of the sand concentrated within each tube. Figures 8, 4a, and 4b show  $q$  the variation of sediment concentration with height  $Z$  for various wind speeds. The logarithm of the amount of sand transport was plotted versus the  $\sqrt{Z}$ . For our studies, the vertical sand concentration variation with height above the ground for a free stream flow velocity of 9 meters per second was interpreted from the two vertical sand concentration profiles between free stream velocities of 8 and 10 meters per second.

### 4). Total Sediment Transport

Table 2 and Figure 3 show the total sediment transport and integral of the transport rate as a function of height for our study compared to results obtained by Horikawa (1960), Kawamura (1951), Bagnold (1954), and O'Brien and Rindlaub (1936). The agreement between our data and their's is good, and, in general,

$$q = f(U_*^3)$$

Since the medium size of our sand is 0.14 mm (which is smaller than sizes between 0.2 to 0.25 mm as used by other investigators) our sand transport rate is greater than others.

Table 2. Comparison of Sand Transport for Different Velocities

| Reference Velocity | Shear Velocity | q [gr/cm-sec] |          |         |                      |                         | Present Study Vertical Sand Trap | Trap Efficiency |
|--------------------|----------------|---------------|----------|---------|----------------------|-------------------------|----------------------------------|-----------------|
|                    |                | Horikawa      | Kawamura | Bagnold | O'Brien and Rindlaub | Present Study Aspirator |                                  |                 |
| 6                  | .186           |               |          |         |                      |                         |                                  |                 |
| 8                  | .307           | 0.014         | 0.026    | 0.055   | 0.062                | 0.099                   | 0.052                            | .52             |
| 10                 | .351           | 0.03          | 0.043    | 0.069   | 0.085                | 0.158                   | 0.09                             | .57             |
| 13                 | .596           | 0.23          | 0.30     | 0.25    | 0.25                 | 0.340                   | 0.28                             | .82             |

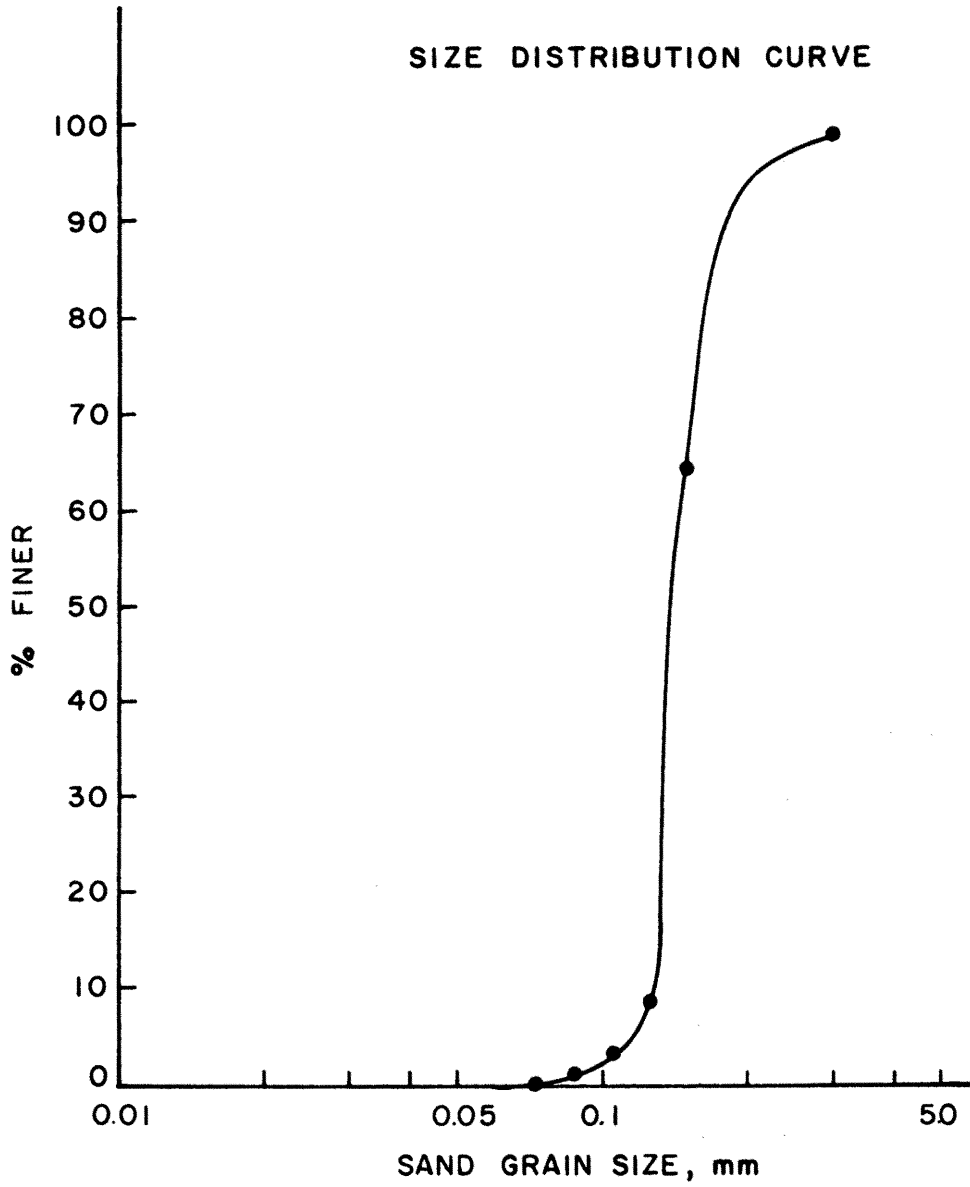


Figure 7. Sand Size Distribution

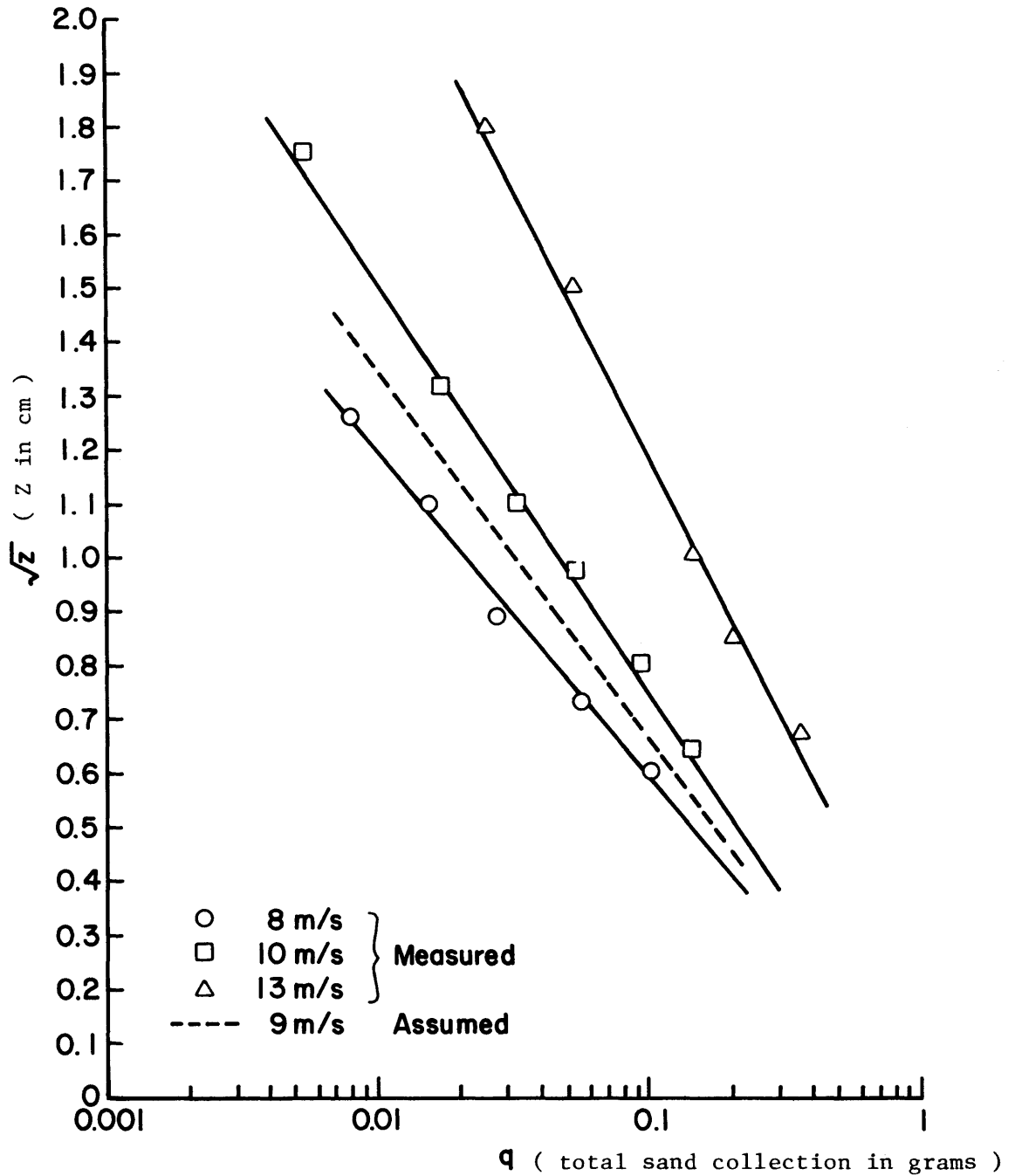


Figure 8. Vertical Sand Transport Rate Distribution, Measured by Aspirator (see Appendix B for description of aspirator)

### III. SAND TRAP SAMPLERS

#### A. Horizontal Trap Samplers

Three horizontal sand trap samplers were provided to us by Mr. Al Hinai of the Research Institute of the University of Petroleum and Minerals. As shown in Figure 9, there are three sizes with respective diameters of 34 mm, 16.5 mm and 12 mm. The largest sampler, with a diameter of 34 mm, is used in the field. Figure 10a and Table 3 show the actual accumulation rates for samplers set at ground level for three different free stream wind speeds. Table 4 and Figure 10b give the trap efficiency of horizontal sand traps samplers set at the ground elevation. Column 1 of Table 4 gives the free stream flow velocity. Column 2 is the inside diameter of the sand trap. Column 3 is obtained from line  $\phi-\phi$  from Figure 3. Column 4, surface creep, is calculated from 20 percent of Column 3. Column 5 is surface creep for each sampler and is taken to be the product of Column 2 and Column 4. Column 6 is the total sand transport for each sampler and is taken to be the product of Column 2 and Column 3. Column 7 gives the actually measured amount of sand accumulation in each sampler. Column 8 gives the trap efficiency of each sampler based on the ratio of the amount of sand trapped and the total sand movement. Column 9 gives the trap efficiency of each sampler based on the ratio of actual amount trapped to the surface creep.

The amount of sand trapped in the field sampler with a diameter of 34 mm is approximately 20 percent of the total sand transport rate. A greater wind velocity would result in a slightly higher trap efficiency. As a general rule, the amount of sand trapped in a 34 mm diameter horizontal trap sampler would be about the same as the amount of surface creep, which is about 20 percent of the total sand transport rate.

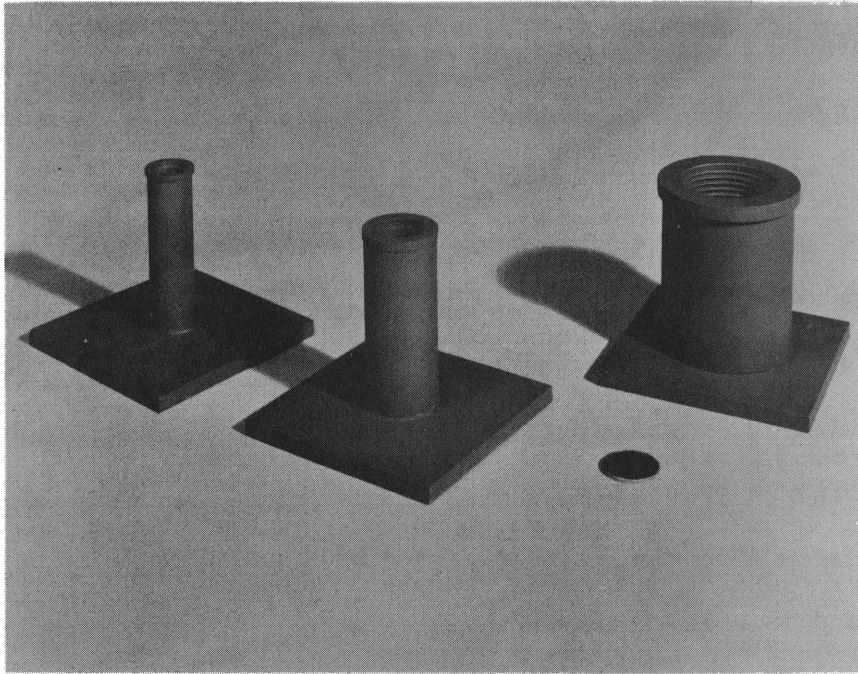


Figure 9. Photograph of Horizontal Traps with inside Diameters of 12 mm, 16.5 mm, and 34 mm

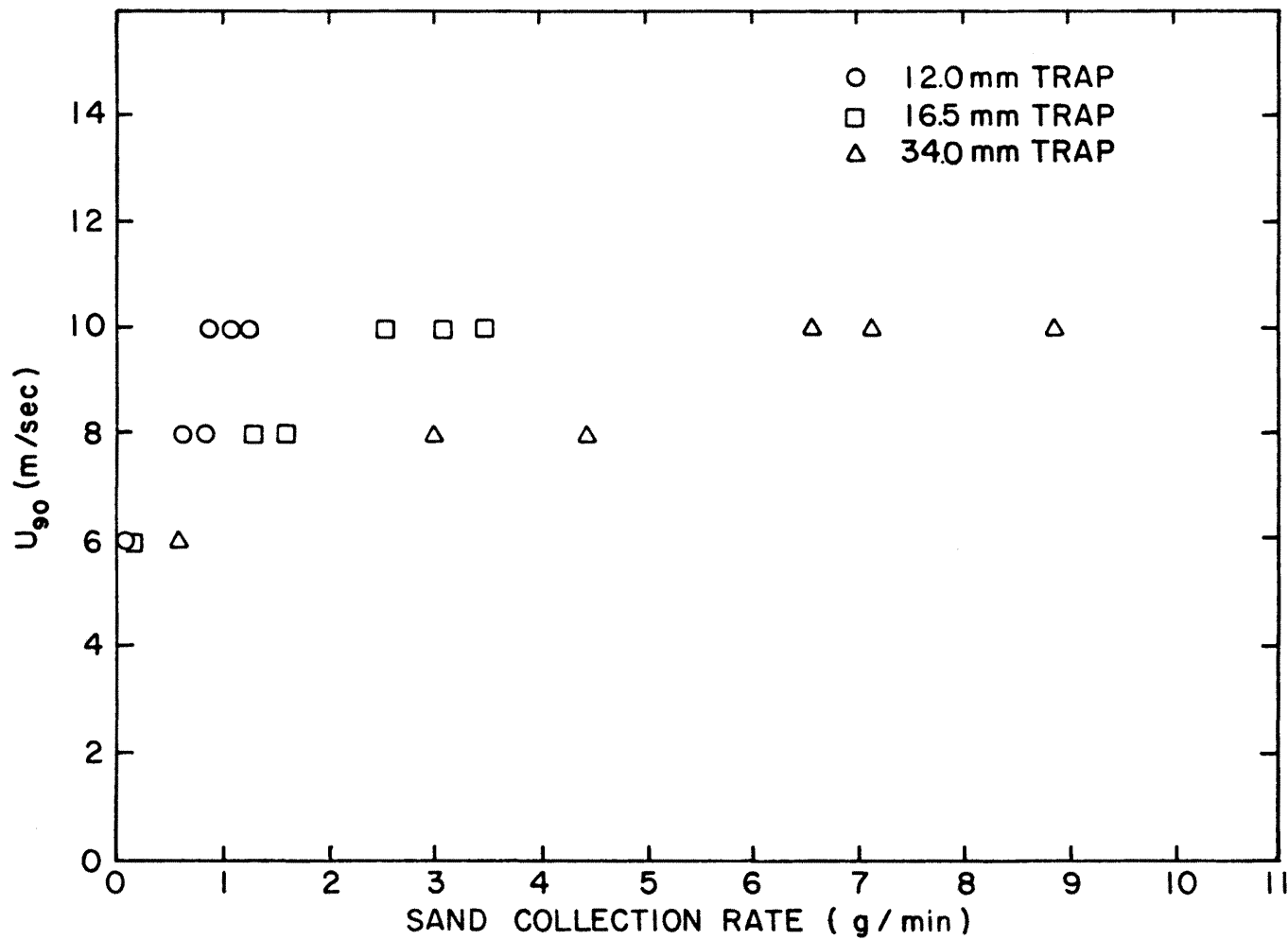


Figure 10a. Sand Collection in Horizontal Traps at Ground Level

Table 3. Horizontal Sand Traps at Ground Level

| Trap Size<br>(mm)                             | Weight of Sand<br>Collected<br>(grams) | Sample<br>Time<br>(min) | Rate of<br>Collection<br>(g/min) |
|---|--|-------------------------|----------------------------------|
| <u><math>U_{90} = 6 \text{ m/sec}</math></u>  |  |                         |                                  |
| 34  | 37.9                                   | 60                      | 0.63                             |
| 16.5  | 12.1                                   | 60                      | 0.20                             |
| 12  | 6.1                                    | 60                      | 0.10                             |
| <u><math>U_{90} = 8 \text{ m/sec}</math></u>  |  |                         |                                  |
| 34  | 35.7                                   | 8                       | 4.46                             |
|   | 23.8                                   | 8                       | 2.98                             |
| 16.5  | 12.8                                   | 8                       | 1.60                             |
|   | 10.6                                   | 8                       | 1.32                             |
| 12  | 6.8                                    | 8                       | 0.85                             |
|   | 5.0                                    | 8                       | 0.62                             |
| <u><math>U_{90} = 10 \text{ m/sec}</math></u> |  |                         |                                  |
| 34  | 44.6                                   | 5                       | 8.92                             |
|   | 21.5                                   | 3                       | 7.17                             |
|   | 26.4                                   | 4                       | 6.60                             |
| 16.5  | 17.4                                   | 5                       | 3.48                             |
|   | 9.3                                    | 3                       | 3.10                             |
|   | 10.2                                   | 4                       | 2.55                             |
| 12  | 8.0                                    | 5                       | 1.60                             |
|   | 5.3                                    | 3                       | 1.77                             |
|   | 5.5                                    | 4                       | 1.38                             |

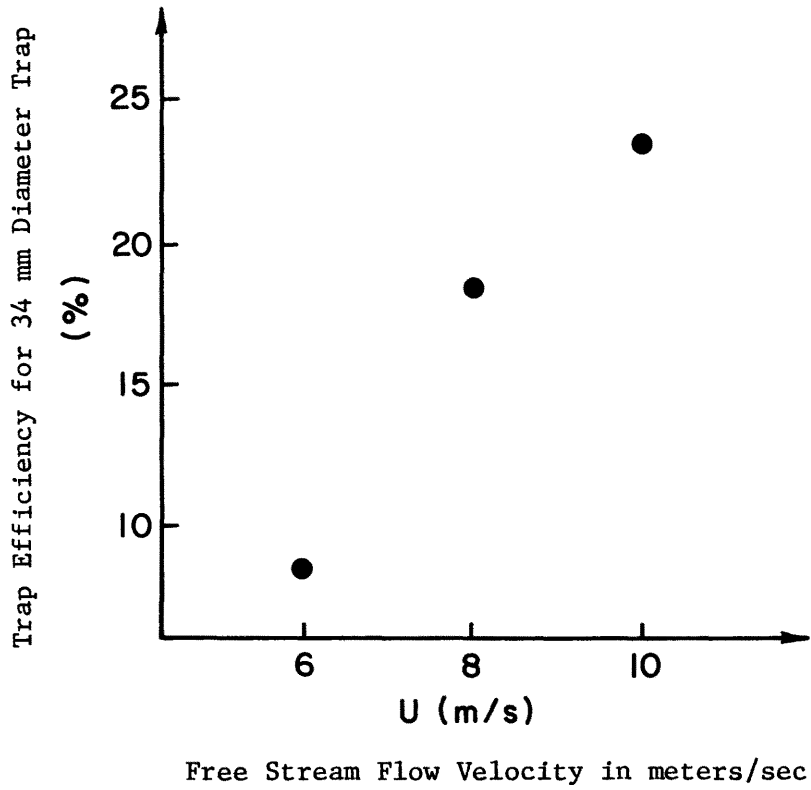


Figure 10b. Trap Efficiency for 34.0 mm inside Diameter Sand Trap Set at Ground Level

Table 4. Comparison of Horizontal Sand Trap Set at Ground Level with Theoretical Values

| (1)                                     | (2)   | (3)  | (4)  | (5)   | (6)   | (7)   | (8)                           |
|---|---|--|--|---|---|---|-------------------------------|
| Free stream<br>flow velocity<br>(m/sec) | D, diameter<br>of horizontal<br>sand trap<br>(mm) | Total transport<br>rate from<br>Figure 3<br>(gm/cm-hr) | Unit surface<br>creep 20% $\times$ (3)<br>(gm/cm-hr) | Calculated<br>surface<br>creep for<br>each sampler<br>(2) $\times$ (4)(gm/hr) | Transport<br>for D (width)<br>(2) $\times$ (3)<br>(gm/hr) | Actual<br>quantity<br>measured<br>in each trap<br>(gm/hr) | Trap<br>Efficiency<br>(7)/(6) |
| 6                                       | 12.0  | 132  | 26.4   | 31.7  | 158   | 6   | 3.8%                          |
| 6                                       | 16.5  | 132  | 26.4   | 43.6  | 218   | 12  | 5.5%                          |
| 6                                       | 34.0  | 132  | 26.4   | 89.8  | 449   | 37.8  | 8.4%                          |
| 8                                       | 12.0  | 356  | 71.2   | 85.4  | 427.2   | 44.1  | 10.32%                        |
| 8                                       | 16.5  | 356  | 71.2   | 117.5   | 534   | 87.6  | 16.4%                         |
| 8                                       | 34.0  | 356  | 71.2   | 242   | 1210  | 223.2   | 18.45%                        |
| 10                                      | 12.0  | 570  | 114  | 136.8   | 684   | 95  | 13.89%                        |
| 10                                      | 16.5  | 570  | 114  | 188.1   | 940.5   | 182.6   | 19.42%                        |
| 10                                      | 34.0  | 570  | 114  | 387.6   | 1938  | 454   | 23.43%                        |

Figures 10c and 10d show the comparison of sand accumulation rates in each of the three samplers when these samplers were set at three different heights above the ground with free stream wind speed of 8 meters per second; sand transport rates at different heights and free stream flow velocities were measured by an aspirator, as described in Appendix B. The following Table 5 gives the ratio between the actual sand accumulated in the horizontal sand traps at different heights and the measured sand transport (by the aspirator) at the same respective heights. For the field sand trap with a diameter of 34 mm, these trap efficiency ratios are given in Column 6.

#### B. Vertical Trap Samplers

Although the testing of these vertical traps shown in Figures 11a and 11b was not included in the original proposal, these tests were conducted. The amounts of total sand accumulated in the vertical sand traps for different free stream flow velocities are given in Figure 12 and Table 6. These values are plotted on Figure 3 and seem to agree with the curves as presented by other investigators, but these traps yield a smaller value than that given by the aspirator. One must remember that our sand size of 0.14 mm is much smaller than that used by other investigators with 0.2 mm to 0.25 mm; thus, a trap efficiency should be applied to our vertical sand trap. The following Table 6 gives the variation of values.

Table 5. Characteristics of Horizontal Sand Traps for 8 m/sec

| (1)                                   | (2)  | (3)                               | (4)   | (5)   | (6)                             |
|---------------------------------------|--|-----------------------------------|---|---|---------------------------------|
| Free stream<br>flow velocity<br>(m/s) | Diameter of<br>horizontal<br>sand trap<br>(mm) | Height<br>above<br>ground<br>(mm) | Estimated<br>Sand Trans-<br>port rate in<br>g/min/cm <sup>2</sup> | Actual<br>measured<br>sand<br>transport<br>rate <sup>2</sup><br>g/min/cm <sup>2</sup> | Trap<br>efficiency %<br>(5)/(4) |
| 8                                     | 34   | 6                                 | 1.62  | 0.0650  | 4.01                            |
| 8                                     | 34   | 12                                | 0.5   | 0.0175  | 3.50                            |
| 8                                     | 34   | 24                                | 0.09  | 0.0010  | 1.11                            |
| 8                                     | 16.5   | 6                                 | 1.62  | 0.025   | 1.54                            |
| 8                                     | 16.5   | 12                                | 0.5   | 0.0083  | 1.66                            |
| 8                                     | 16.5   | 24                                | 0.09  | 0.0015  | 1.66                            |
| 8                                     | 12   | 6                                 | 1.62  | 0.0275  | 1.70                            |
| 8                                     | 12   | 12                                | 0.5   | 0.0068  | 1.36                            |
| 8                                     | 12   | 24                                | 0.09  | 0.001   | 1.11                            |

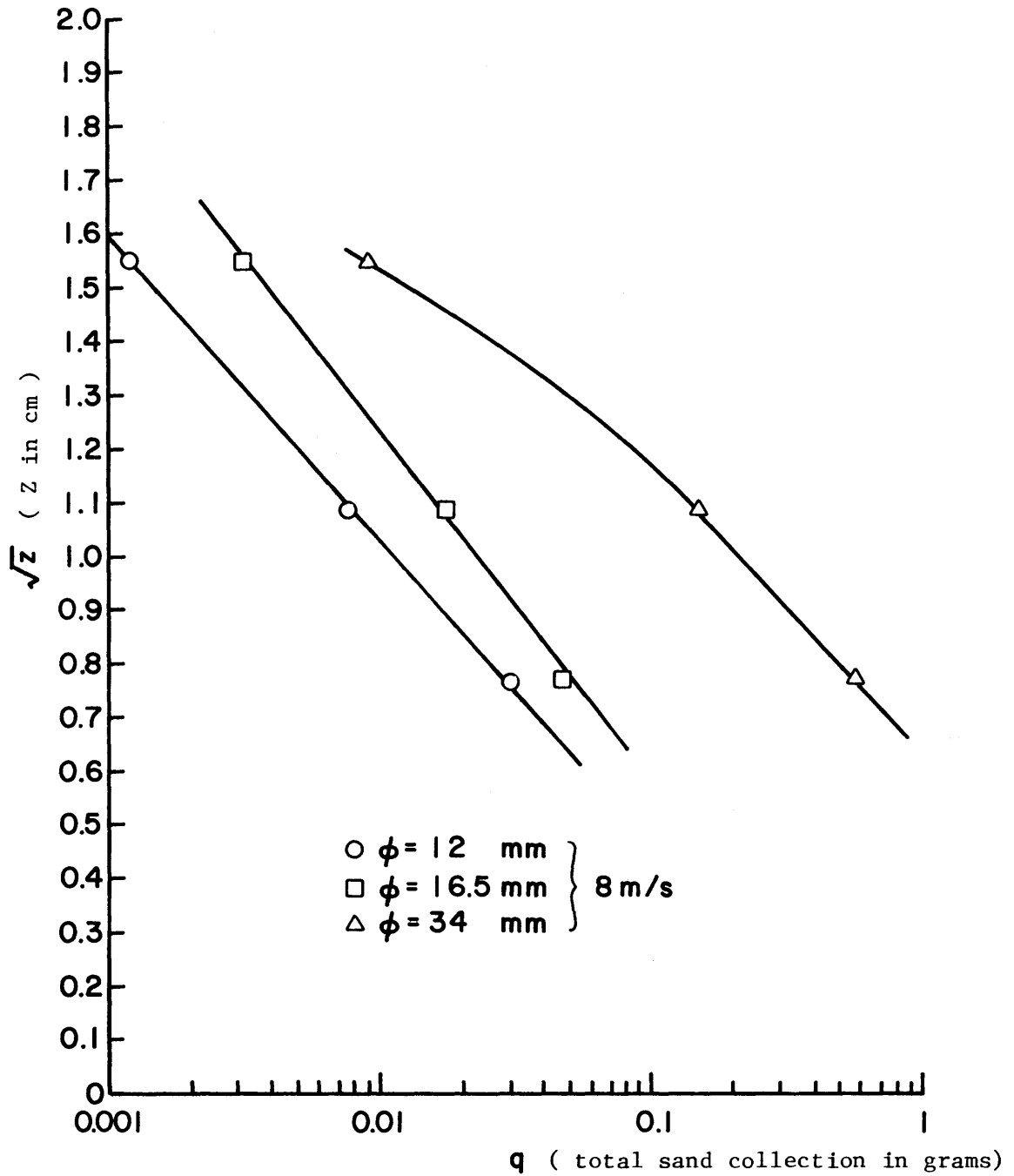


Figure 10c. Vertical Distribution of Sand Trapped by Horizontal Sand Traps

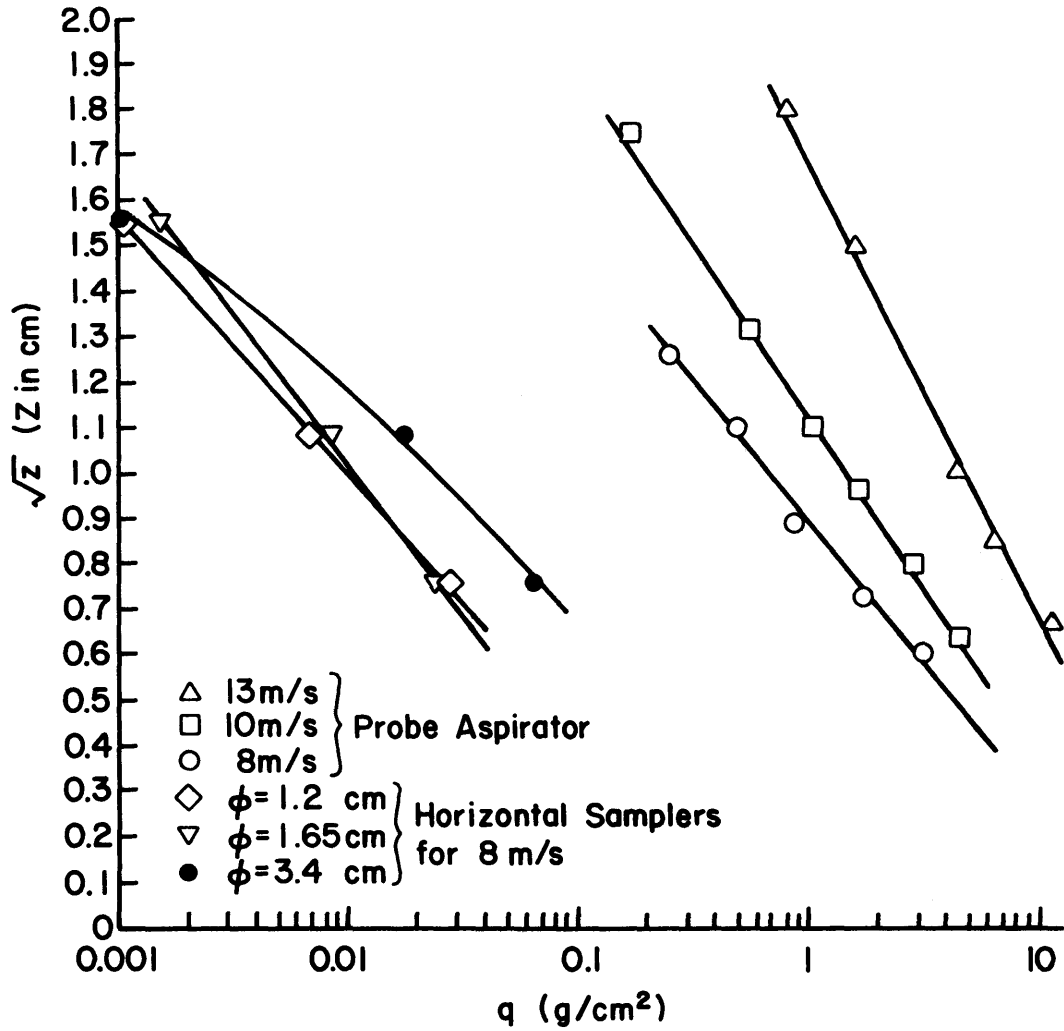


Figure 10d. Comparison of Horizontal Sand Trap Samplers with Aspirator

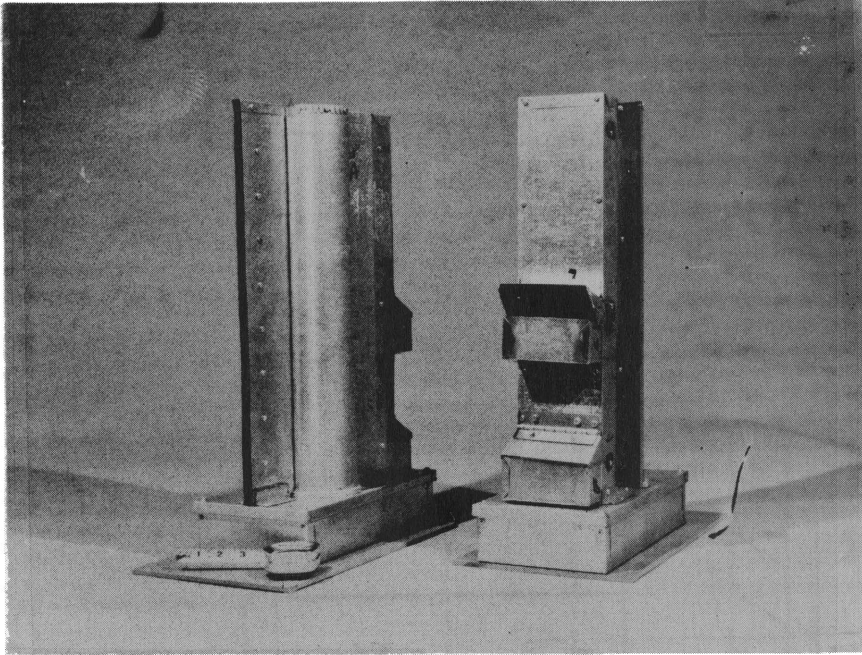
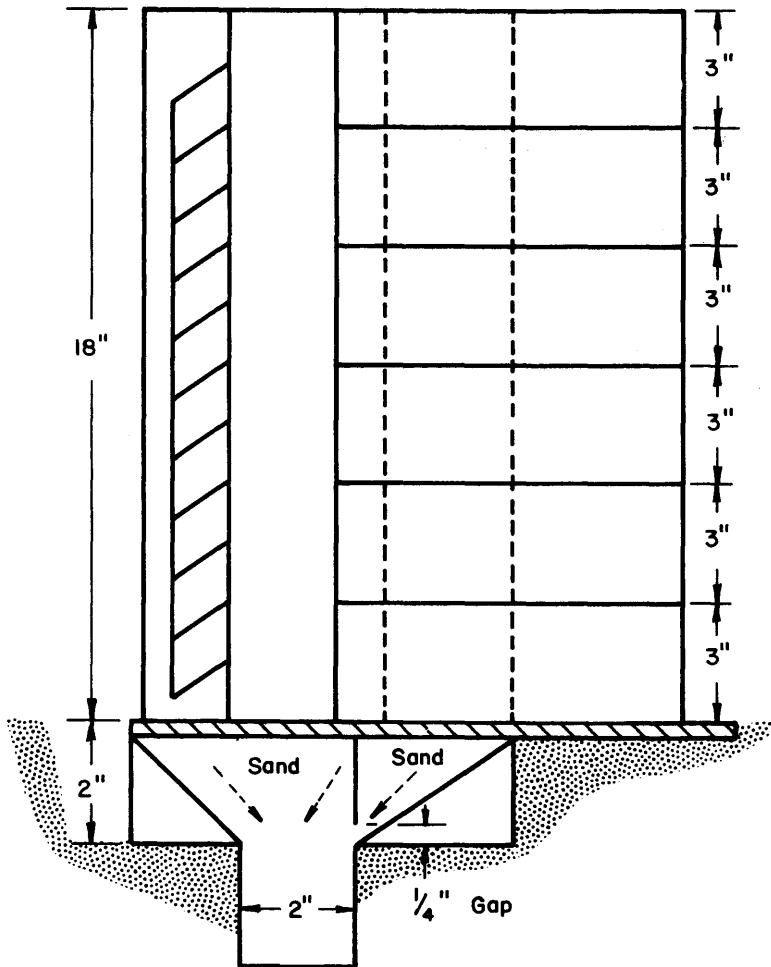
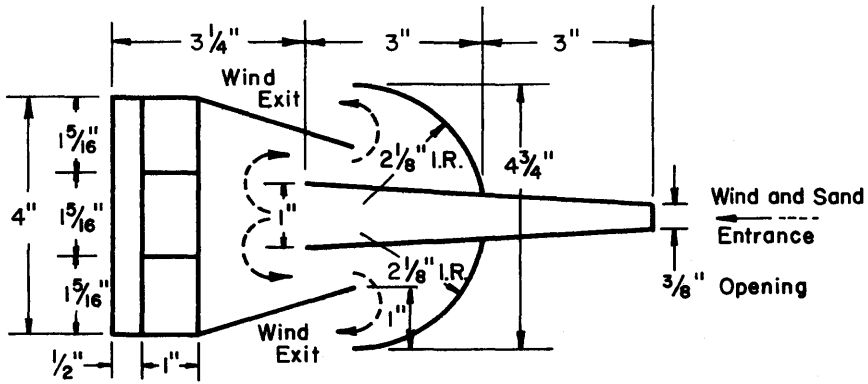


Figure 11a. Photograph of Vertical Sand Traps Developed by Horikawa and Shen (1960) (The left-hand model is facing upstream.)



Conversion Chart

|       |          |    |
|-------|----------|----|
| 1/16" | =0.15875 | cm |
| 1/8 " | =0.3175  | cm |
| 1/4 " | =0.635   | cm |
| 5/16" | =0.79375 | cm |
| 3/8 " | =0.9525  | cm |
| 1/2 " | =1.27    | cm |
| 1 "   | =2.54    | cm |

Figure 11b. Schematic Diagram of Vertical Sand Traps Developed by Horikawa and Shen

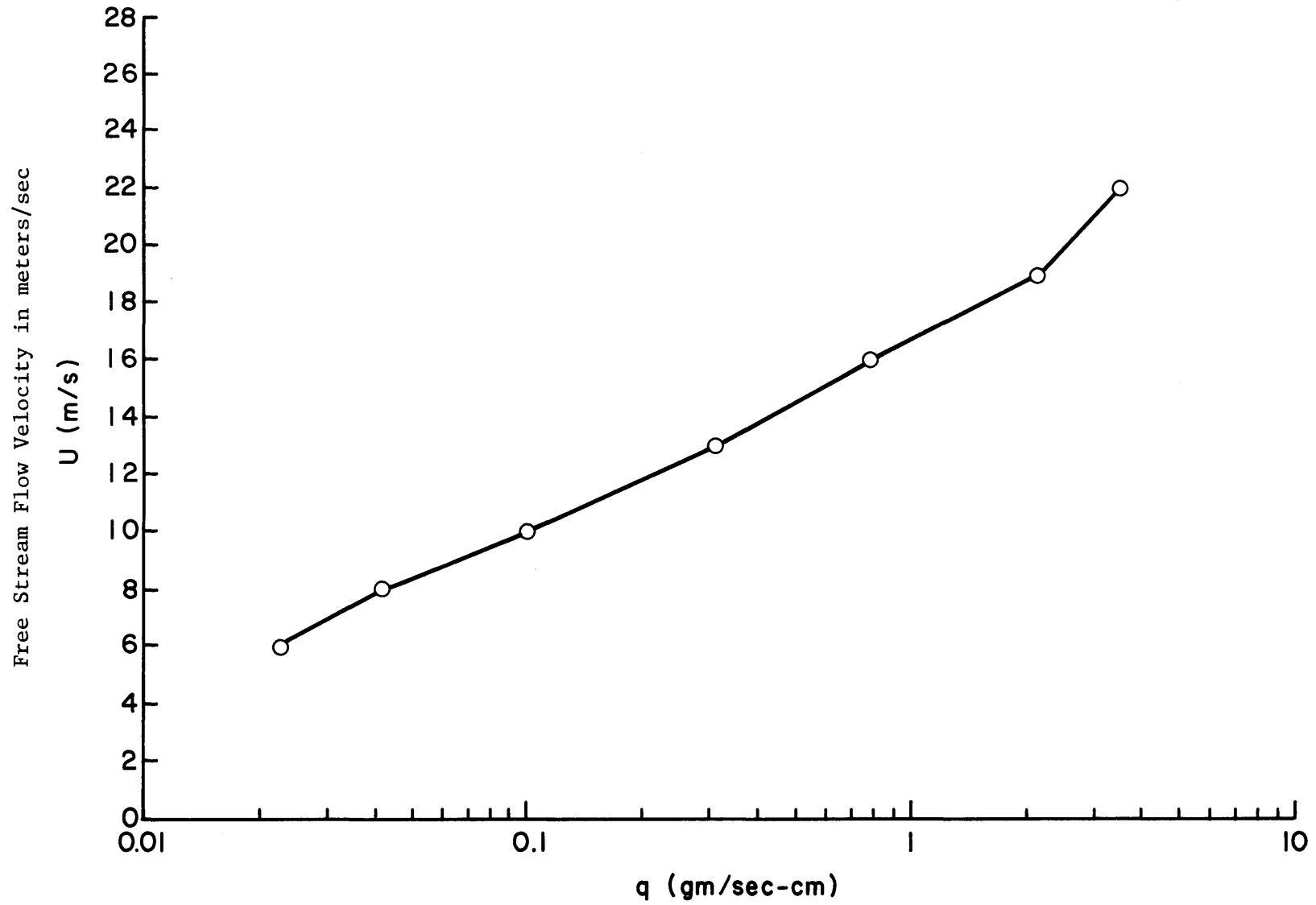


Figure 12. Amount of Sand Trapped by Vertical Sand Traps

Table 6. Trap Efficiency for Vertical Sand Trap as Developed by Horikawa and Shen (1960)

| Wind Speed | Total Sand Measurements by Aspirator (g/cm sec) | Total Sand Measurements by Vertical Trap (g/cm sec) | Efficiency (3)/(2) |
|------------|---|---|--------------------|
| 6          | 0.037   | 0.023   | .62                |
| 8          | 0.099   | 0.044   | .44                |
| 9          | 0.127   | 0.065   | .51                |
| 10         | 0.158   | 0.100   | .63                |
| 13         | 0.340   | 0.315   | .93                |

### C. Conclusions

Although a rough order of magnitude estimation on the magnitude of sand transport rate can be obtained by the 34 mm diameter horizontal sand traps, better sand traps are needed to obtain more reliable values. One should always remember that during periods of high winds, the wind may even erode sand away from the horizontal samplers, if the sand deposit nearly reaches the top.

The vertical sand trap sampler as developed by Horikawa and Shen (1960) performed reasonably well in the wind tunnel. With high wind speeds of 13 meters per second, the trap efficiency of this vertical sand trap was nearly unity. However, this particular sand trap collects samples well only when its narrow entrance is aligned perfectly with the wind direction.

Most of the field costs are incurred by the salary of personnel and transportation. A set of reliable field samplers is definitely urgently needed to obtain reliable samples.

### IV. ROADWAY MODELS

At the special request of Mr. Al Hinai, a series of experimental runs was made regarding the characteristics of sand movements over selected types of roadways.

As the wind carries sand over the roadway, the sand drift may create hazardous conditions for the traffic on the roadway. The main purpose of this series of preliminary tests was to investigate the characteristics of sand movements over selected types of roadways.

#### A. Roadway Models Tested and Sequence of Testing

Figure 13 shows the different roadway models and their respective priorities for testing. This figure was provided by Mr. Al Hinai. The prototype heights of roadways for these models are 1 meter (for the existing roadway), 5 meters, 6 meters, and 8 meters; the angles of approach are  $32^\circ$ ,  $26.57^\circ$ ,  $18.43^\circ$ ,  $14.04^\circ$ , and  $9.46^\circ$ . Although at this stage it is not possible

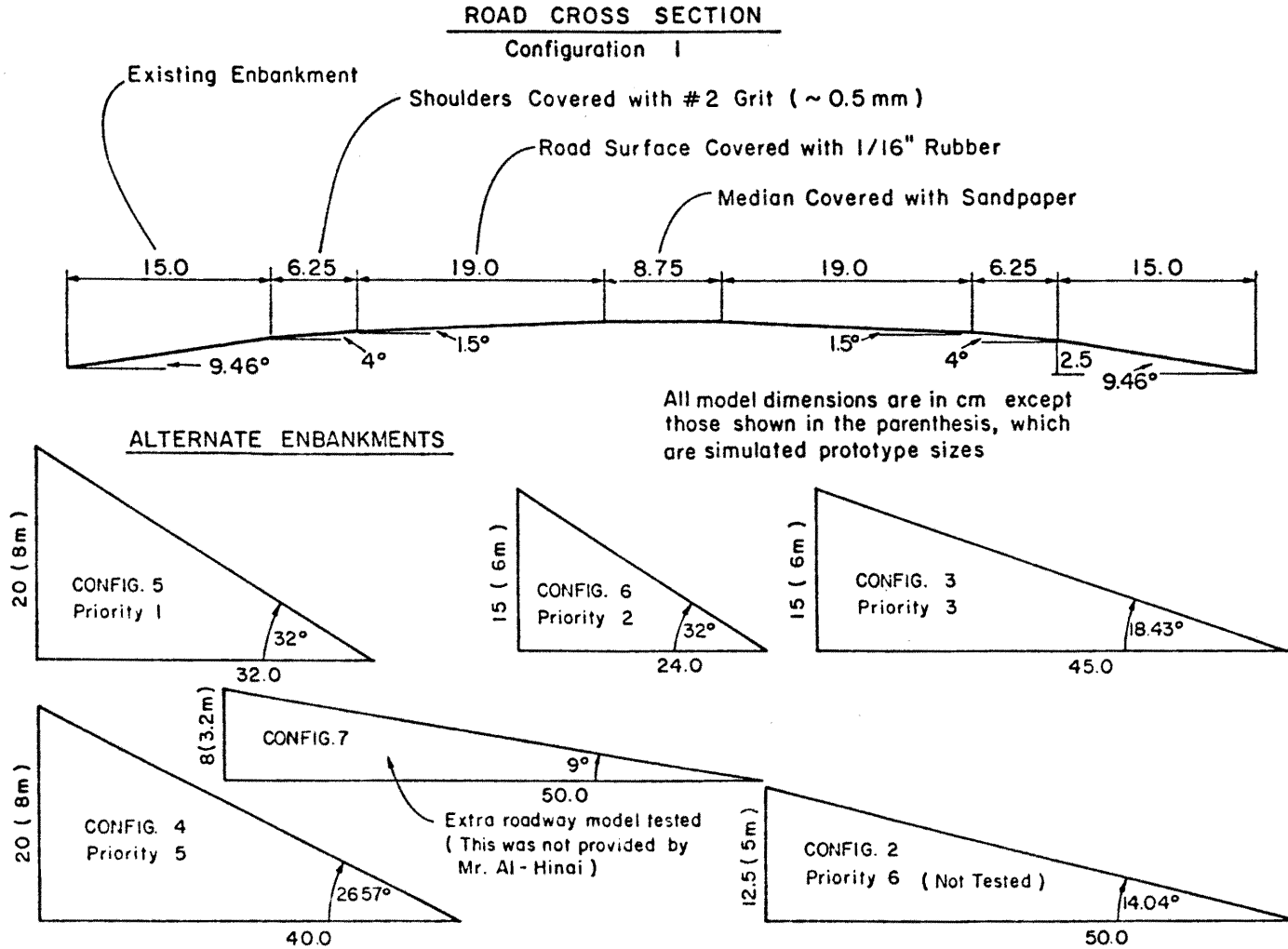


Figure 13. Roadway Cross Sections and Alternater Embankments for Wind-Tunnel Testing (all model dimensions are in cm)

to determine a correct model scale ratio without proper measurements from the field, a "possible" model-prototype scale ratio of 1 to 40 is assumed. Thus, the heights of the models are 2.5 cm, 12.5 cm, 15 cm, and 20 cm. The "possible" model-prototype scale ratio will be discussed in the future research needs, Section VIII. It is noticed that Configuration 2 is rather close to Configuration 3; since Configuration 2 has the lowest priority, it was thus abandoned. Instead, a new extra roadway model was created (Configuration 7). This model has a height of 8 cm (about half way between the existing roadway model with a height of 2.5 cm and the next higher model with a height of 15 cm) and an approach angle of  $9.1^\circ$ . This particular angle is selected because it is rather close to the average upslope angle of natural sand dunes.

We adopted a rational approach for the sequence of testing rather than the assigned model priorities. Since the average upslope angle of natural sand dunes is between 9 and 10 degrees, there is reason to believe that sand may be able to migrate (without any deposition) over the roadway, having an approach angle within the range of 9 to 10 degrees. Thus, Configurations 1 and 7 were tested first. Configurations 5 and 4 were tested next because these are the tallest roadway models, having a height of 20 centimeters. Configuration 3 and 6 were tested last because they have a medium height. The free stream wind tunnel speed was kept at 12 meters per second which is approximately the greatest convenience speed in our wind tunnel for this type of sand. The sand size distribution is shown in Figure 7. The sand particles are rather uniform with a medium size of 0.115 mm and are easy to operate. For the last model, Configuration 6, two different speeds of 9 and 7 meters per second were used to investigate the effect of wind speeds on sand accumulations.

## B. Testing Results

Table 7 provides a brief summary of the testing program. Column 1 gives the model roadway configuration numbers. One should refer to Figure 1 for the sketches of all configurations. Columns 2 and 3 give, respectively, the angle of approach to each roadway and the height of the roadway. Column 4 states the wind tunnel speeds; Column 5 presents the sand accumulation taken for the stated hours and minutes since initiation of each experimental run. The last Column 6 gives the average rate of sand deposit in the first x cm upstream from the model. The values of x in centimeters are given in parentheses for all the runs.

The sand accumulations at different times for each roadway model are shown in Figures 14a, 14b, 14c, 14d, 14e, 14f, and 14g respectively for model Configurations 1, 7, 5, 4, 3 and 6. Figures 14a and 14b clearly indicate that sand deposition occurred continuously at the upslope face of the roadways with an approach angle of approximately 9 degrees until the level of sand deposition nearly reached the top of the roadway. Once this level of deposition was achieved, sand particles migrated over the roadway without significant deposition on the roadway. Although this is not part of the stated testing program, it is believed that sand deposition can occur on the roadway if sufficient roughness elements are present. As indicated in Column 6 of Table 7, the rate of sediment deposition upstream from the roadway decreased only slightly with time. If one assumes that the sediment supply rate from upstream was constant, the amount of sand drifting over the roadway increased only slightly as sand particles were continuously being deposited upstream from the roadway. This nearly constant sand drift rate over the roadway is a desirable feature for the roadway traffic.

The next series of tests was conducted for Configurations 5 and 4, having the tallest roadway heights of 20 cm. Again, sand particles were

Table 7. Roadway Models Tested

| (1)<br>Roadway Model<br>Configuration | (2)<br>Approached<br>Embankment<br>Angle ° | (3)<br>Model<br>Embankment<br>height (cm) | (4)<br>Tunnel Wind<br>Speed | (5)<br>Sand Accumulation<br>Taken in Hours +<br>Minutes | (6)<br>Deposits/Hour During Time<br>Intervals for the First<br>(x cm) Upstream from the<br>Model |
|---------------------------------------|--|---|-----------------------------|---|--|
| 1 (existing<br>roadway)               | 9.46°                                      | 2.5                                       | 12                          | 1 + 00<br>2 + 00<br>3 + 40                              | 227.0<br>173<br>44<br>(x = 280 cm)   |
|                                       |  |   | 8                           | 1 + 40  | 43.7<br>(x = 200 cm)   |
| 7                                     | 9.1 °                                      | 8   | 12                          | 1 + 30<br>3 + 20<br>4 + 53<br>6 + 23                    | 383.3<br>383.6<br>348.7<br>327.6<br>(x = 280 cm)   |
| 5                                     | 32 °                                       | 20  | 12                          | 1 + 43<br>4 + 01<br>7 + 15<br>9 + 40<br>10 + 25         | 247.1<br>342.1<br>300.7<br>271.0<br>251.9<br>(x = 280 cm)  |
| 4                                     | 26.57°                                     | 20  | 12                          | 1 + 54<br>3 + 54<br>5 + 40<br>9 + 19                    | 298.4<br>425.9<br>293.0<br>286.0<br>(x = 280 cm)   |
| 3                                     | 18.43°                                     | 15  | 12                          | 2 + 00<br>4 + 45<br>9 + 02                              | 237.5<br>256.4<br>249.4<br>(x = 280 cm)  |

Table 7 (continued).

| (1)<br>Roadway Model<br>Configuration | (2)<br>Approached<br>Embankment<br>Angle ° | (3)<br>Model<br>Embankment<br>height (cm) | (4)<br>Tunnel Wind<br>Speed | (5)<br>Sand Accumulation<br>Taken in Hours +<br>Minutes | (6)<br>Deposits/Hour During Time<br>Intervals for the First<br>(x cm) Upstream from the<br>Model |
|---------------------------------------|--|---|-----------------------------|---|--|
| 6                                     | 32 °                                       | 15  | 9.14                        | 1 + 29<br>2 + 55<br>4 + 55                              | 139.9<br>112.7<br>65.5<br>(x = 190 cm)   |
| 6                                     | 32 °                                       | 15  | 7                           | 5 + 28<br>6 + 45  | 32.9<br>58.9<br>(x = 180 cm)   |

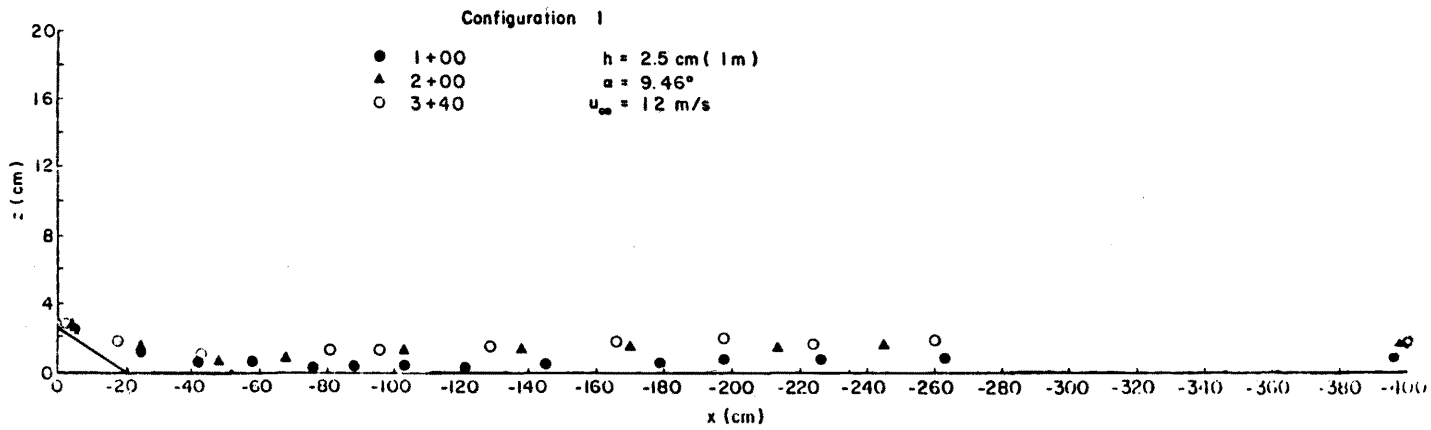


Figure 14a. Sand Accumulation for Configuration 1 (existing roadway)

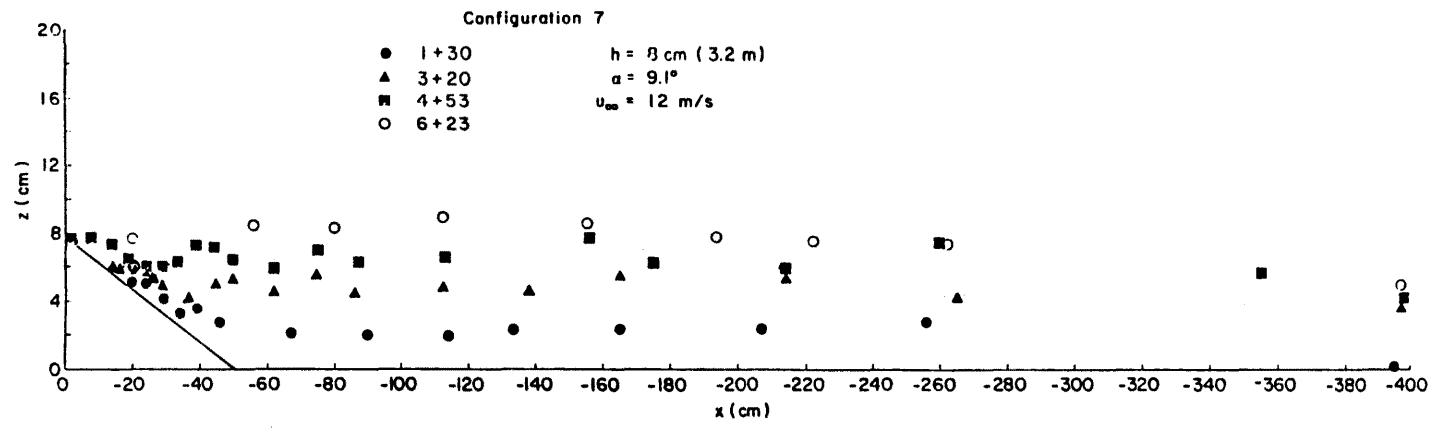


Figure 14b. Sand Accumulation for Configuration 7 (added)

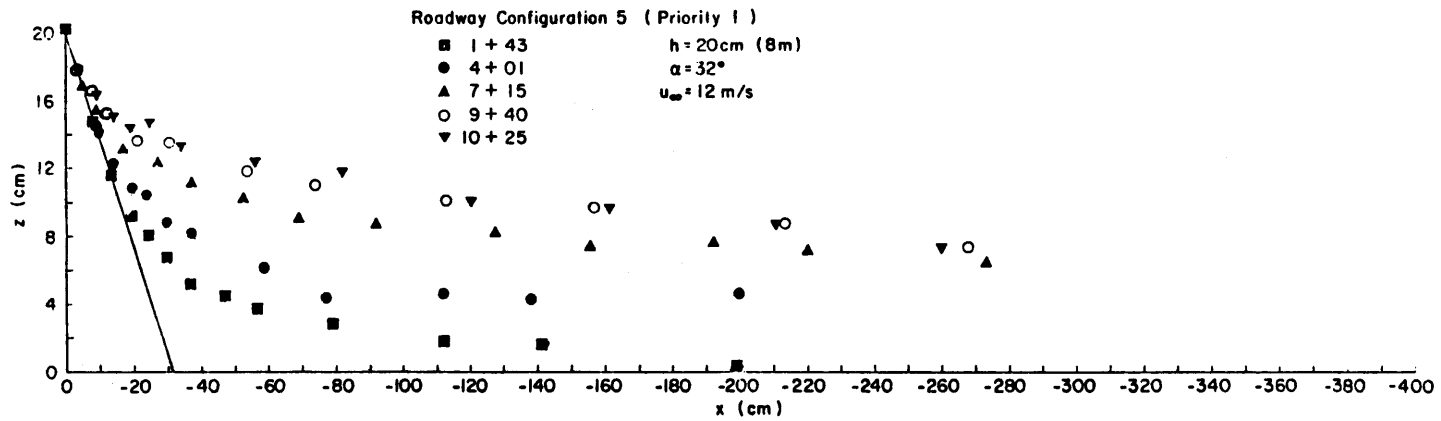


Figure 14c. Sand Accumulation for Configuration 5 (priority 1)

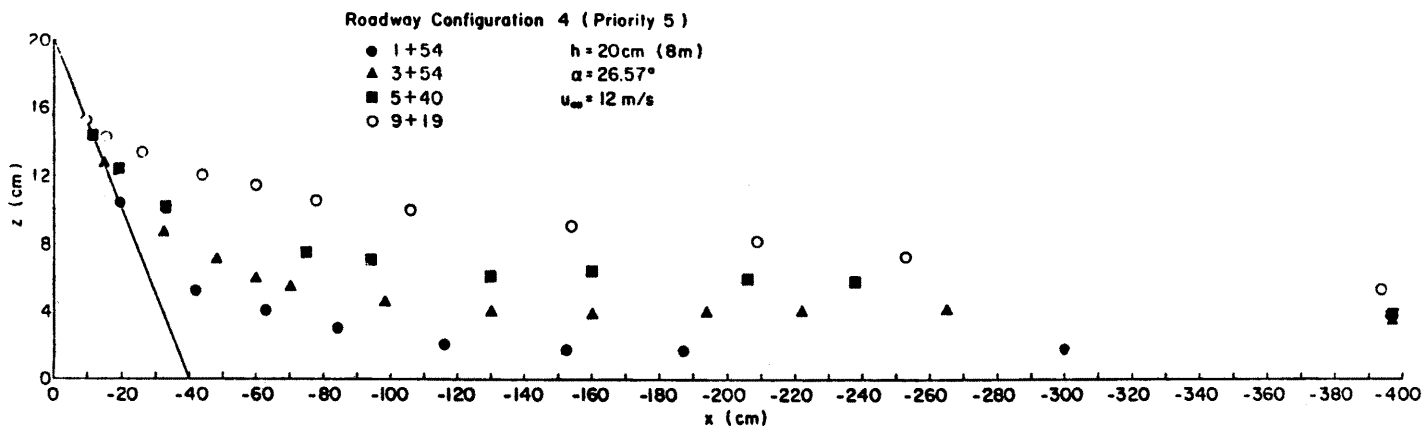


Figure 14d. Sand Accumulation for Configuration 4 (priority 5)

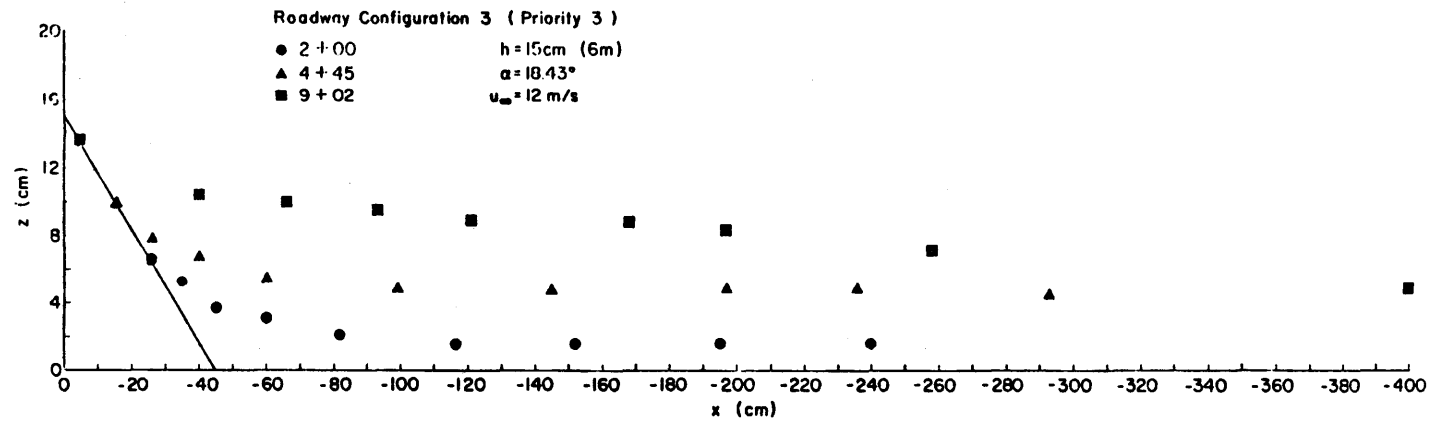


Figure 14e. Sand Accumulation for Configuration 3 (priority 3)

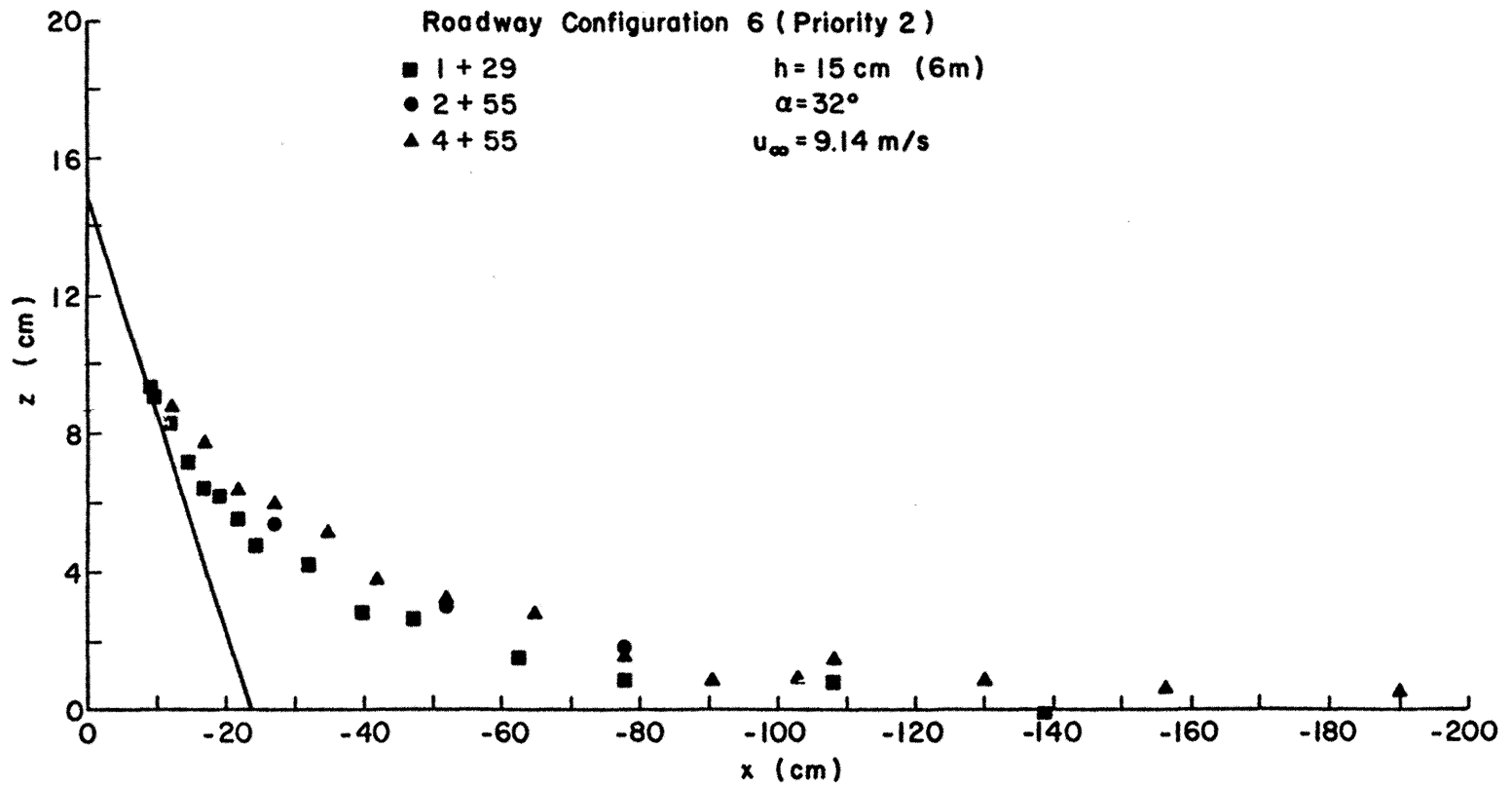


Figure 14f. Sand Accumulation for Configuration 6 (priority 2),  
Wind Speed 9.1 meters per second

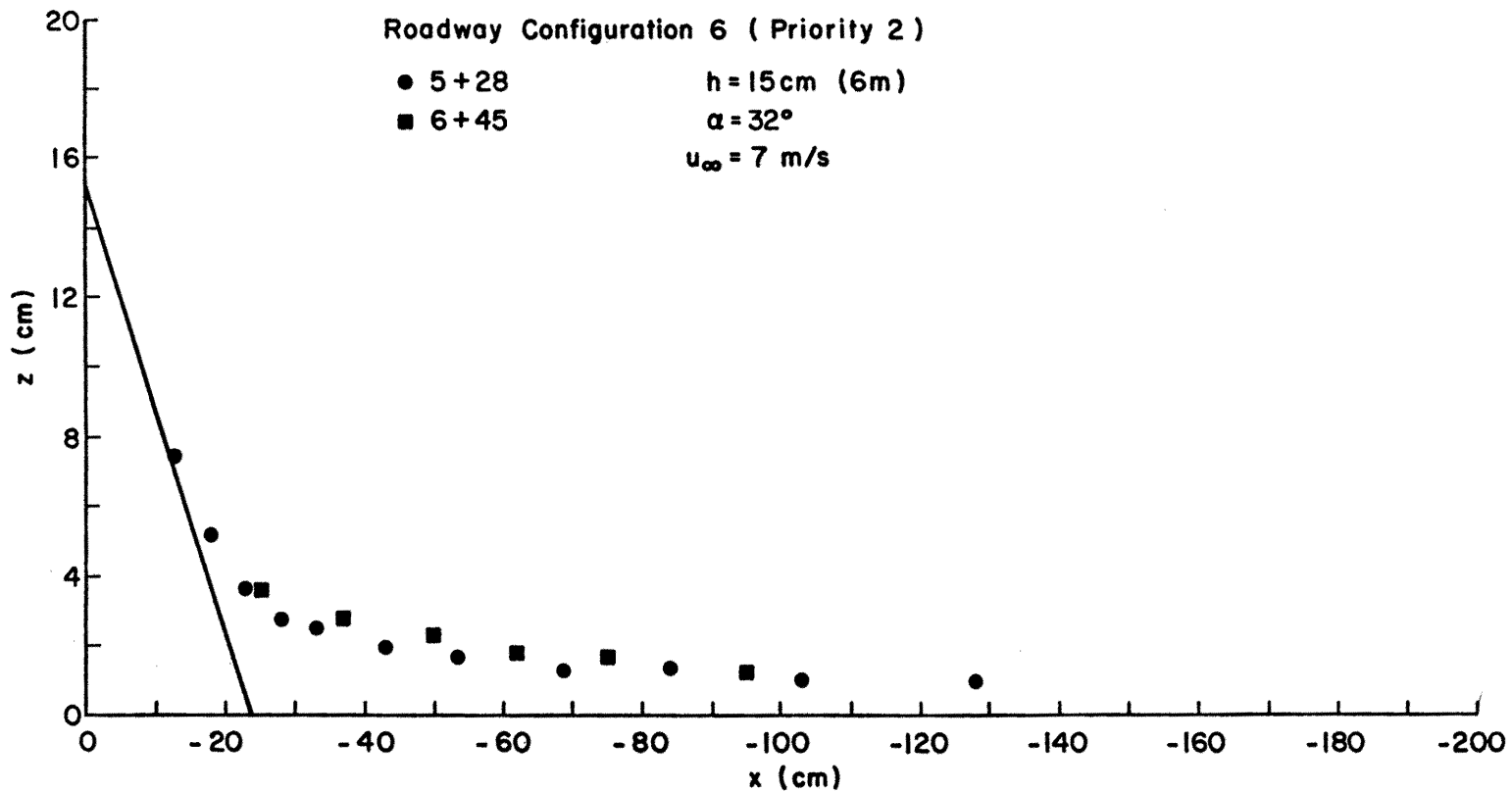


Figure 14g. Sand Accumulation for Configuration 6 (priority 2),  
Wind Speed 7 meters per second

continuously deposited by the flow at the upstream slope of the roadway. As shown in Column 6 of Table 7, the rate of deposition first increased, and then decreased to the initial value as deposition continuously occurred. It is difficult to evaluate the significance of this phenomenon, which may even result from measurement errors. Once the upslope angle of the sand deposition fell below three degrees, the experiment was stopped because it is quite clear that the sand would be continuously deposited at the upstream end of the roadway until the entire sand deposition reached the roadway, as experienced during the first series of tests with Configurations 3 and 4.

The last series of tests was conducted for Configurations 3 and 6, having roadway heights of 16 cm. The only difference between these two models is the approach angle. As with the other models, the sand particles were again deposited upslope from the roadway (see Figure 14e). This experiment was stopped after the upstream sand deposition angle fell below five degrees. After the testing of all these models, it became rather apparent that unless some other factors enter in, the sand particles will be continuously deposited at the upslope of the roadway until the level of sand deposition nearly reaches the top of the roadway.

It was then decided to test Configuration 6 for different wind speeds of 9 and 7 meters per second. The sand accumulation for these two speeds are shown respectively in Figures 14f and 14g. Both experiments were stopped for the following two reasons: i) the variations of the slope of the upslope sand depositions were quite similar to other models previously tested; thus, it appeared that the sand deposit would again reach the top of the roadway. ii) time was running out. As agreed by Mr. Al Hinai and Dr. J. E. Cermak, the Colorado State University research team would conduct special preliminary tests of sand migration over a roadway for a total period of 7 days, but the actual testing period was longer than anticipated. Each model was tested for

approximately 9 to 10 hours, with frequent stops for data measurements; therefore, the total testing period lasted 18 days.

Figures 15a and 15b are photographs of roadway model Configuration 5 at the end of the experimental runs. Figure 15c is a photograph of the sand drift over roadway model Configuration 3. The direction of flow was from right to left. This photograph clearly shows the heavy concentration of sand particles migrating over the roadway. Several movies were taken for different experiments. Once processed, these movies will be sent to Saudi Arabia.

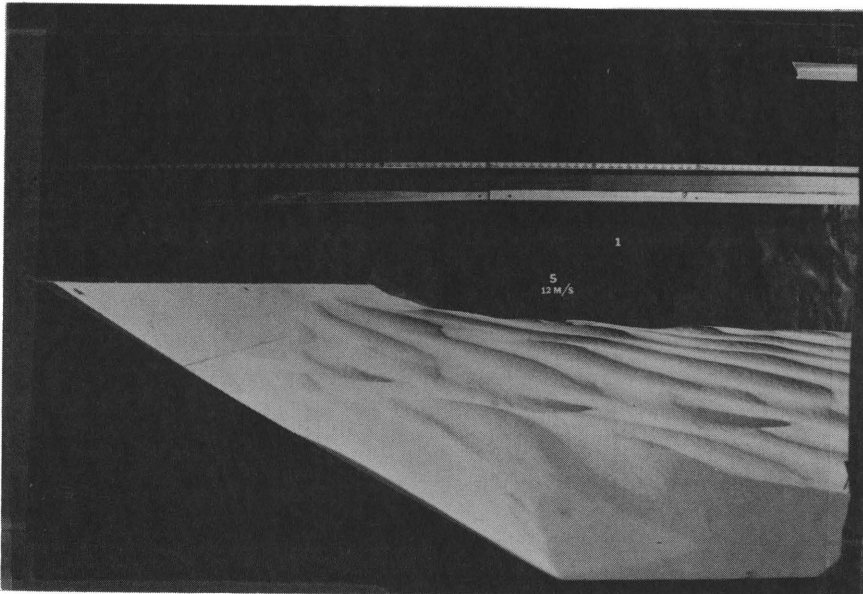


Figure 15a. Side View of Sand Deposition at the Upstream Slope of Roadway Model Configuration No. 5 (after 10 hours and 25 minutes of running time with a wind speed of 12 meters per second)

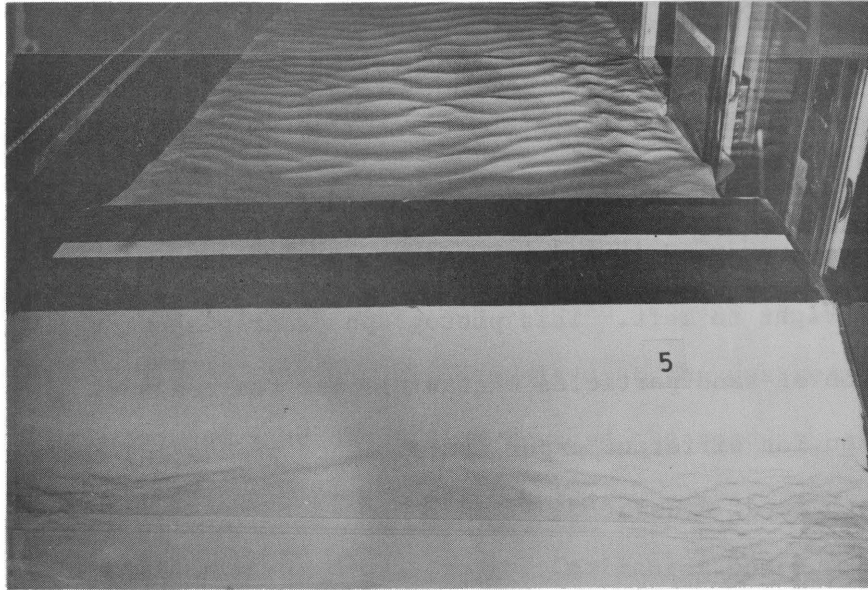


Figure 15b. Upstream View of Sand Deposition near the Roadway Configuration No. 5 (after 10 hours and 25 minutes of running time with a wind speed of 12 meters per second)

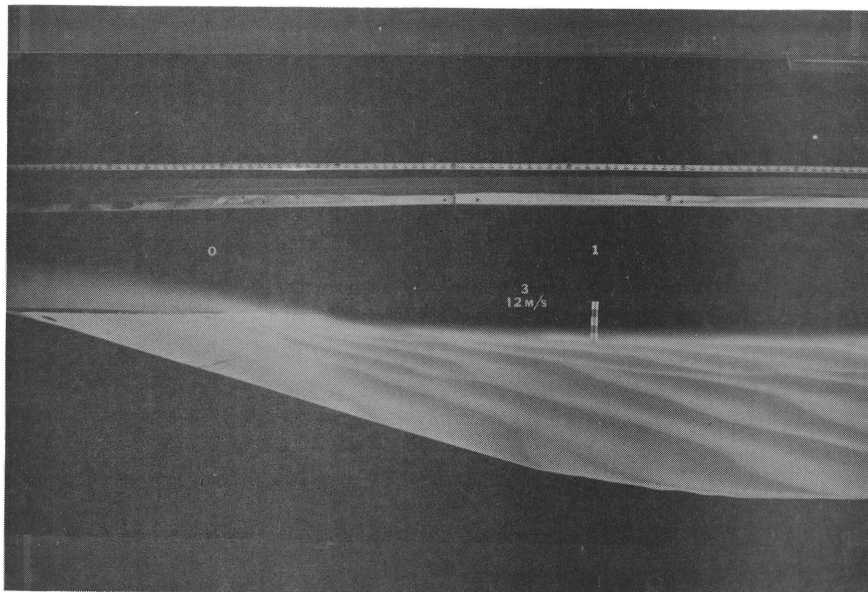


Figure 15c. Side View Showing the Migration of Sand Particles over Roadway Model Configuration No. 3 (with a wind speed of 12 meters per second)

It can be generally concluded from this series of testing that sediment particles will be continuously deposited upstream from all model roadways until the tops of the sand deposition reach the top of the roadway. The upslope approach angle of the roadway model varied between 9.1 degrees and 32 degrees; the heights of the approach to the roadway model varied between 2.5 centimeters and 20 centimeters.

### C. Summary and Conclusions

From the laboratory tests of six roadway models (with a range of approach roadway angles between 9.1 degrees and 32 degrees and heights between 2.5 cm and 20 cm), it is concluded that:

- 1) Under constant wind speeds, the sand particles would continuously be deposited at the upslope of the roadway models until the sand deposition level reached the top of the roadway, if a sufficient amount of sand particles is available from upstream.
- 2) No proven prototype-model scale is available at present, and this should be investigated based on all available information. However, if the thickness of the sand layer can be used as a governing factor, the laboratory model results can be applied to field conditions. More field data for the vertical distribution of sand particles should also be collected.
- 3) If a great deal of roadway construction is anticipated, a much more comprehensive series of laboratory tests should be conducted to investigate the wind velocity distribution and vertical sand distribution over the roadway for different shapes of roadways to determine an optimum roadway shape so that extremely high wind and sand drifts would not occur near the traffic level.

## V. SINGLE ROW OF SAND FENCES

### A. Introduction

The purpose of this section is to describe the results of wind-tunnel tests on sand accumulation by a single row of fences in our meteorological tunnel.

In accordance with the agreement between Mr. Al Hinai and Dr. J. E. Cermak, the following fence shapes were tested: i) horizontal slats, ii) vertical slats, iii) special vertical spires, and iv) solid fence. Within a total of 25 days of testing, we have investigated the effects i) of fence shape, ii) of fence porosity, iii) of opening distribution, iv) of scour at the bottom of fences, and v) of absolute sizes of the slats.

Another series of tests was conducted to investigate the behavior of horizontal sand traps, provided by the client.

Appendix A describes the instrumentation used for the collection of data.

### B. Review of Literature and Analysis

#### 1). Flow Fields Around the Fence

Figure 16 shows the different flow zones in the neighborhood of a fence.

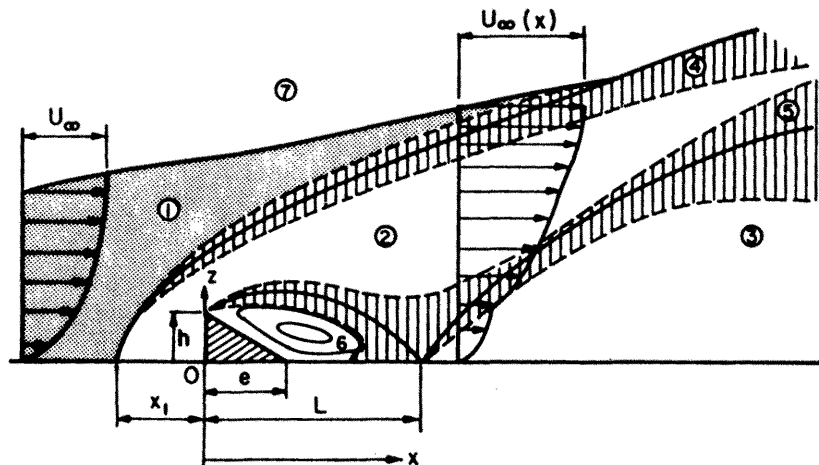


Figure 16. The Flow Zones of a Boundary Layer Disturbed by Fence (Fence is set at the origin with a vertical height of  $h$ --after Plate (1971))

Seven different regions can be distinguished:

1. Region of undisturbed boundary layer.

The flow is mostly determined by conditions in the undisturbed boundary layer far upstream from the wedge.

2. Region of hill influence.

The flow is displaced and distorted due to the presence of the wedge.

3. Region of reestablishing boundary layer.

This region is characterized by a highly retarded flow.

4. Blending regions between region 1 and region 2.

5. Blending region between inner and middle layers (region 3 and region 2).

Wind gradually increases in velocity. A new and thicker boundary layer is formed which adjusts to the local boundary conditions at the ground until the effect of the obstruction can only be inferred by comparing the boundary layer thickness with that which would have existed if the wedge had not been there.

6. Standing eddy zone.

When the wedge is solid, back flow may occur, leading to a separation bubble with a reattachment point at a distance  $L$  downstream from the wedge.

7. Region of potential outer flow.

The flow fields in the sheltered region behind a solid fence:

A detailed study of this flow has been made in a wind tunnel by Chang (1966) at Colorado State University. The upper parts of some of the mean velocity profile obtained in this case are shown in Figure 17a (where  $U_{\infty}$  is the potential flow velocity;  $U$  is the mean flow velocity as a function of vertical distance  $z$ ;  $u'$ ,  $v'$ , and  $w'$  are the fluctuating

flow velocities in  $x$ ,  $y$ , and  $z$  directions, respectively;  $p$  is the pressure and  $p_\infty$  is the pressure above the boundary layer).

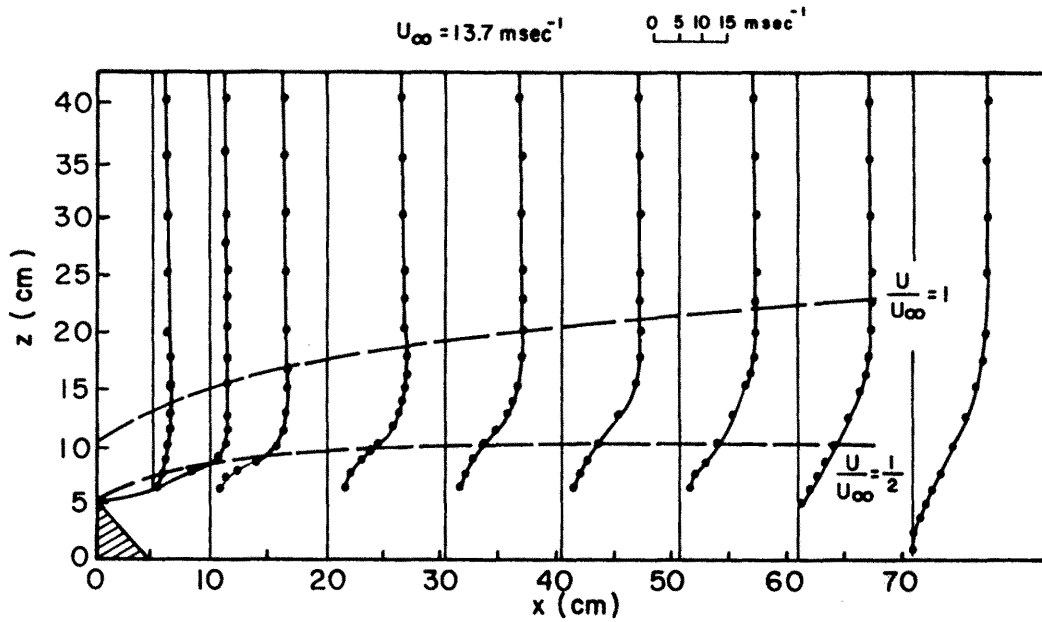


Figure 17a. Mean Flow Velocity Profile after Chang (1966)

Figure 17b shows the turbulence characteristics of the same flow.

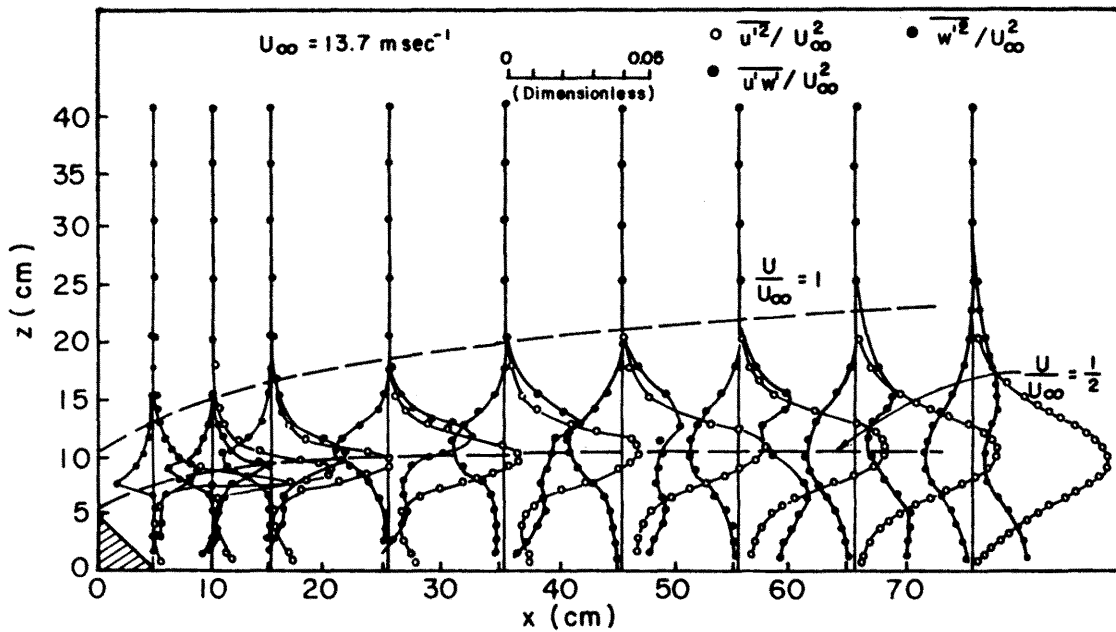


Figure 17b. Turbulence Characteristics after Chang (1966)

As shown in Figure 17c, significant change of turbulent velocity characteristics occurred across the curve at which  $\frac{U}{U_\infty} = 1/2$ . Figure 17c presents the large pressure gradients which exist in the lee of a solid fence.

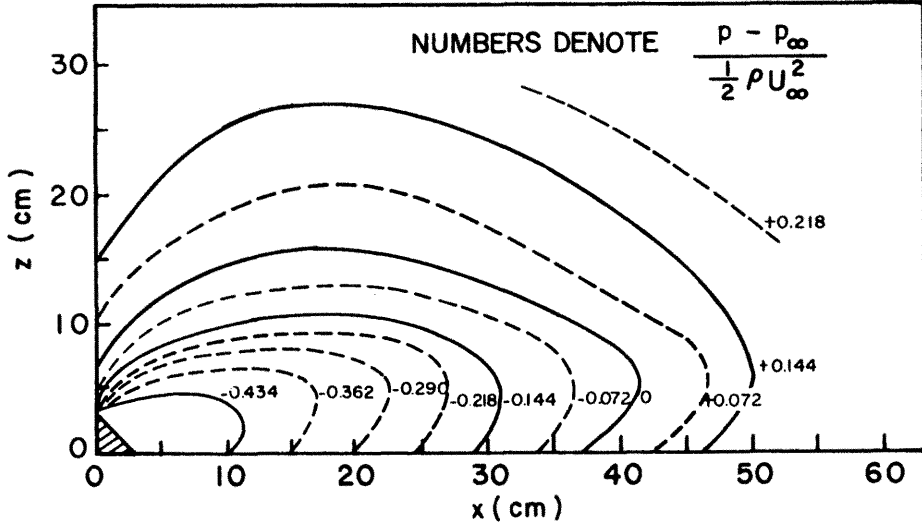


Figure 17c. Pressure Distribution Behind Solid Fence after Chang (1966).

If one assumes that the shear stress is a function of  $\rho$ , the fluid density;  $\epsilon$  the eddy viscosity; and  $\partial U/\partial z$  then:

$$\tau = \rho \epsilon \frac{\partial U}{\partial z} \quad (4)$$

and

$$\epsilon = \frac{1}{4\sigma^2} U_\infty^2 \quad (5)$$

where  $\sigma^2$  is an empirical constant (see Schlichting, 1968).

The resulting velocity distribution can be expressed as

$$U = \frac{U_\infty}{2} (1 + \operatorname{erf} \xi) \quad (6)$$

where the error function

$$\text{erf} = \frac{2}{\sqrt{\pi}} \int_0^{\xi} e^{-m^2} dm \quad (7)$$

Chang (1966) experimentally found the validity of Equation (6) for a solid fence, as shown in Figure 18.

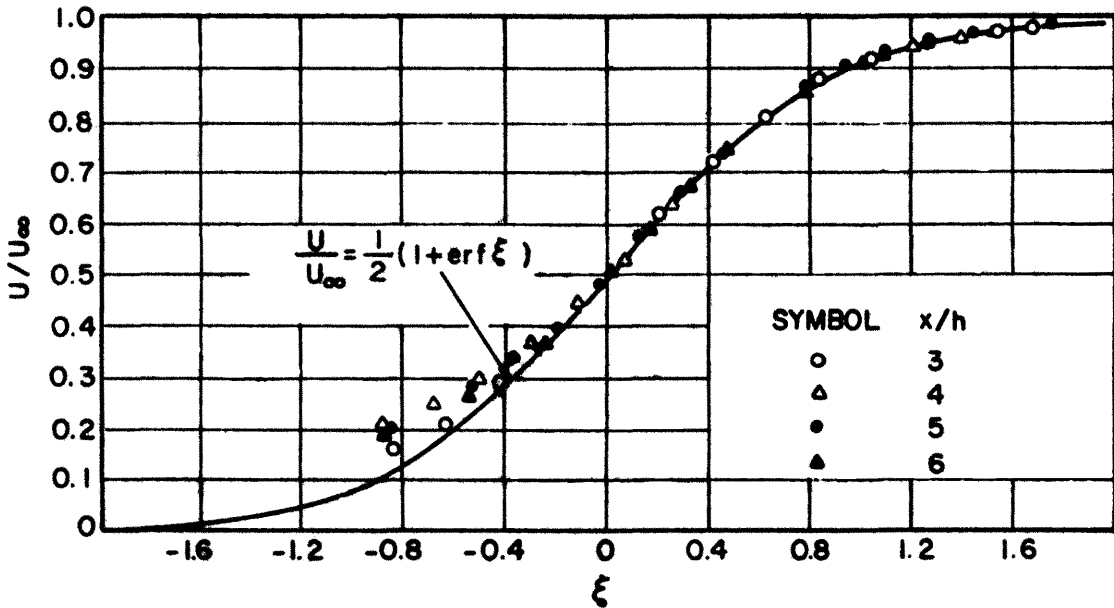


Figure 18. Experimental Verification of Equation (6) after Chang (1966)

Chang also found the value of  $\sigma$  had a mean value of 14.5 as shown in

Figure 19.

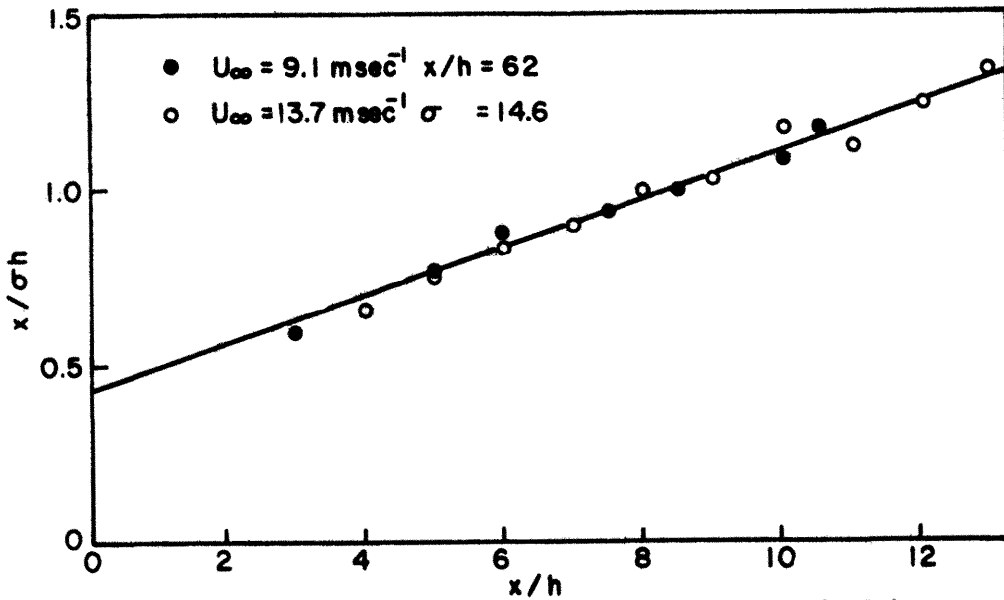


Figure 19. The Determination of  $\sigma$  after Plate (1971)

The flow fields behind a porous fence:

Following the approach to flow around a solid fence, one may introduce a flow field with  $U_b$  as the velocities through the porous fences at various locations. It is further assumed that  $U_b$  can be superimposed on the velocity distribution behind a solid fence. Of course, this assumption is not strictly precise and must be corrected by experimental evidence. First, Equation (5) must be modified to

$$\varepsilon = \frac{1}{4\sigma} (U_\infty + U_b) \quad (8)$$

and Equation (6) must be modified to

$$U = \frac{U_\infty + U_b}{2} \left[ 1 + \left( \frac{U_\infty - U_b}{U_\infty + U_b} \right) \operatorname{erf} \xi \right] \quad (9)$$

The flow fields in Figure 16 may be changed into a simplified model as shown in Figure 20.

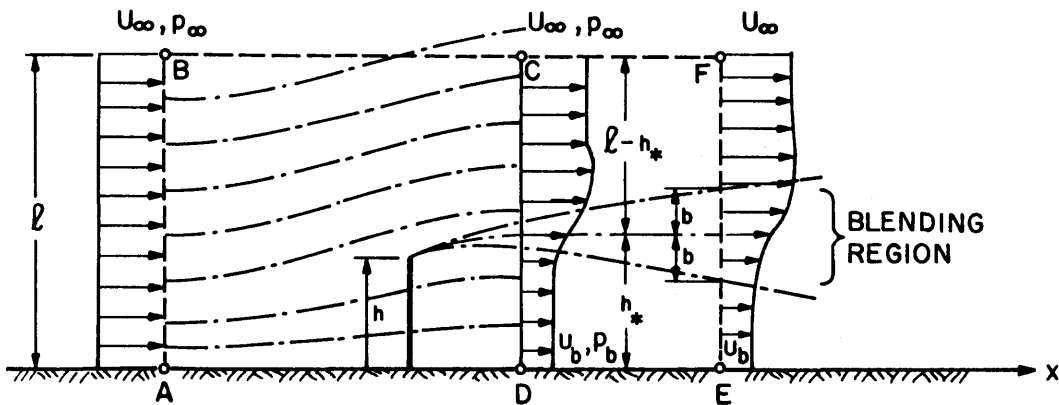


Figure 20. Flow Fields around Porous Fence with a Height of  $h$ --after Plate (1971)

In Figure 20, the effect of the lower boundary layer is neglected, and the ground elevation is assumed to be a streamline. The streamline displacements due to the obstruction of the porous fence may be obtained by the application of the conservation of both mass and momentum.

Figures 21a and 21b give the actual velocity distribution for two porous fences with porosities  $\beta = 0.182$  and  $0.425$ , respectively.

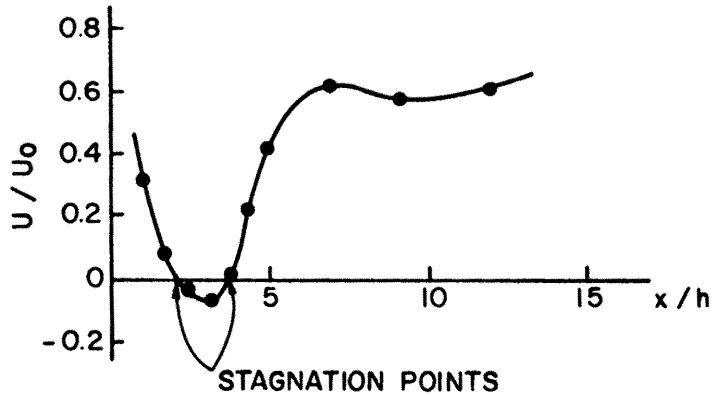


Figure 21a. Velocity Distribution across a Fence of Porosity  $\beta = 0.182$ , after I. P. Castro (1971)

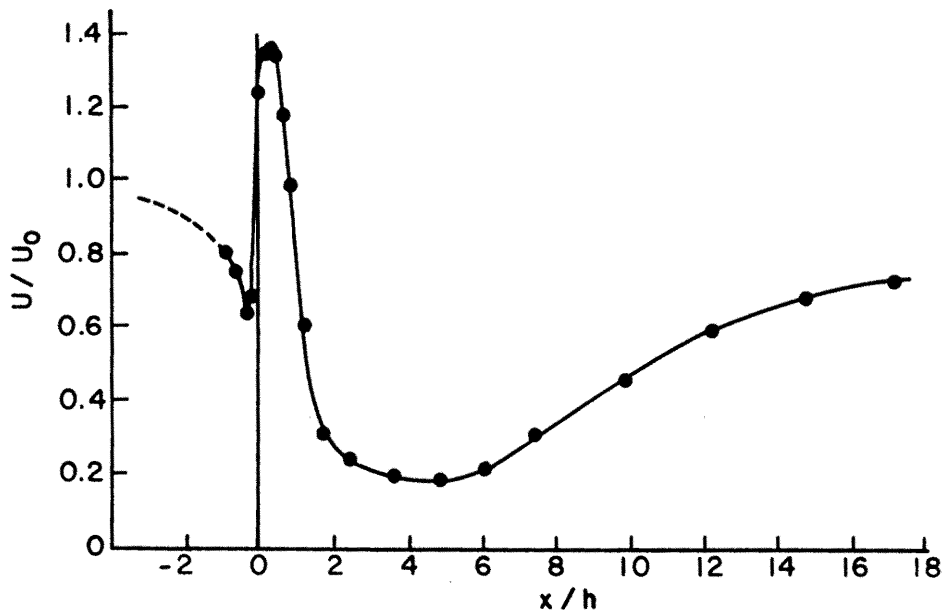


Figure 21b. Velocity Distribution across a Fence of Porosity  $\beta = 0.425$ , after I. P. Castro (1971)

In Figure 20, the effect of the lower boundary layer is neglected, and the ground elevation is assumed to be a streamline. The streamline displacements due to the obstruction of the porous fence may be obtained by the application of the conservation of both mass and momentum.

Figures 21a and 21b give the actual velocity distribution for two porous fences with porosities  $\beta = 0.182$  and  $0.425$ , respectively.

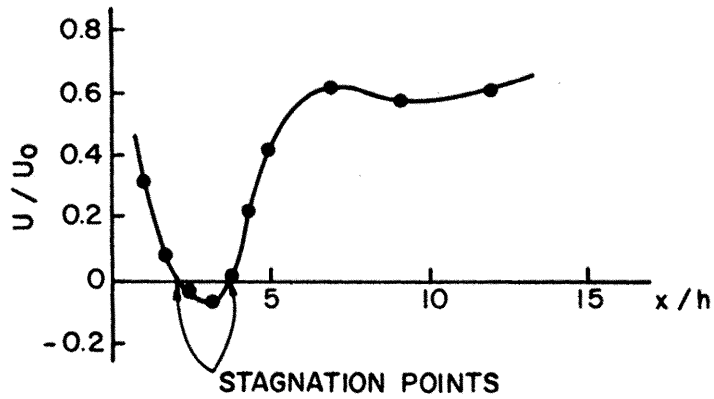


Figure 21a. Velocity Distribution across a Fence of Porosity  $\beta = 0.182$ , after I. P. Castro (1971)

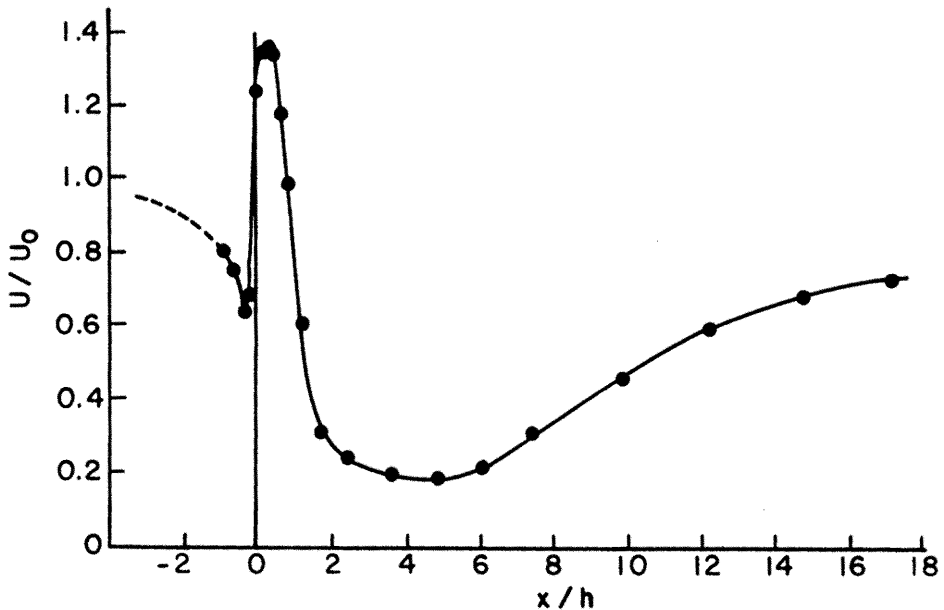


Figure 21b. Velocity Distribution across a Fence of Porosity  $\beta = 0.425$ , after I. P. Castro (1971)

The turbulence characteristics of flow behind these two porous fences are shown in the following Figures 22a and 22b.

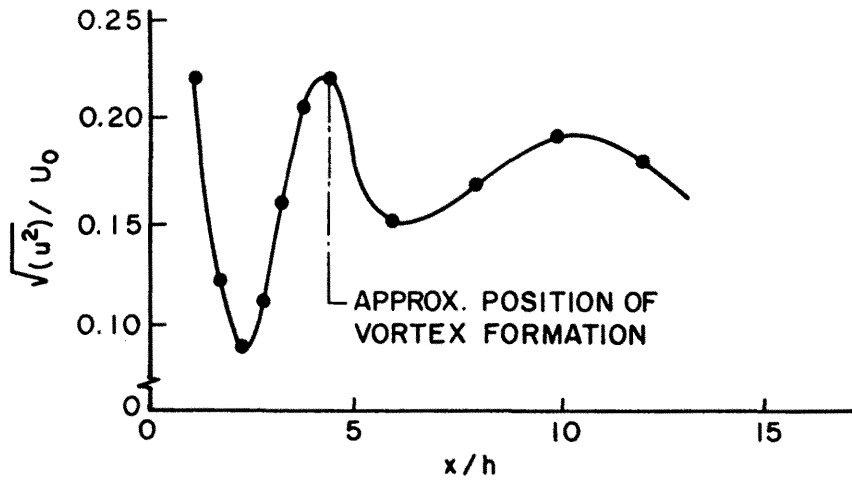


Figure 22a. Turbulence Downstream from a Fence of Porosity  $\beta = 0.182$ , after I. P. Castro (1971)

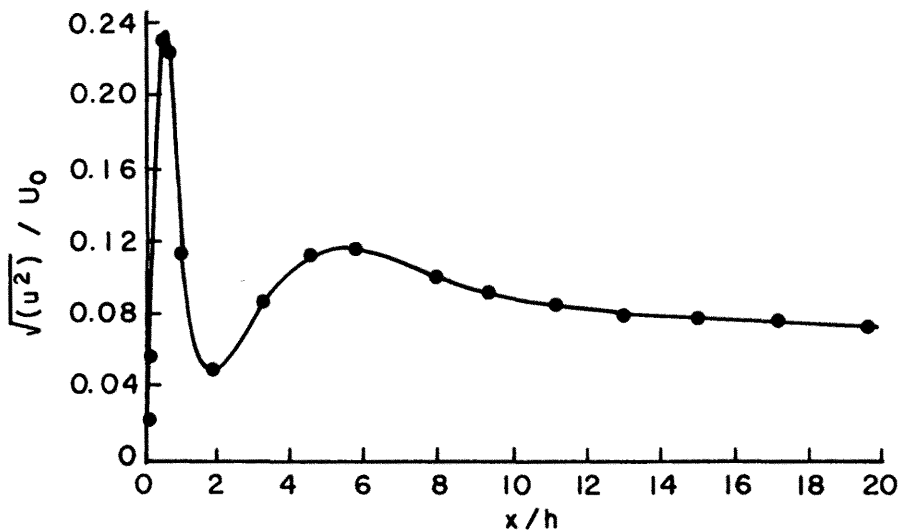


Figure 22b. Turbulence Downstream from a Fence of Porosity  $\beta = 0.425$ , after I. P. Castro (1971)

Kind (1976) and Iversen (1980) have selected the four basic similarity parameters for the modeling of flow around fences. Those four parameters are:

$$\frac{z}{z_0} \quad \text{Geometric scaling parameter,}$$

$$\frac{\sqrt{U'^2}}{U_0}$$

Similarity of profile of turbulent intensity,

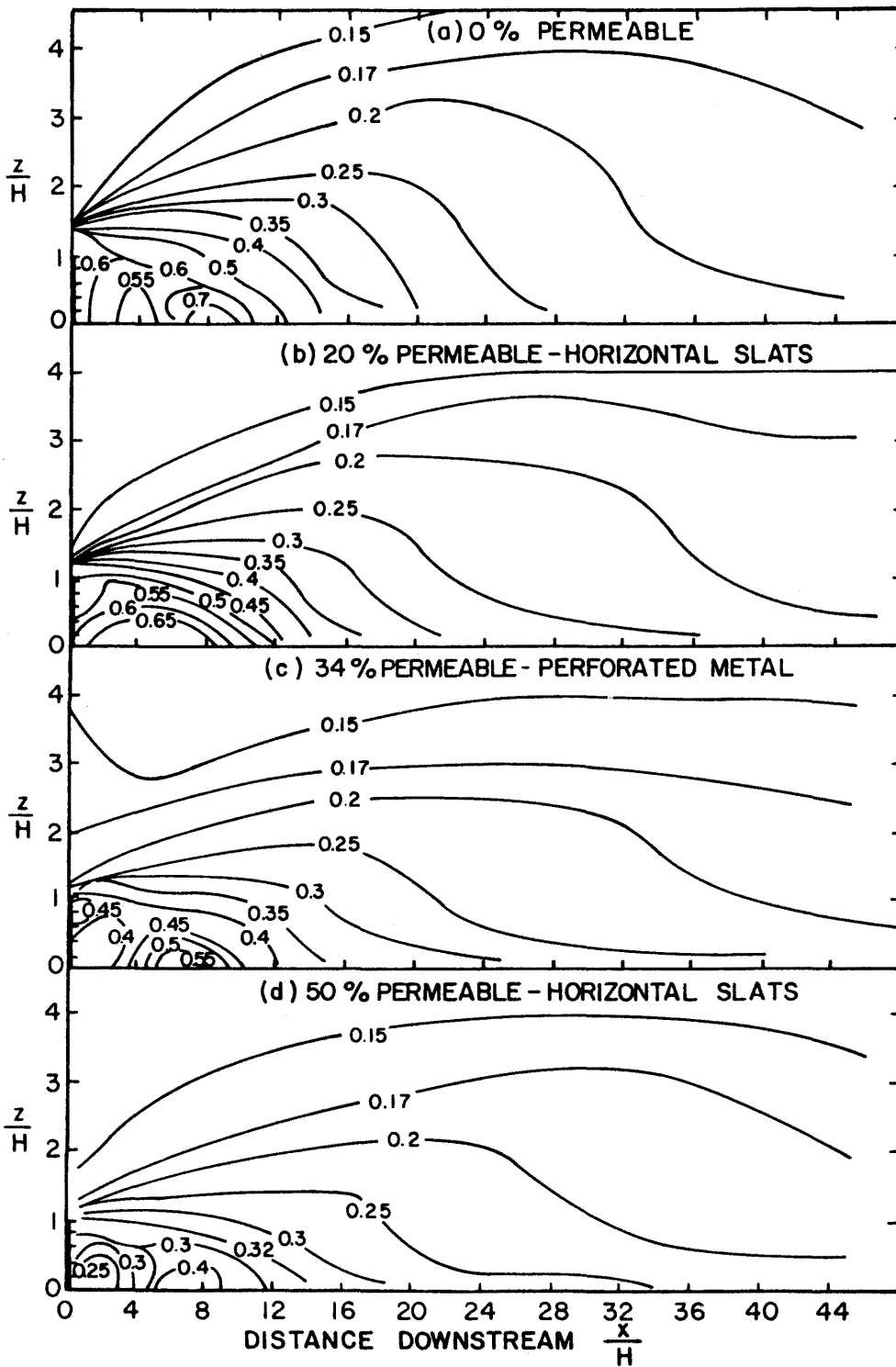
$$\frac{Lu_{x_0}}{z_0}$$

Similarity of profile of integral scale of turbulence,

$$\frac{U z}{K_{m_0}}$$

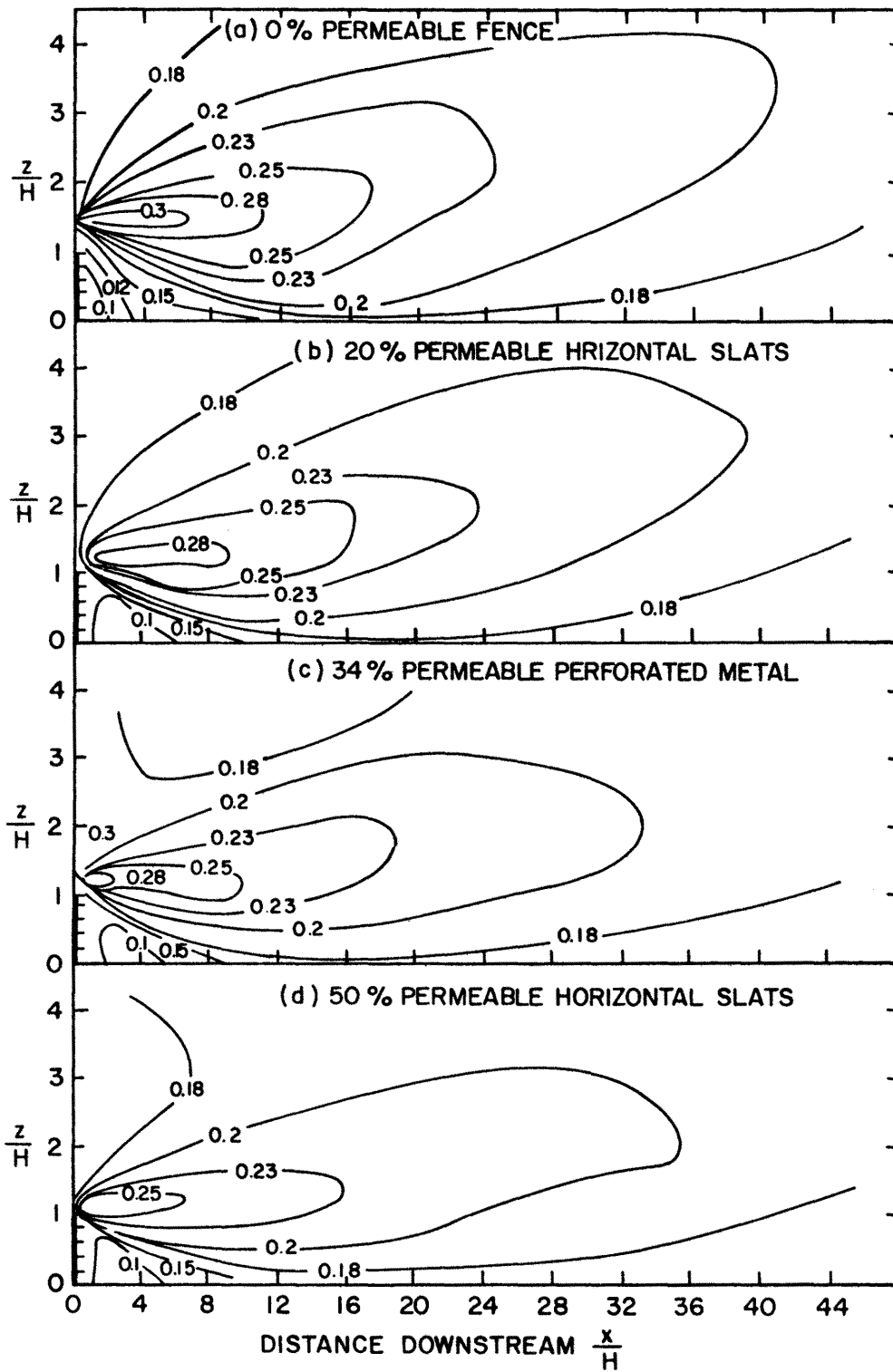
Similarity of shear-stress profile and momentum transfer processes.

Raine and Stevenson (1977) determined the flow velocity distributions for different fence porosities as shown in the following Figures 23a and 23b. Greater mean velocity reduction occurred immediately downstream from the fence with decreasing fence permeability, as expected. Scale tests also showed that a greater velocity reduction occurred with an increasing fence height. The model fence height should be chosen rather carefully.



$\bar{U}/U_0$  Isotachs Downstream of Fences of Different Permeability

Figure 23a. Isotachs Downstream from Fences of Different Permeabilities after J. K. Raine and D. C. Stevenson (1977)



$u'/\bar{U}$  Isoturbs Downstream of Fences of Different Permeability

Figure 23b. Isoturbs Downstream from Fences of Different Permeabilities after J. K. Raine and D. C. Stevenson (1977)

### C. Accumulation of Sand Particles around the Fence

Theoretically, the best type of fence has the greatest efficiency in blocking sand particle movements and thus results in greatest accumulation of sand particles near the fence.

Savage (1963) tested different types of fences in the sand beach near the Drum Inlet, North Carolina, U.S.A. Table 8 provides his results.

Table 8. Volumes of Sand Collected by Sand Fences on Core Banks from Installation to July 1961

| <u>Single-Fence Sections</u>         |                             |  |
|--------------------------------------|-----------------------------|--|
| <u>Section</u>                       | <u>Type</u>                 | <u>Cubic Yards<br/>per Foot of Beach</u> |
| A                                    | Straight brush              | 2.00                                     |
| B                                    | Straight snow               | 2.62                                     |
| C                                    | Zigzag brush                | 2.52                                     |
| D                                    | Zigzag snow                 | 2.38                                     |
| E                                    | Straight brush with spurs   | 1.89                                     |
| F                                    | Straight snow with spurs    | 1.77                                     |
| K                                    | Straight snow raised 1 ft   | 2.28                                     |
| L                                    | Straight snow raised 2 ft   | 2.22                                     |
| P                                    | Brush fence 25% porosity    | 2.97                                     |
| Q                                    | Straight snow raised 1 ft   | 2.66                                     |
| R                                    | Straight snow raised 2 ft   | --                                       |
| S                                    | Straight snow               | 2.53                                     |
| T                                    | Straight snow               | 2.54                                     |
| U                                    | Straight brush on 2-ft bank | <u>1.20</u>                              |
| Average of all single fence sections |                             | 2.28                                     |

The brush fence with 25 percent porosity had the most accumulation of sand particles. He also concluded that:

1. Single fencing which is initially 4 feet high appears to hold about 3 cubic yards of sand per lineal foot of fencing. However, during the first 7 months of this study, the average volume of sand trapped by all of the fence sections, single and double, was about 2.5 cubic yards per lineal foot of beach.

2. Brush fencing apparently traps about 5 percent more sand than comparable snow fencing. However, brush fencing installed costs approximately twice as much as snow fencing installed. Therefore, the use of brush fencing is not economically justified.

3. Straight fencing appears to trap and hold more sand than either straight fencing with side spurs or zigzag fencing.

4. The effective height of sand fencing can be increased by installing it with the bottom one foot off the ground. However, fencing installed in this manner fills slower immediately after installation than fencing set at ground level.

5. The rate of filling and final trapping capacity of fencing with a porosity of approximately 25 percent appears to be larger than that of fencing with a porosity of approximately 50 percent.

P. Brumm (1970) tested the accumulation of sand around the fences with five different widths of vertical slats (all with 50% porosity) in wind tunnels at the University of Florida. He found that the narrowest width of 1.5 inches resulted in a greater accumulation of sand than others.

C. J. Trossel (1981) and Al Ain International Airport Preliminary Design Report (1980) field studies from Saudi Arabia indicated that slats of medium porosity, between 40 to 50 percent with a bottom gap of 30 cm, appeared to accumulate the most sand.

Sketches of sand accumulation for a solid fence and 45 percent porosity fence (D.R. = 45%) are given in Figure 24.

Iversen (1981) conducted a comparison of field and model test results for the accumulation of snow around snow fences. He concluded that small model results (with a fence height of 0.0254 meter) agreed rather well with full scale field tests (with fence heights of 2.44, 3.17, and 3.78 meters).

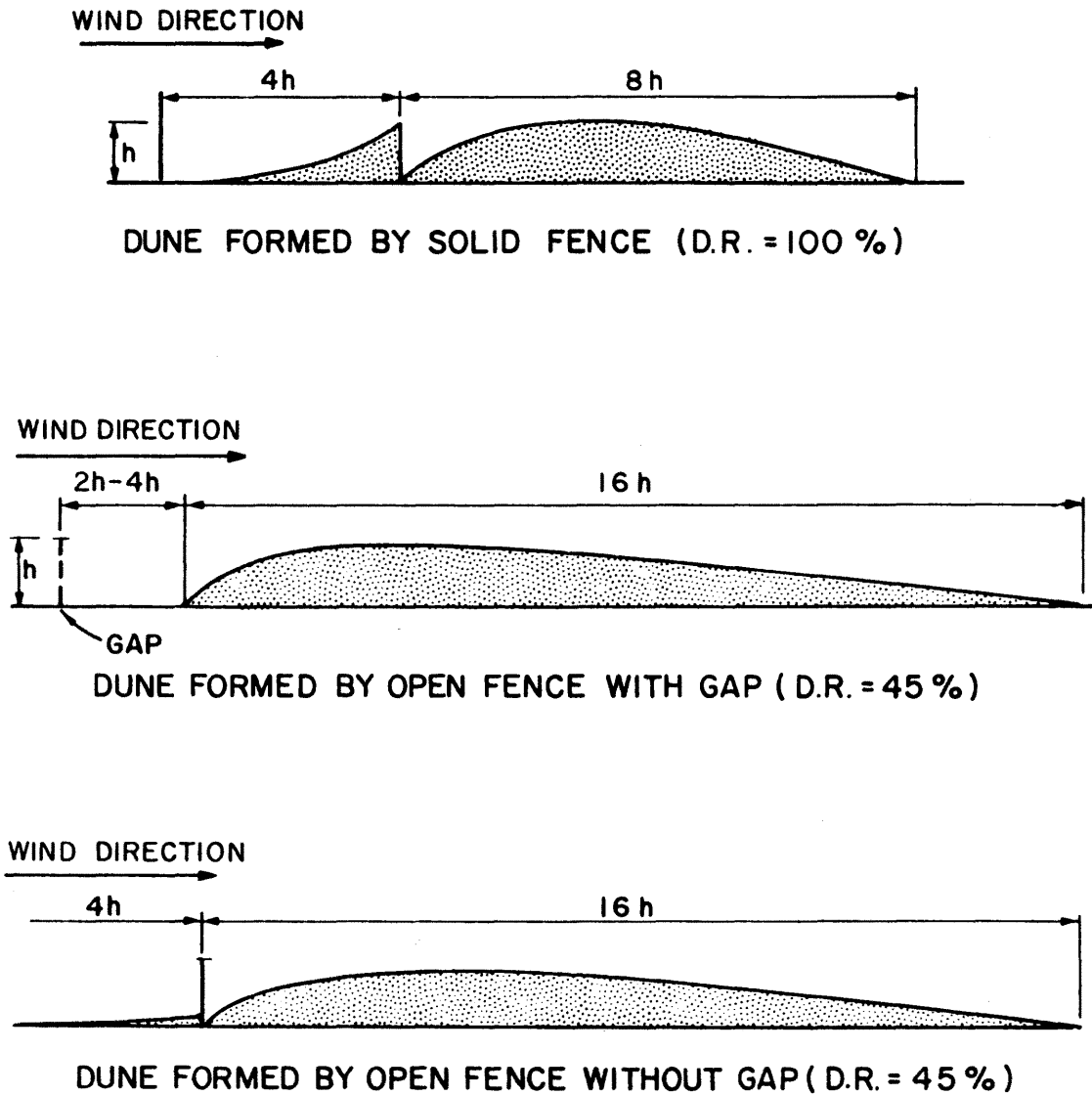


Figure 24. Different Sand Accumulations after Al Ain International Airport Preliminary Design Report (1980)

His tests also showed that fences with 0 percent and 25 percent porosity had respectively only 30 percent and 60 percent efficiencies as compared with fences with 50 percent porosity.

Tabler (1980, a, b, c, d) found that Wyoming snow fences with horizontal slats of 50 percent porosity with a bottom gap between 0.10 to 0.15 fence height were 20 percent more effective than Canadian snow fences with vertical slats of 60 percent porosity.

#### D. Testing Program

As stated previously, the main emphasis of this period is to obtain experimental results for sand accumulations around a single row of fences. According to the agreement between Mr. Al Hinai and Dr. J. E. Cermak, fences with the following shapes were tested: i) the solid panel, ii) the vertical slats, iii) the horizontal slats, and iv) a special vertical spires shape.

The following Table 9 shows the different types of fences tested during this period. Figures 25 through 30 give the sketch of dimensions of each type of fence tested. The length of each fence in this series of tests was equal to the wind-tunnel test-section width. This "two-dimensional" configuration was chosen to reduce three-dimensional effects in order to identify more clearly the effects of fence geometry and porosity.

We also tested the 1/8" vertical slat fence for 30 and 60 percent angles from the line perpendicular to the flow direction. Run 14 for 30 degrees with the line perpendicular to the wind direction is shown in Figure 31a. Run 15 for 60 degrees with the line perpendicular to the wind direction is shown in Figure 31b. These two runs were conducted at the special request of the client.

Table 9. Experimental Runs for Different Configurations for Single Row of Fences

| Number | Description                           | Porosity | Gap at<br>Fence<br>Bottom<br>(%) | Sub-Sand<br>Barrier | Wind<br>Speed<br>(m/s) | Total<br>Running<br>Time<br>(hrs) |
|--------|---------------------------------------|----------|----------------------------------|---------------------|------------------------|-----------------------------------|
| 1      | 1/16 in. Horizontal<br>Slats          | 50       | 0                                | NO                  | 8                      | 22                                |
| 2      | 1/8 in. Horizontal<br>Slats           | 50       | 20                               | NO                  | 8                      | 16                                |
| 3      | 1/16 in. Horizontal<br>Slats          | 50       | 20                               | NO                  | 9                      | 17                                |
| 4      | 1/8 in. Horizontal<br>Slats           | 50       | 20                               | YES                 | 9                      | 20                                |
| 5      | 1/8 in. Vertical<br>Slats             | 50       | 0                                | NO                  | 9                      | 16                                |
| 5A     | 1/8 in. Vertical<br>Slats             | 50       | 0                                | YES                 | 9                      | 16                                |
| 6      | Solid Panel                           | 0        | 0                                | YES                 | 9                      | 16                                |
| 7      | 1/16 in. Vertical<br>Slats            | 50       | 0                                | NO                  | 9                      | 18                                |
| 8      | 1/8 in. Horizontal<br>Slats           | 66       | 0                                | NO                  | 9                      | 20                                |
| 9      | Vertical Spires I                     | 80       | 0                                | YES                 | 9                      | 10                                |
| 10     | 1/8 in. Horizontal<br>Slats           | 33       | 0                                | NO                  | 9                      | 10                                |
| 11     | 1/8 in. Horizontal<br>Slats           | 33       | 0                                | YES                 | 9                      | 12                                |
| 12     | 1/8 in. Vertical<br>Slats             | 60       | 0                                | YES                 | 9                      | 42                                |
| 13     | 1/8 in. Slats<br>(draft fence height) | 60       | 0                                | YES                 | 9                      | 30                                |
| 14     | Vertical Spires II                    | 50       | 0                                | YES                 | 9                      | 24                                |
| 15     | 1/8 in. Vertical<br>("30° angle")     | 60       | 0                                | YES                 | 9                      | 16                                |
| 16     | 1/8 in. Vertical<br>("60° angle")     | 60       | 0                                | YES                 | 9                      | 20                                |

1/16 inch = 0.15875 cm; 1/8 inch = 0.3175 cm.

Fence for Run #1  
1/16 in. Slats and Gaps  
50% Porosity

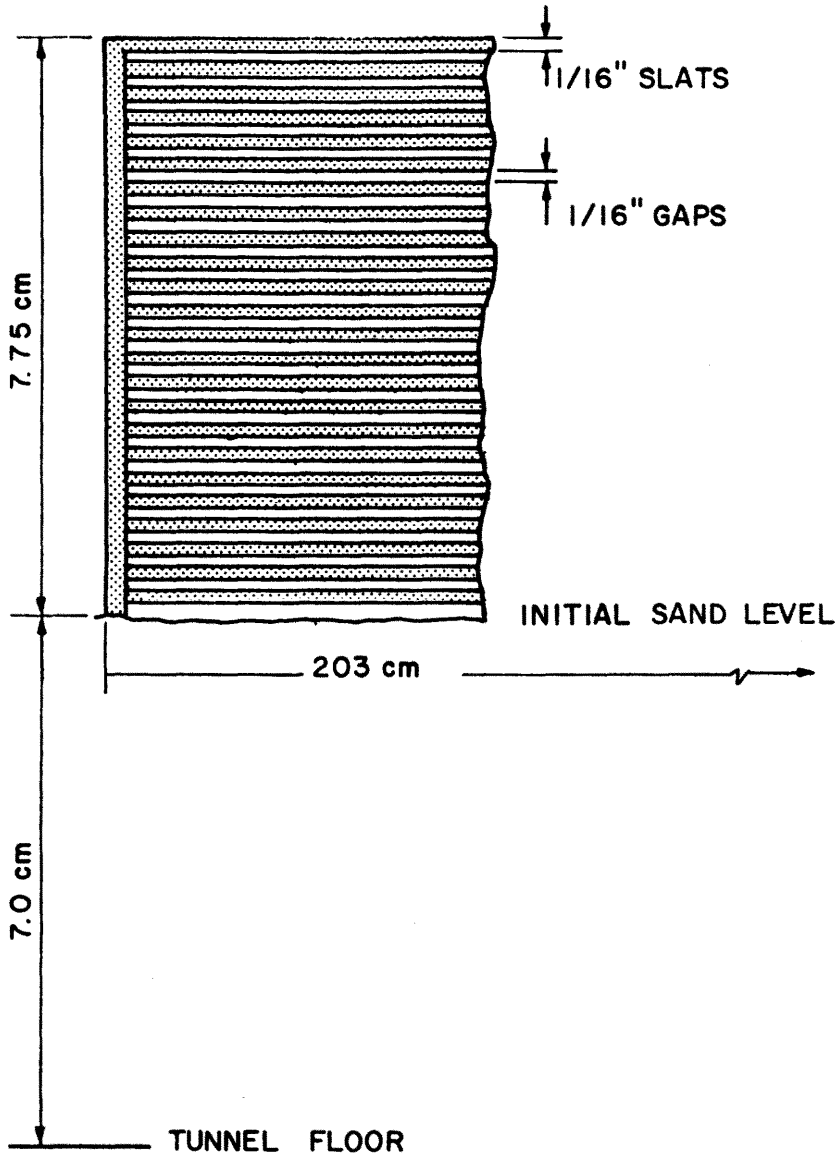


Figure 25a. Different Fence Configurations - horizontal slat, 1/16 inch slats, 1/16 inch gaps, 50% porosity (1/16 inch - 0.15875 cm)

Fence for Run #8  
 1/8 in. Slats  
 1/4 in. Gaps  
 66% Porosity

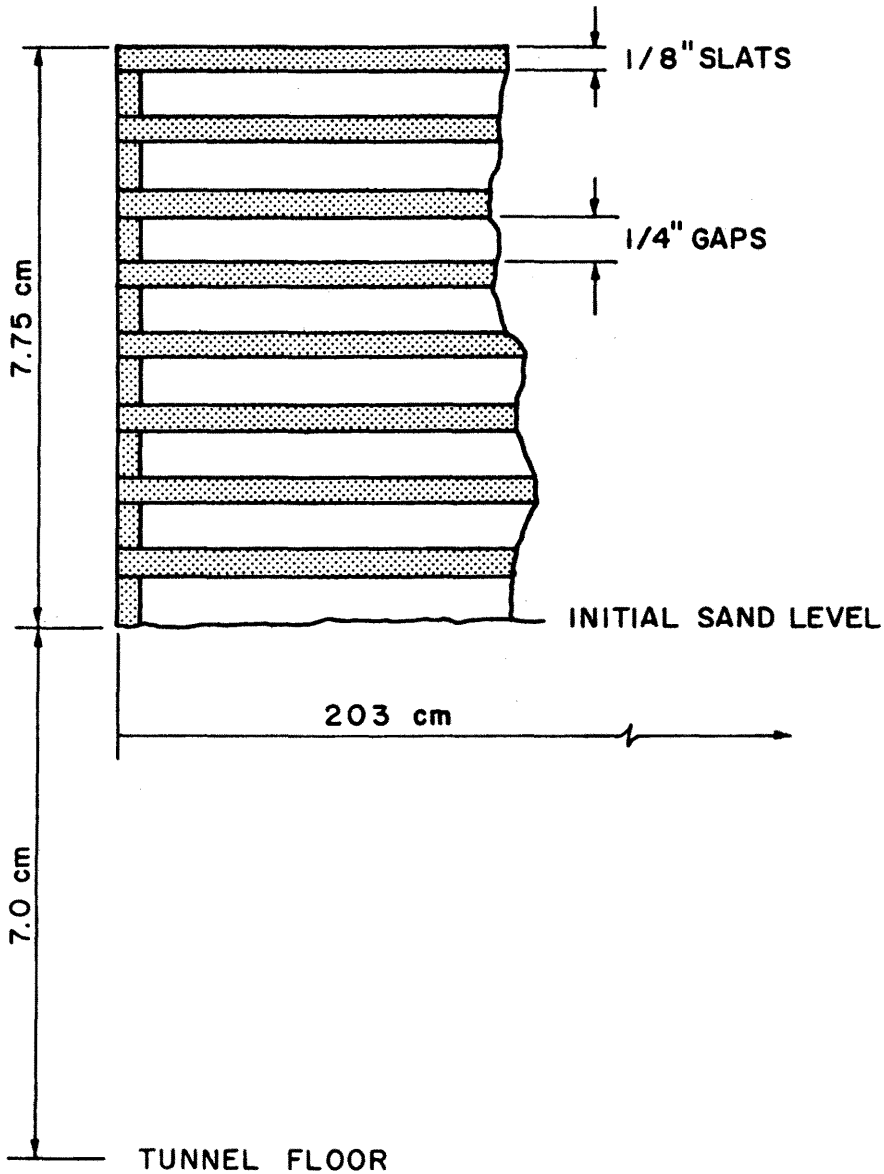


Figure 25b. Different Fence Configurations - horizontal slat , 1/8 inch slats, 1/4 inch gaps, 66% porosity (1/8 inch = 0.3175 cm, 1/4 inch = 0.635 cm)

Fence for Run #10  
 1/8 in. Slats  
 1/16 in. Gaps  
 33% Porosity

Fence for Run #11  
 Same, except sub-sand  
 barrier installed to  
 prevent scour.

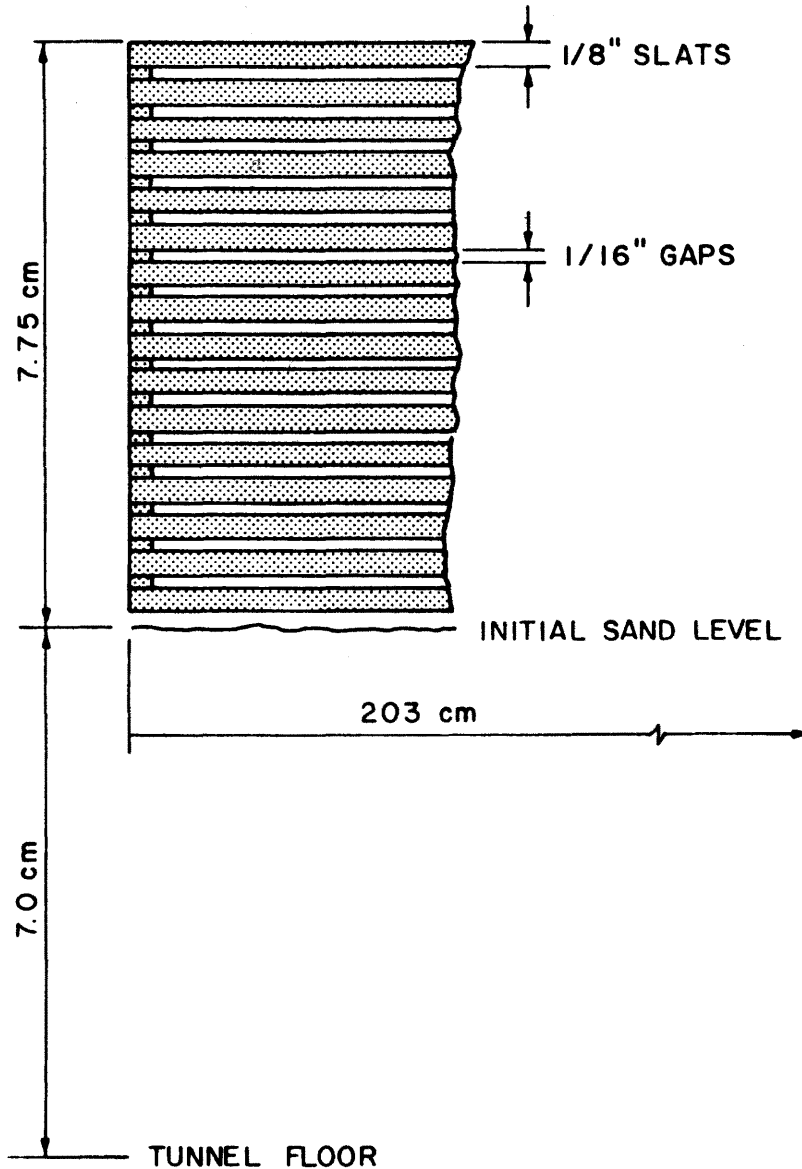


Figure 25c. Different Fence Configurations - horizontal slat, 1/8 inch slats, 1/16 inch gaps, 33% porosity (1/16 inch = 0.15875 cm, 1/8 inch = 0.3175 cm)

Fence for Run #2  
 1/8 in. Slats and Gaps  
 50% Porosity

Fence for Run #4  
 Same, except sub-sand  
 barrier installed to  
 prevent scour.

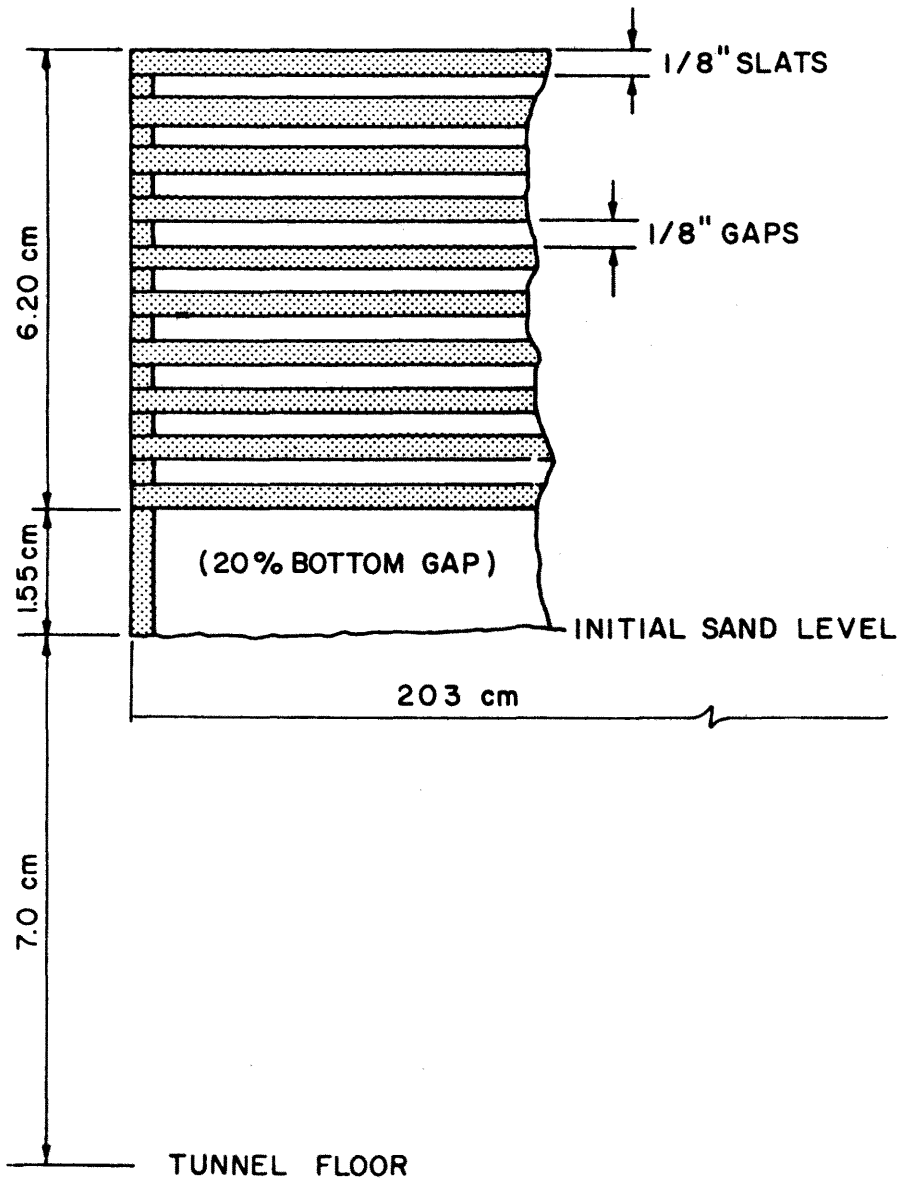


Figure 26a. Different Fence Configurations - horizontal slat, with 20% bottom gap, 1/8 inch slats, 1/8 inch gaps, 50% porosity (1/8 inch = 0.3175 cm)

Fence for Run #3  
 1/16 in. Slats and Gaps  
 50% Porosity

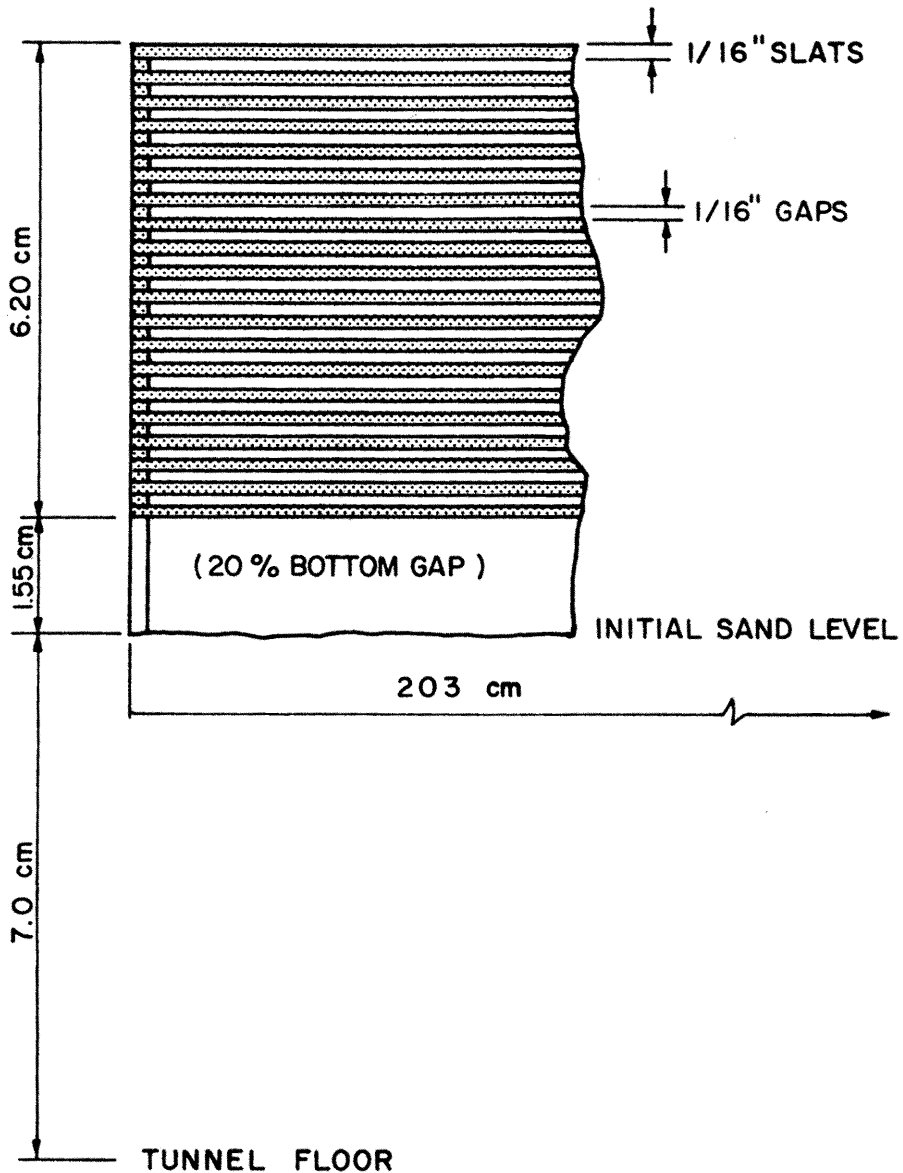


Figure 26b. Different Fence Configurations - horizontal slat, with 20% bottom gap, 1/16 inch slats, 1/16 inch gaps, 50% porosity (1/16 inch = 0.15875 cm)

Fence for Run #5  
 1/8 in. Slats and Gaps  
 50% Porosity

Fence for Run #5A  
 Same, except sub-sand  
 barrier installed to  
 prevent scour.

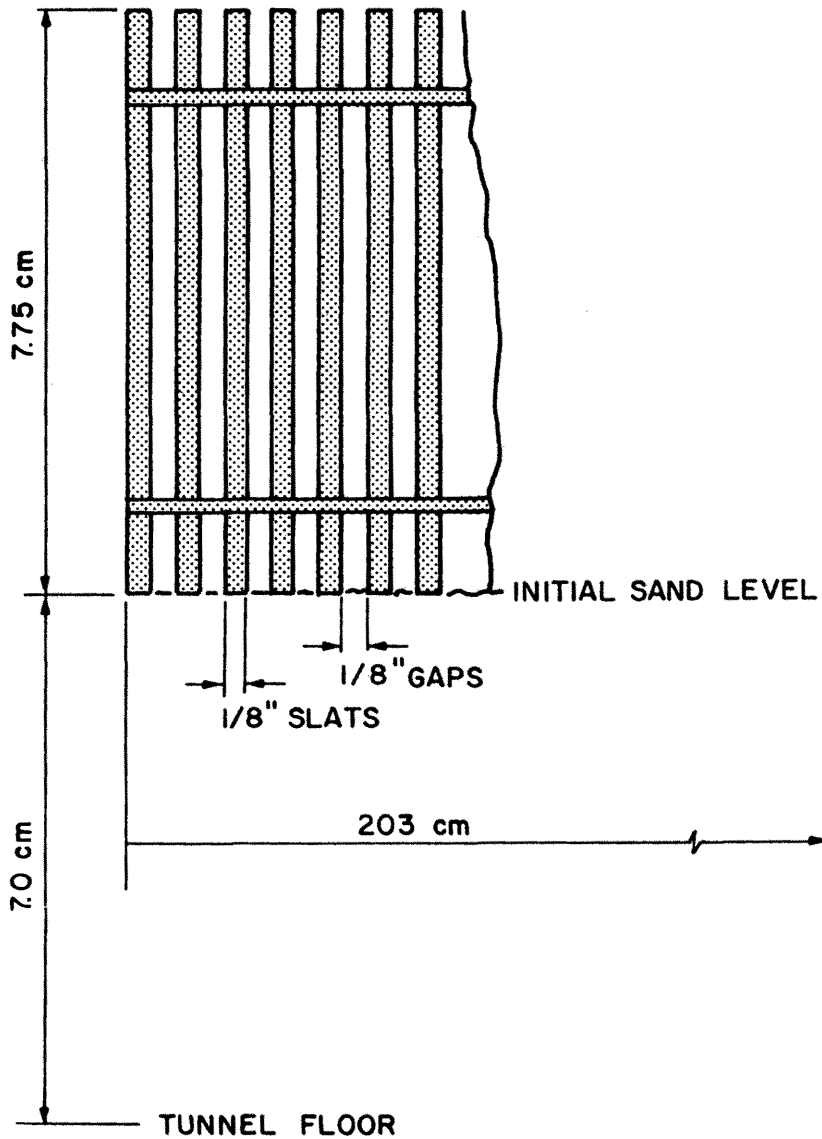


Figure 27a. Different Fence Configurations - vertical slat, 1/8 inch slats, 1/8 inch gaps, 50% porosity (1/8 inch = 0.3175 cm)

Fence for Run #7  
1/16 in. Slats and Gaps  
50% Porosity

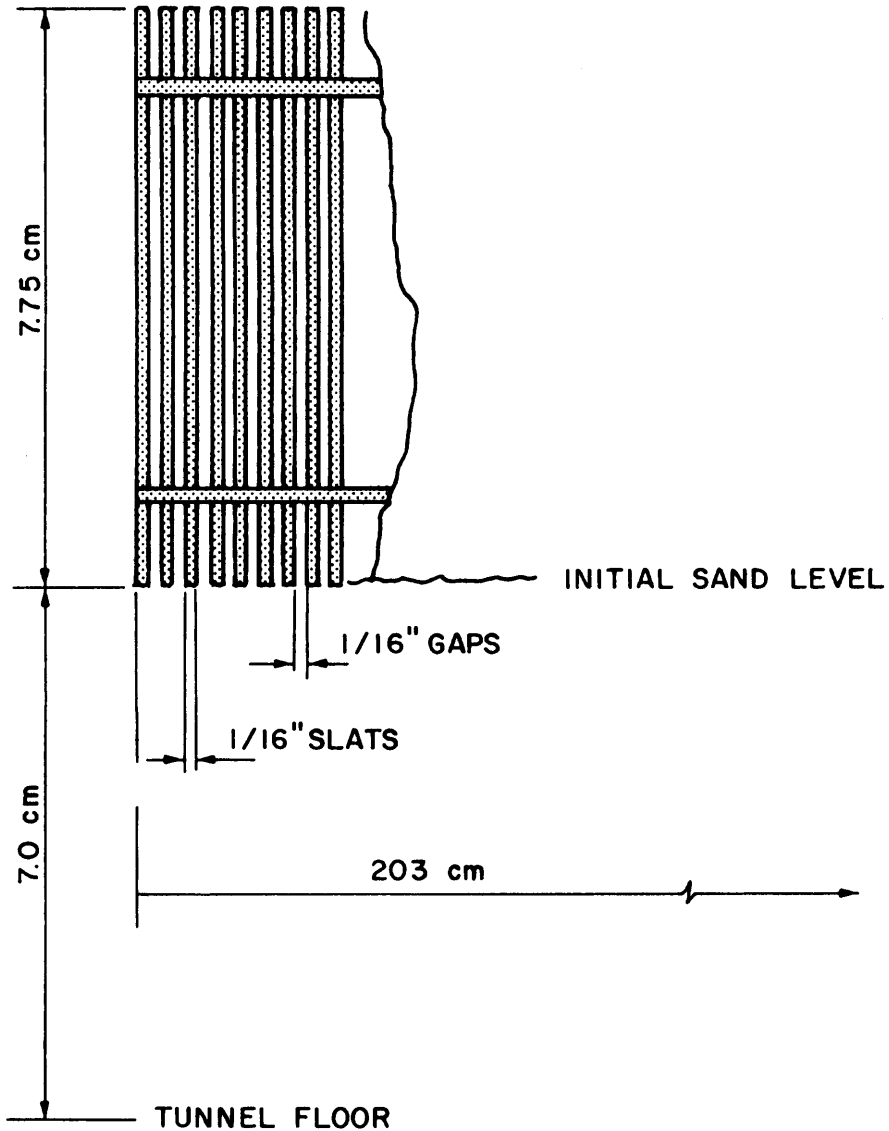


Figure 27b. Different Fence Configurations - vertical slat, 1/16 inch slats, 1/16 inch gaps, 50% porosity (1/16 inch = 0.15875 cm)

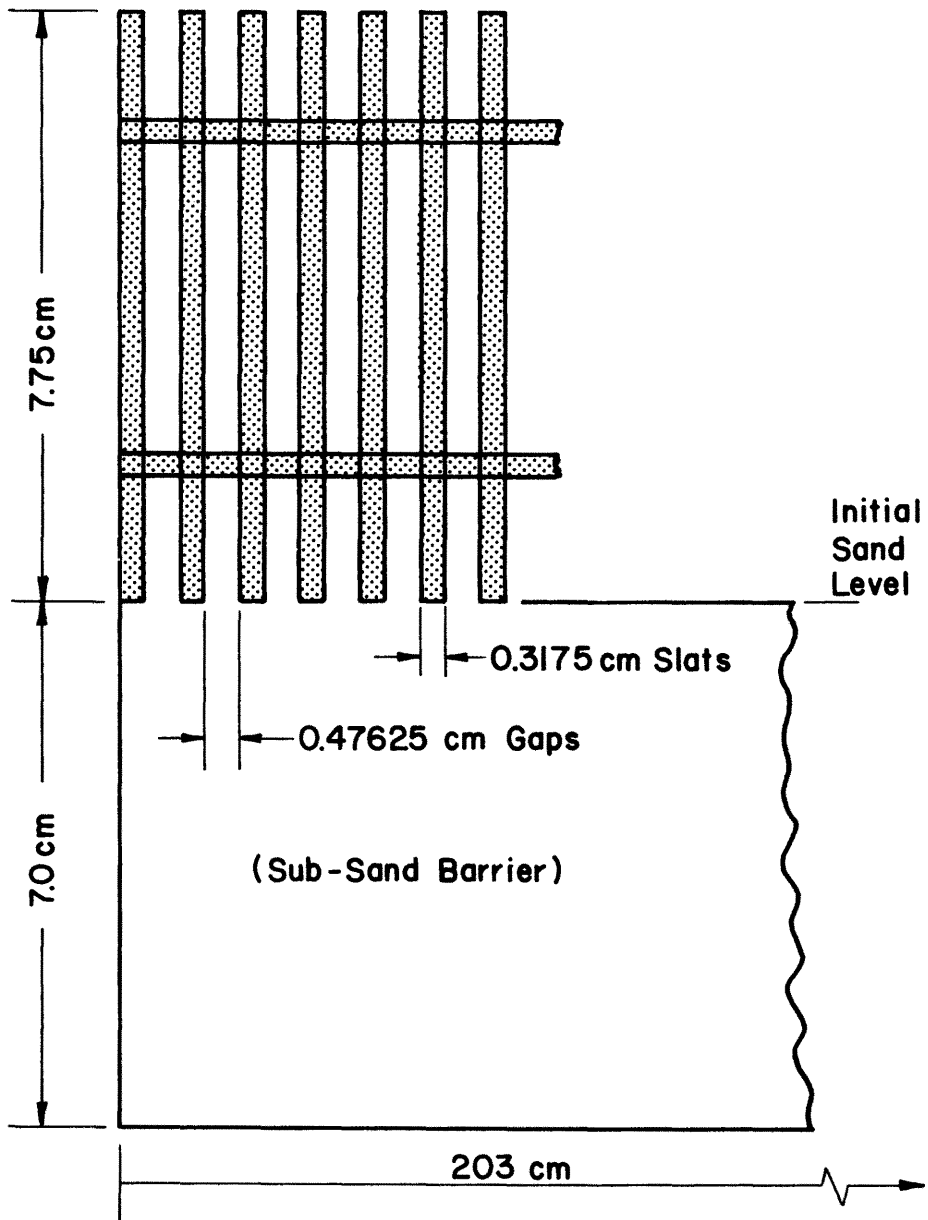


Figure 27c. Different Fence Configurations - 1/8 inch vertical slat fence with 60% porosity (1/8 inch = 0.3175 cm)

Fence for Run #6  
Solid Panel  
0% Porosity

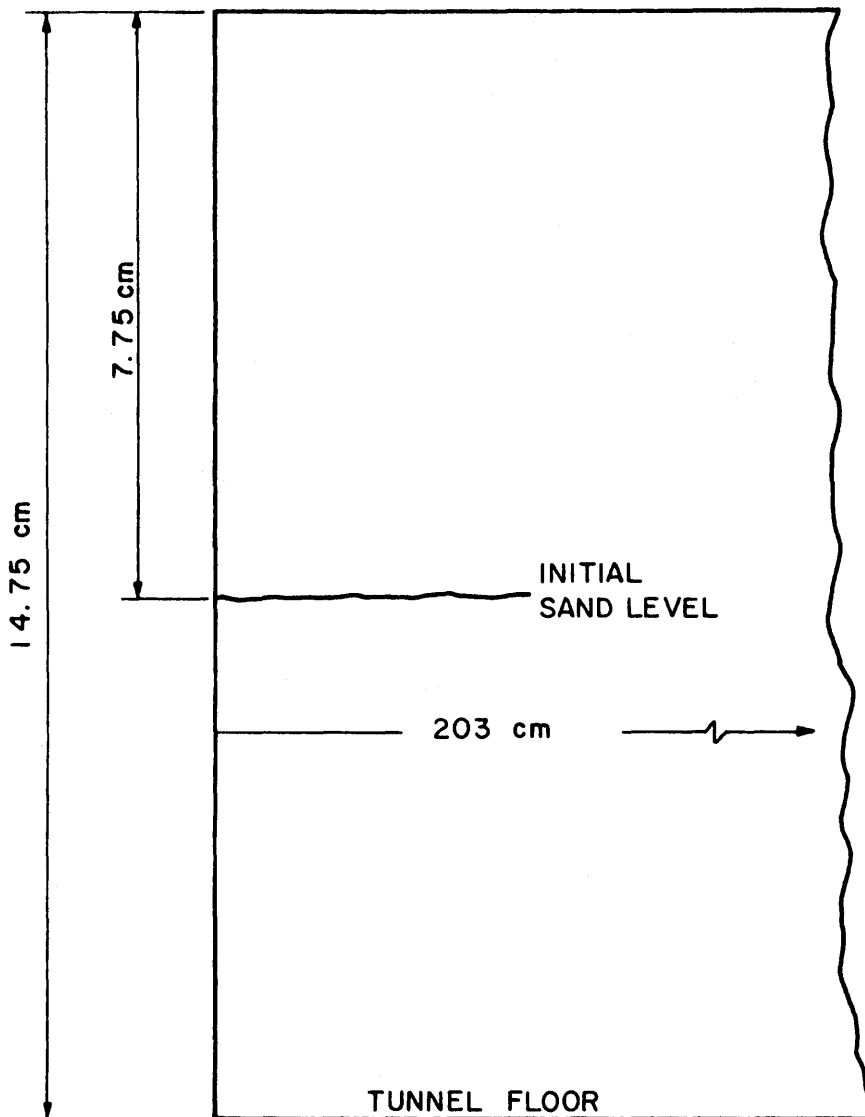


Figure 28. Different Fence Configurations - solid panel fence with 0% porosity

Fence for Run #9  
Vertical Spires  
80% Porosity

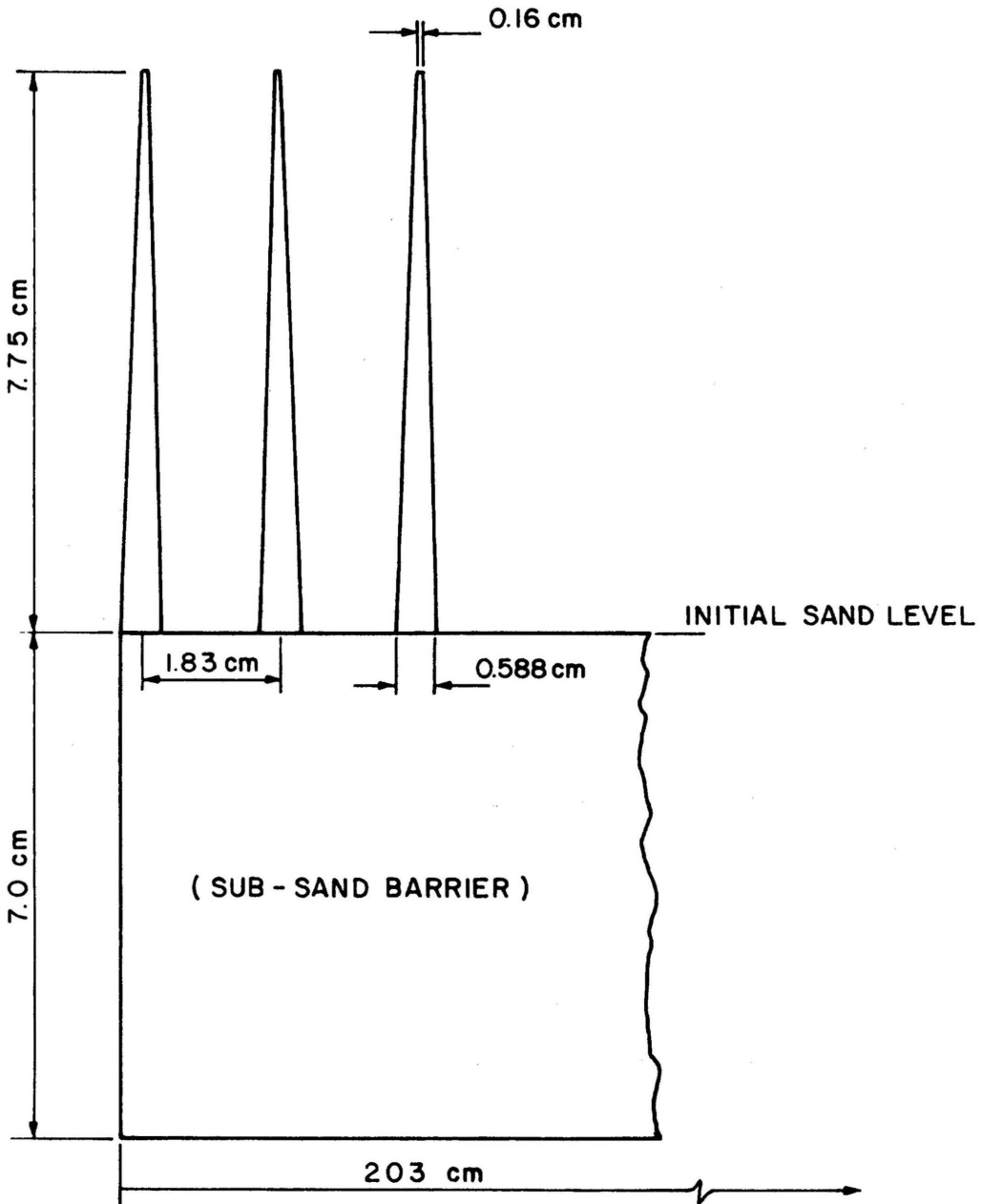


Figure 29. Different Fence Configurations - vertical spires I, 80% porosity

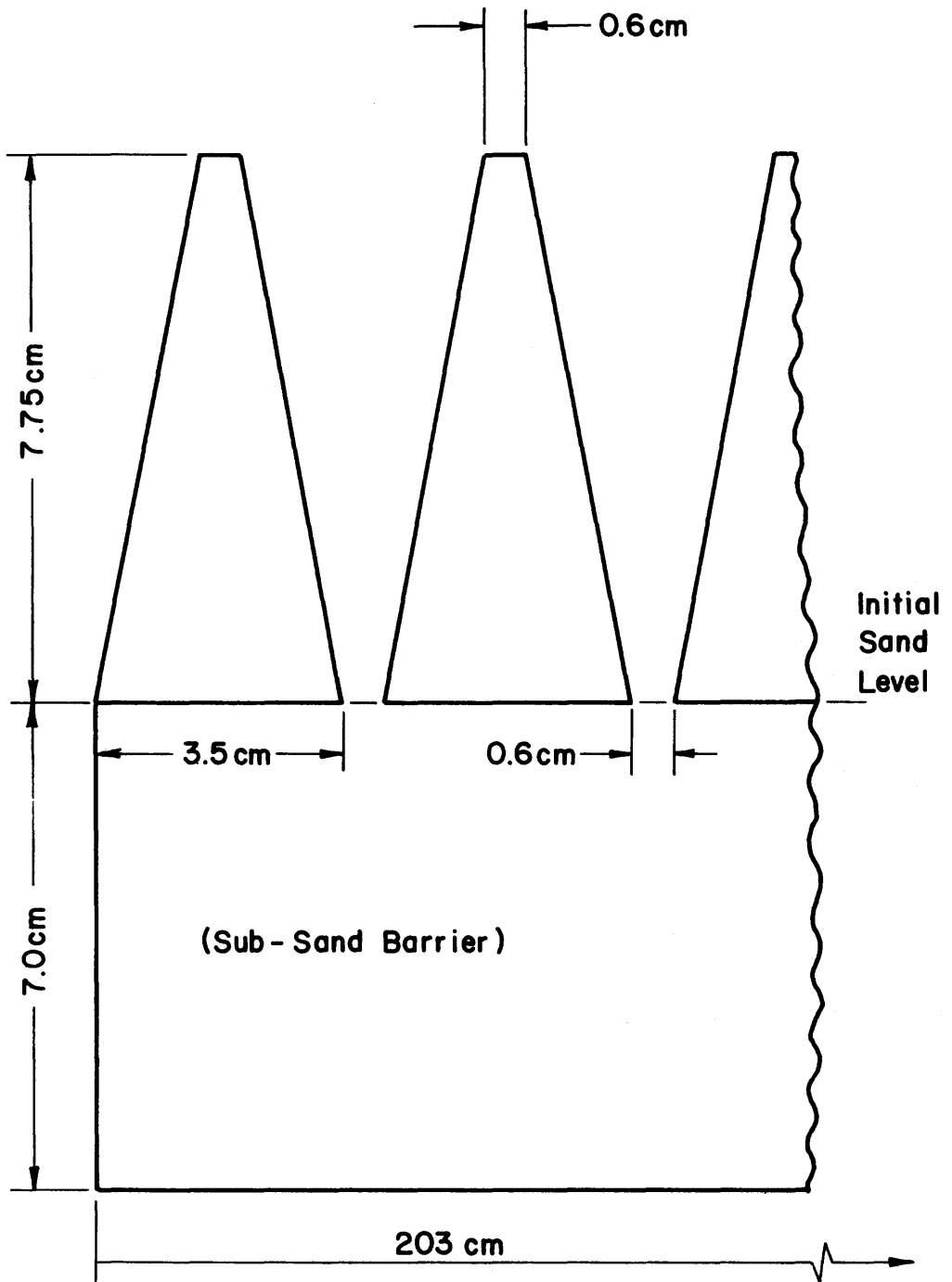


Figure 30. Different Fence Configurations - vertical spires II, 50% porosity

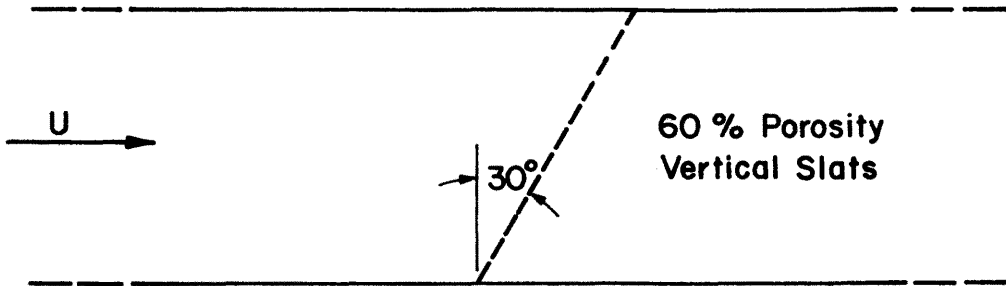


Figure 31a. Schematic Diagram, Top View, for a 30-degree Inclined Fence

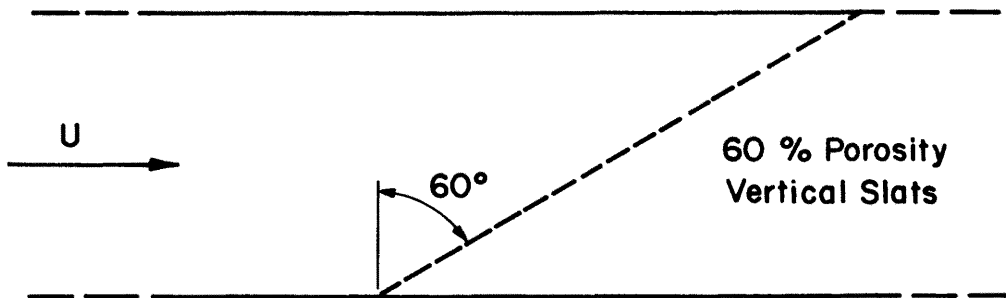


Figure 31b. Schematic Diagram, Top View, for a 60-degree Inclined Fence

Note that the 20 percent bottom opening in the horizontal slats has an opening height of 1.55 cm which is about half of the thickness of the moving sand layer depth. Note that a different sand was used than that for the exploratory studies reported in the First Progress Report.

#### E. Experimental Results

Figures 32a and 32b reveal the mean flow and turbulent flow intensity at respective distances of 2, 6, 10, and 15 fence heights downstream from horizontal slat fences with 50 percent uniform porosity (Experimental Run 10). The turbulent flow near the bed increased significantly from the corresponding values without the fence. However, we must point out that these high turbulent intensity values are difficult to evaluate. If these measurements are correct, both the mean velocity and turbulent characteristics did not change significantly within a distance between two fence heights to fifteen fence heights.

#### F. Sand Accumulation Around Each Type of Fence

Sand accumulation around each type of fences is shown in Figures 33, 34, 35, 36, 37, 38, 39, 40, 41, 42, 43, 44, 45, 46, 47, 48, and 49.

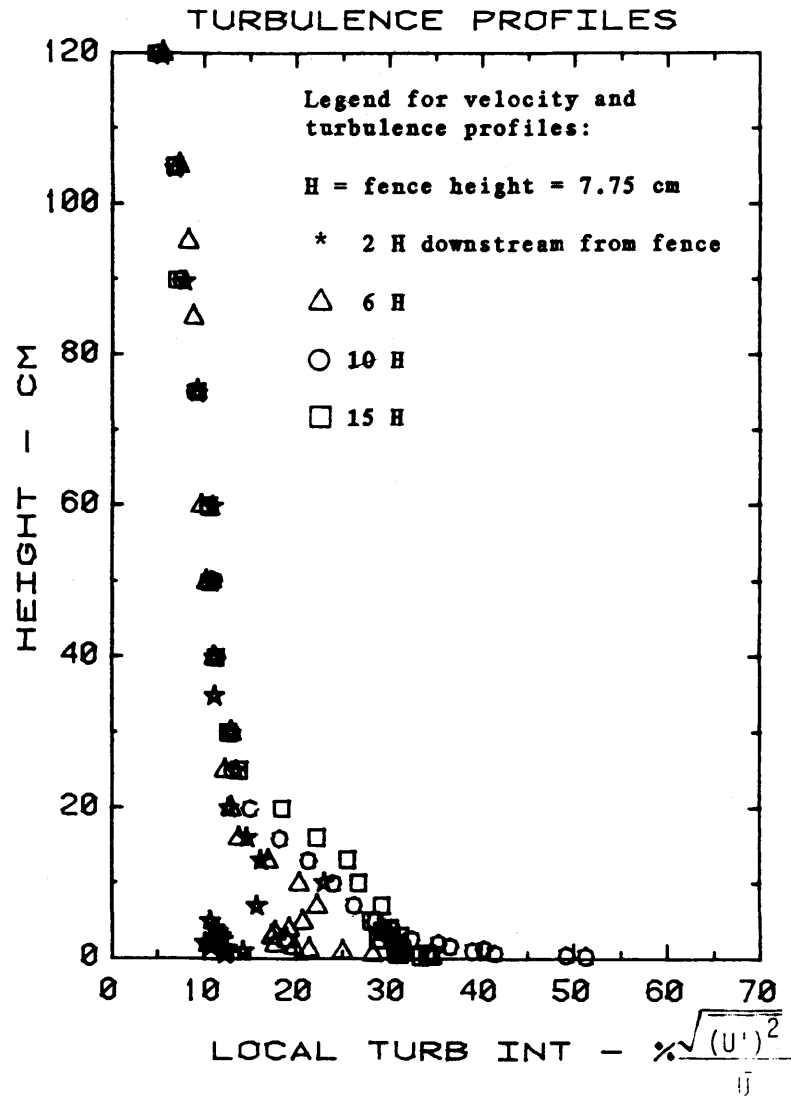
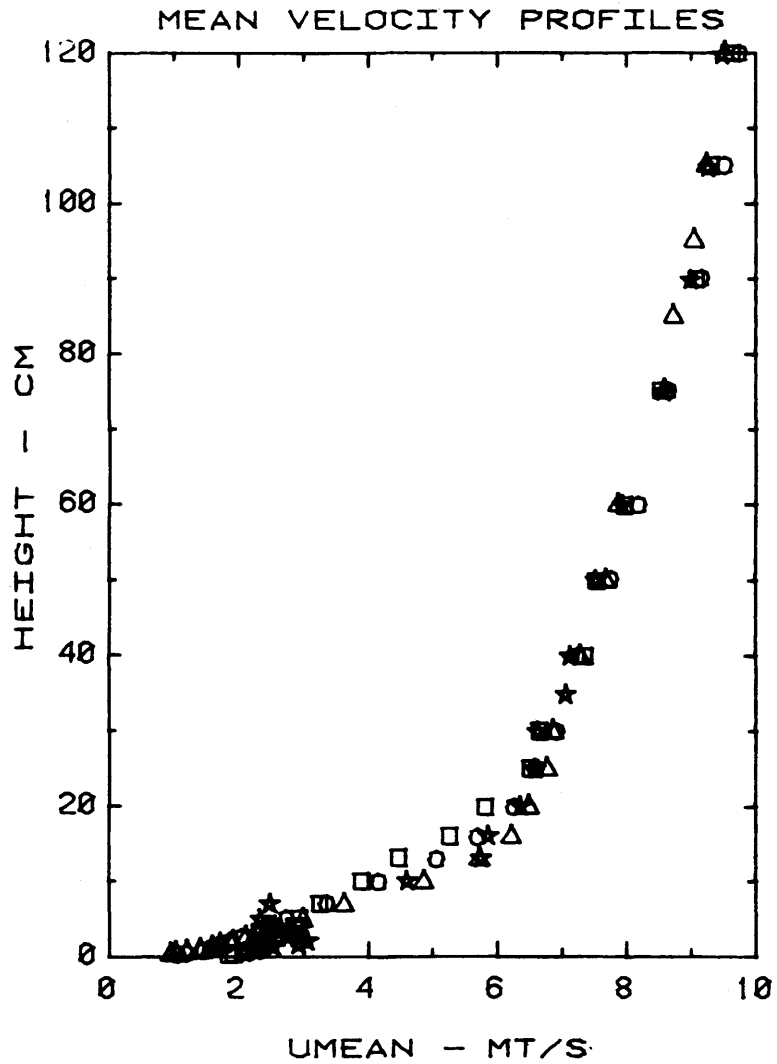


Figure 32a. Flow Characteristics Downstream from Horizontal Slat Fence with 50% Uniform Porosity (Run 1)

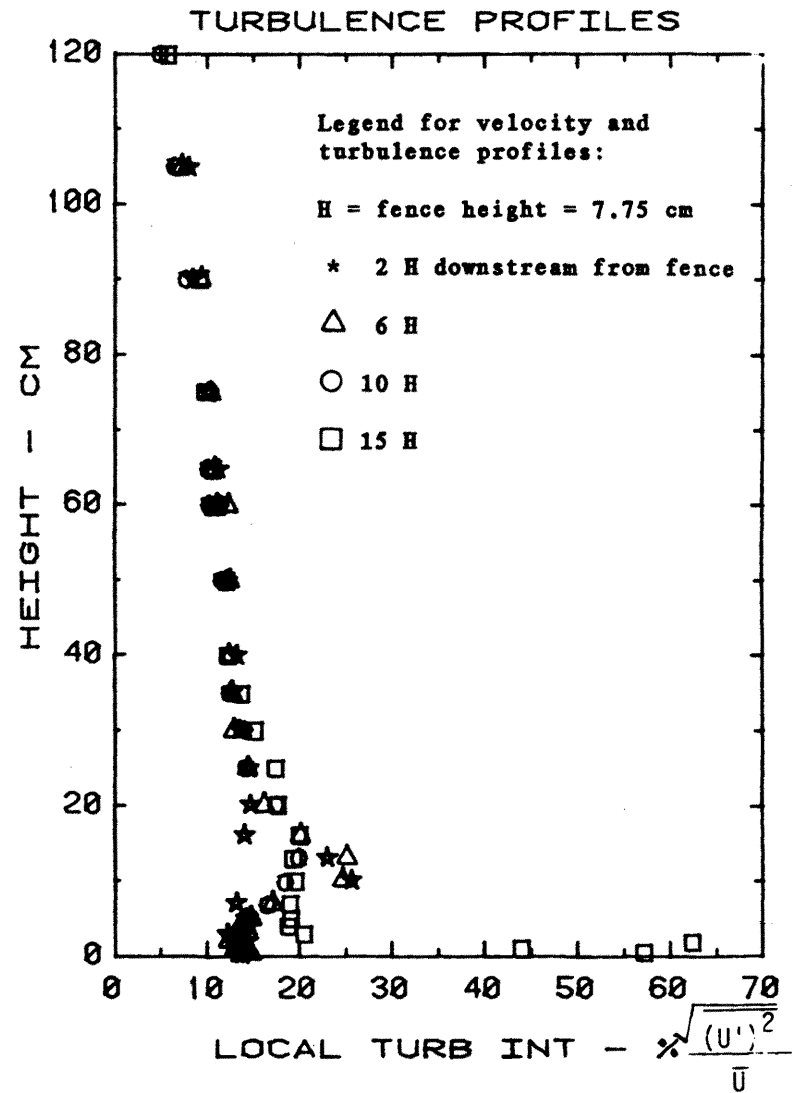
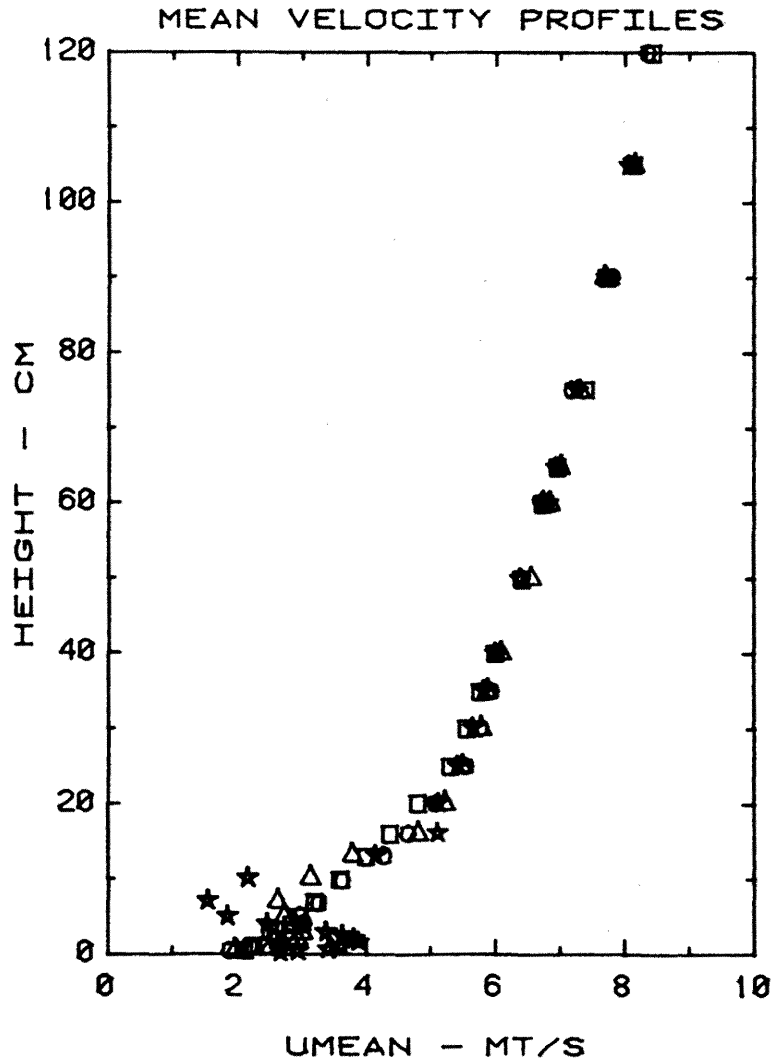
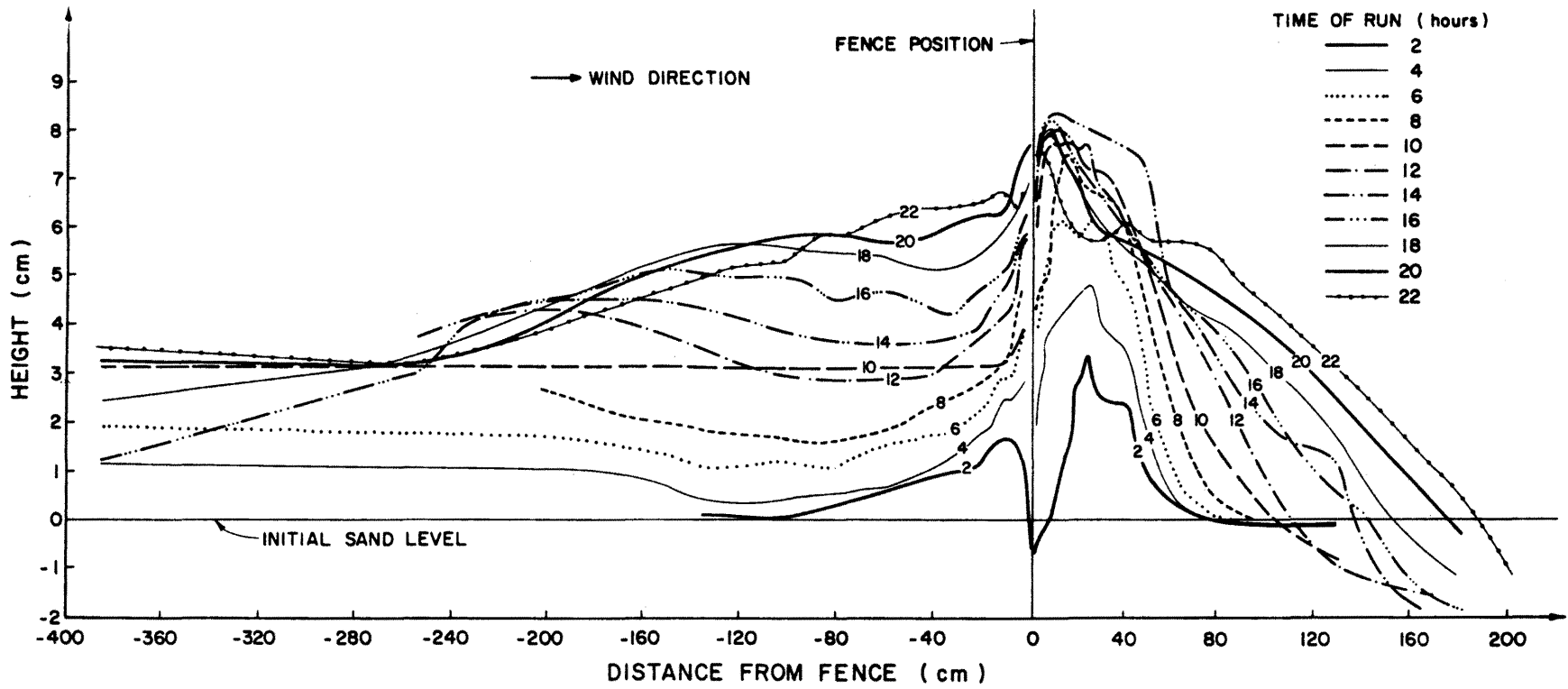
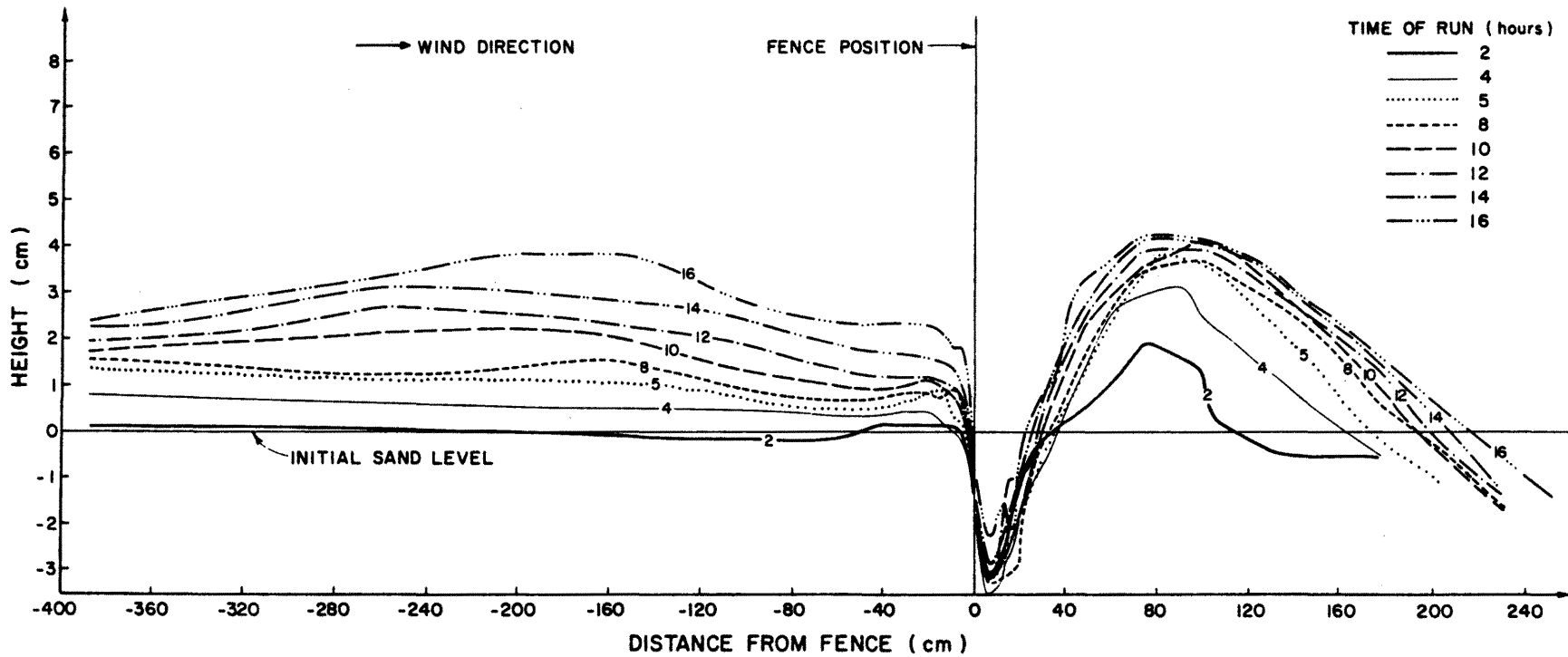


Figure 32b. Flow Characteristics Downstream from Horizontal Slat Fence of 50% Porosity with a 20% Bottom Gap (Run 2)



1/16 inch = 0.15875 cm

Figure 33. Sand Accumulation Profiles for a 1/16 inch Horizontal Slat Fence with 50% Uniform Porosity (Run 1)



1/8 inch = 0.3175 cm

Figure 34. Sand Accumulation Profiles for a 1/8 inch Horizontal Slat Fence with 50% Porosity and 20% Opening at the Bottom (Run 2)

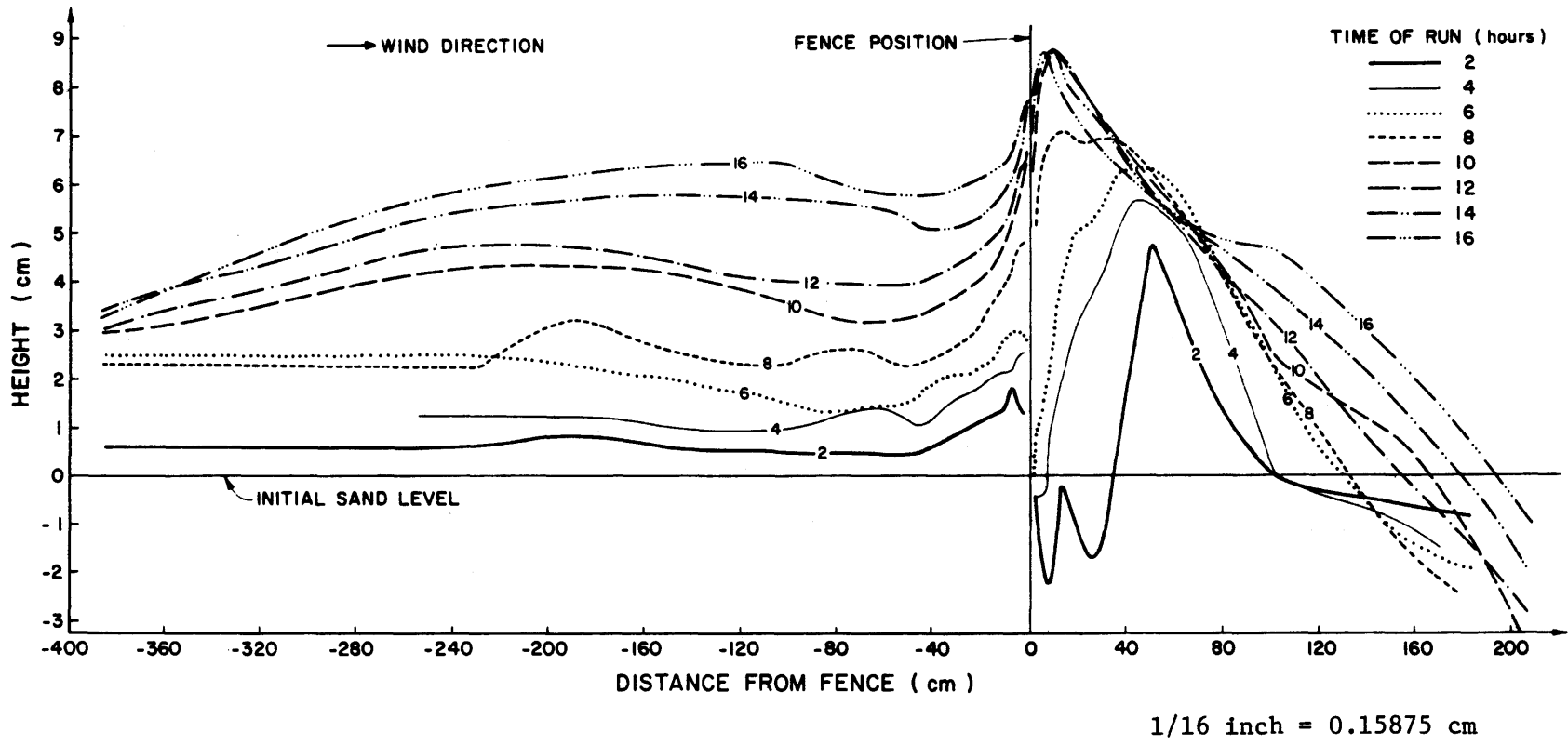
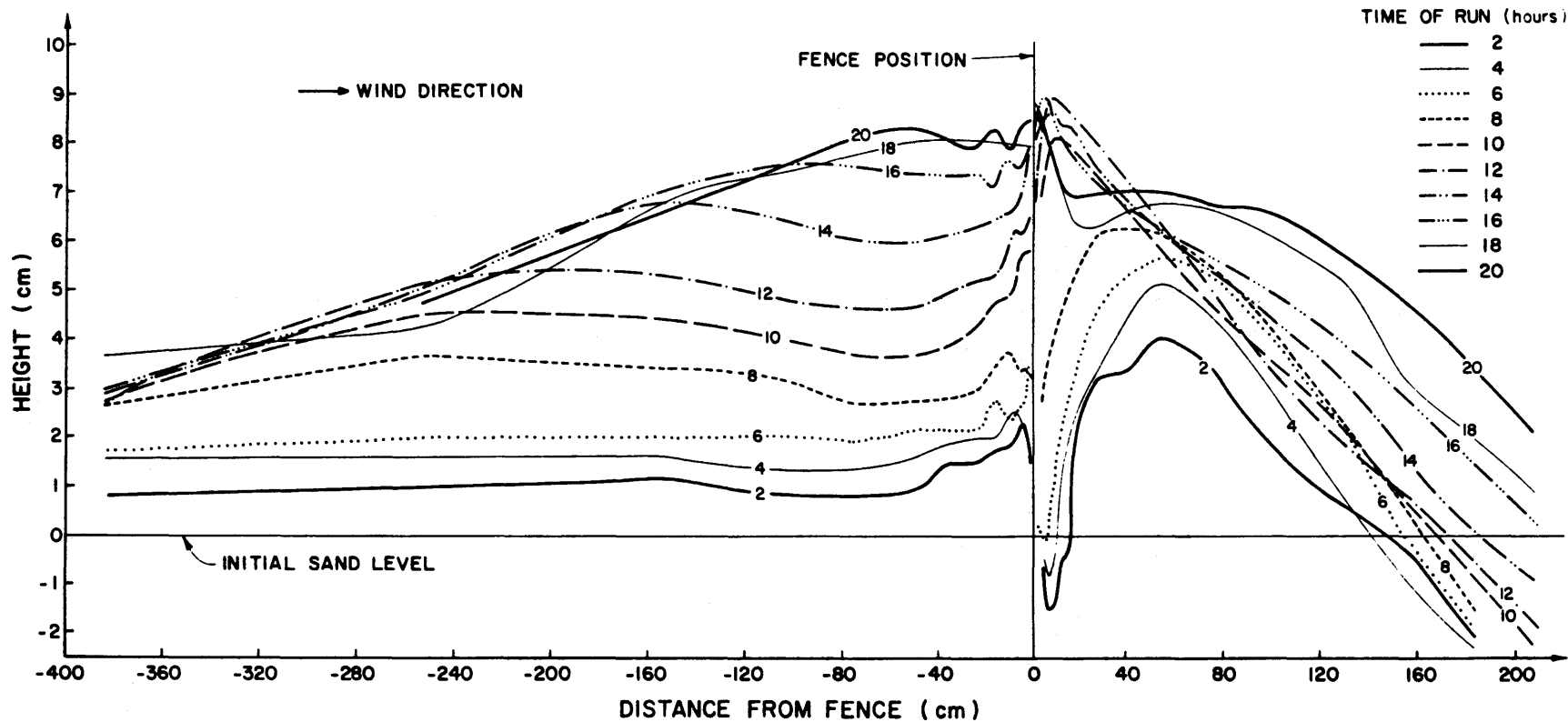
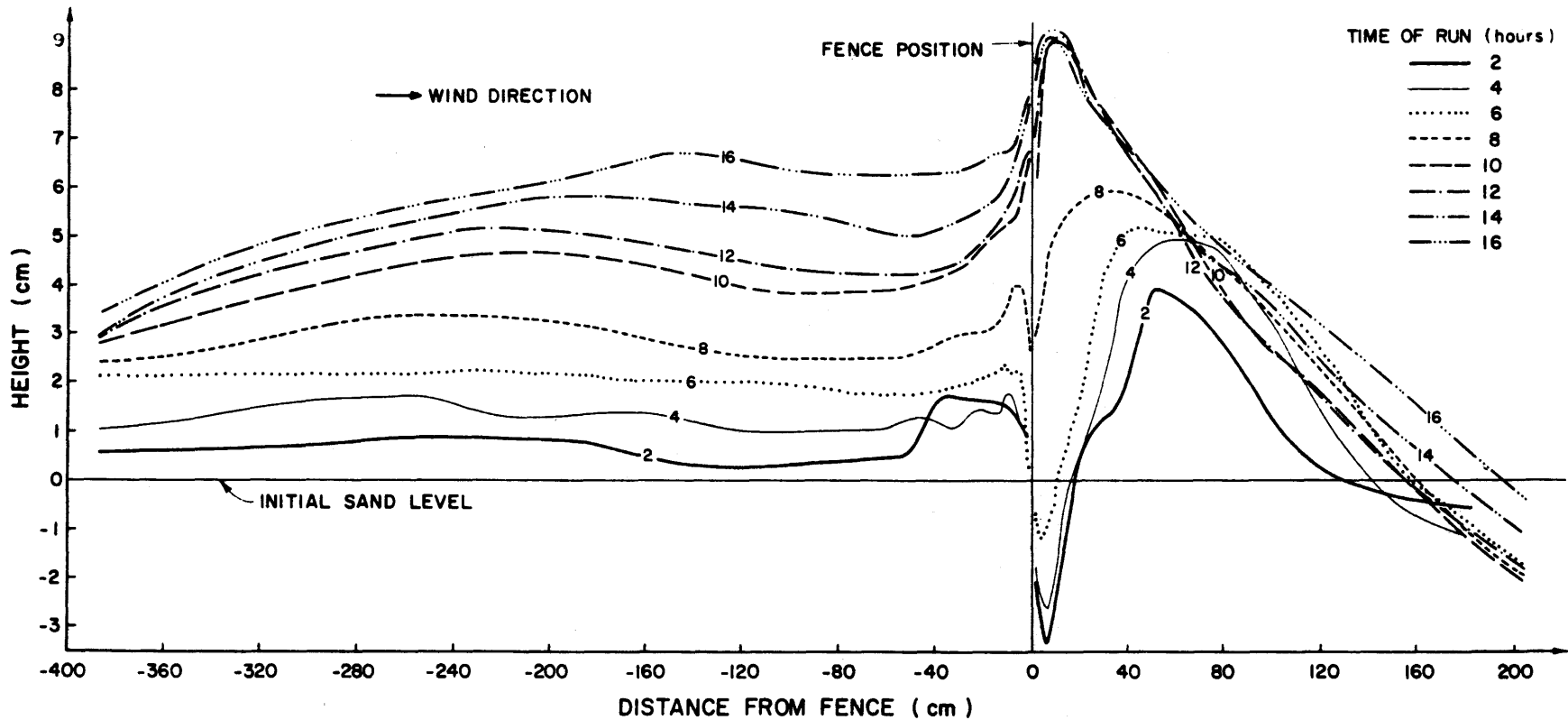


Figure 35. Sand Accumulation Profiles for a 1/16 inch Horizontal Slat Fence with 50% Porosity and 20% Opening at the Bottom (Run 3)



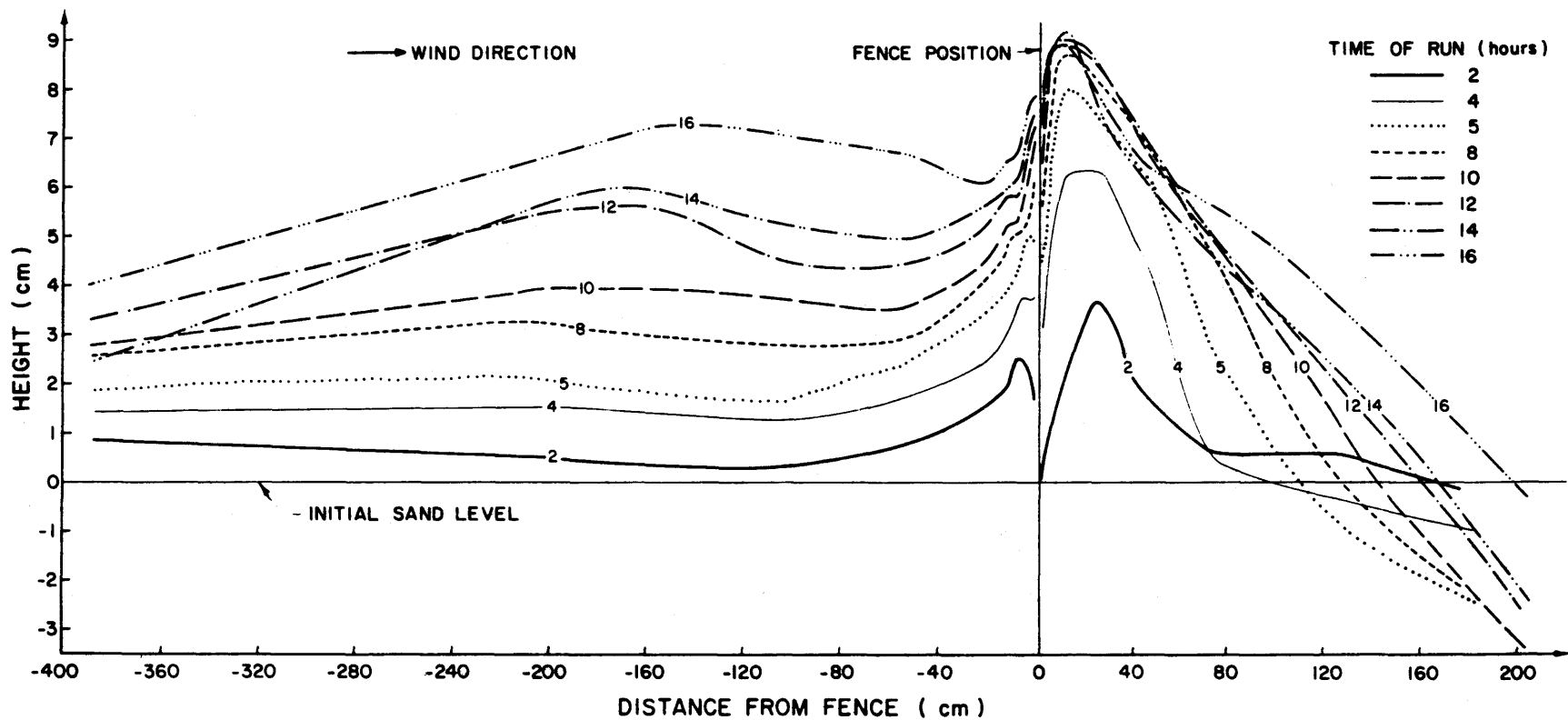
1/8 inch = 0.3175 cm

Figure 36. Sand Accumulation Profiles for a 1/8 inch Horizontal Slat Fence with 50% Porosity, 20% Opening at the Bottom, and a Subsurface Barrier Installed (Run 4)



1/8 inch = 0.3175 cm

Figure 37. Sand Accumulation Profiles for a 1/8 inch Vertical Slat Fence with 50% Uniform Porosity (Run 5)



1/8 inch = 0.3175 cm

Figure 38. Sand Accumulation Profiles for a 1/8 inch Vertical Slat Fence with 50% Uniform Porosity and a Subsurface Barrier Installed (Run 5A)

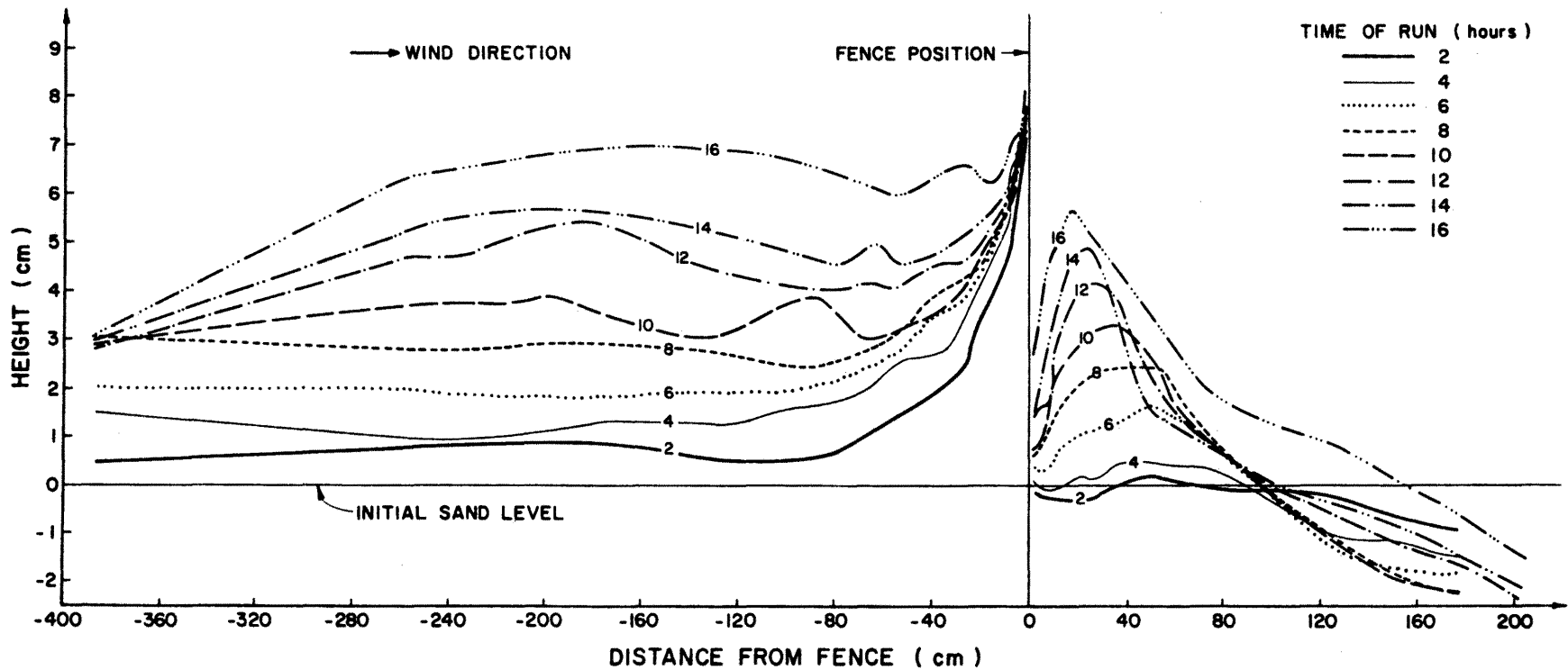
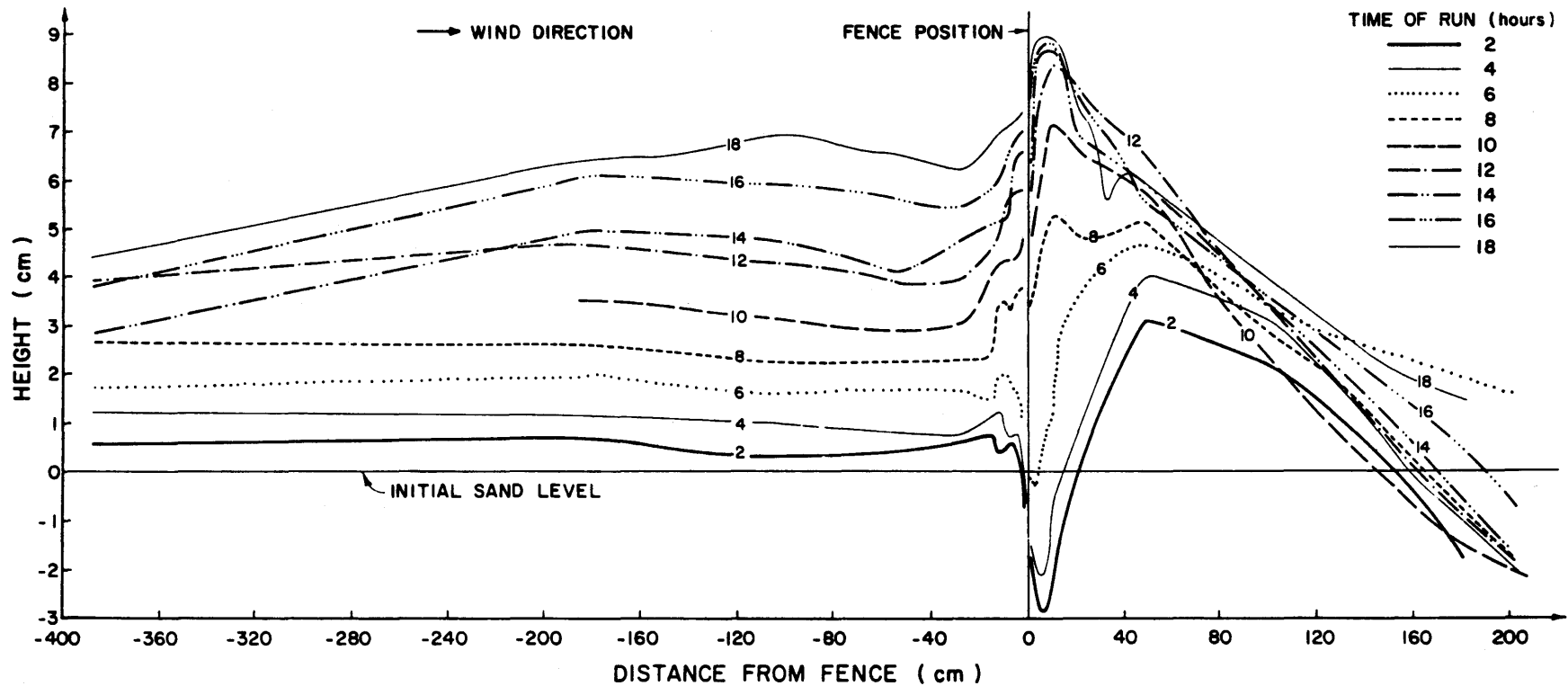
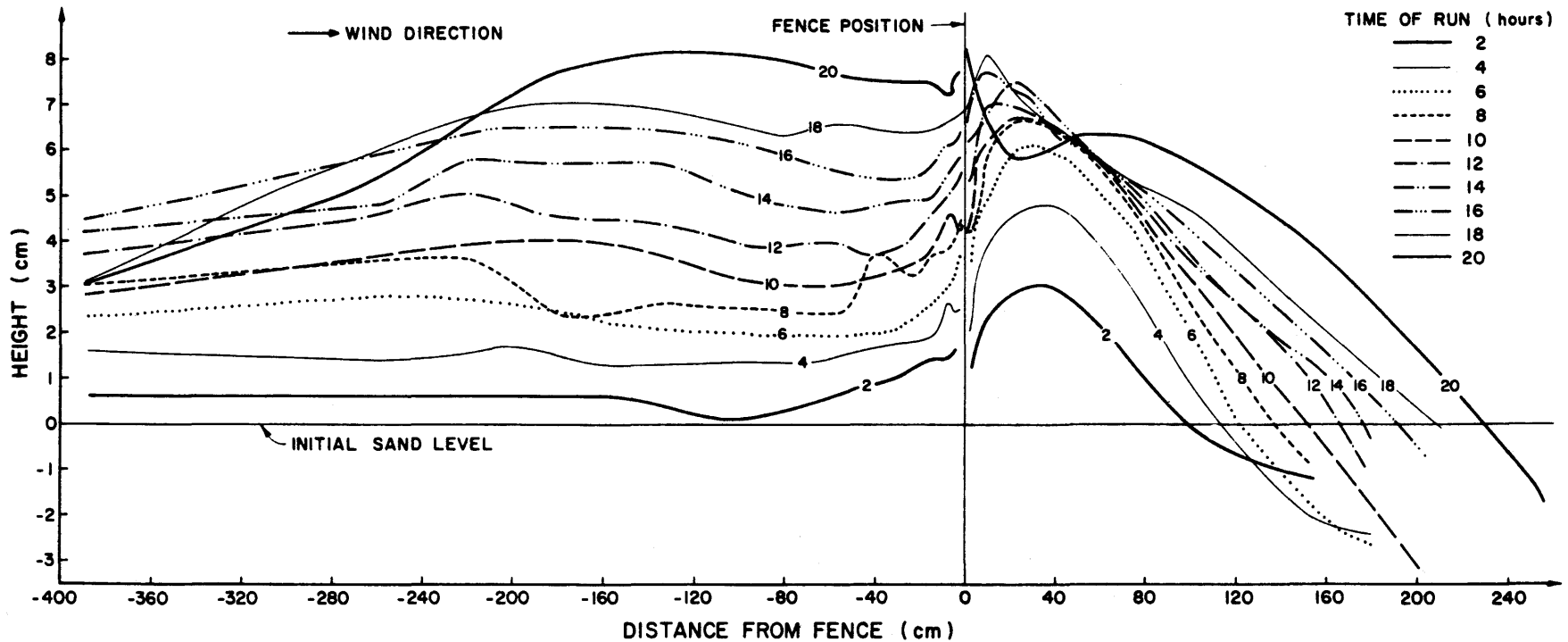


Figure 39. Sand Accumulation Profiles for a Solid Panel Fence (0% porosity) with a Subsurface Barrier Installed (Run 6)



1/16 inch = 0.15875 cm

Figure 40. Sand Accumulation Profiles for a 1/16 inch Vertical Slat Fence with 50% Uniform Porosity (Run 7)



1/8 Inch = 0.3175 cm

Figure 41. Sand Accumulation Profiles for a 1/8 inch Horizontal Slat Fence with 66% Uniform Porosity (Run 8)

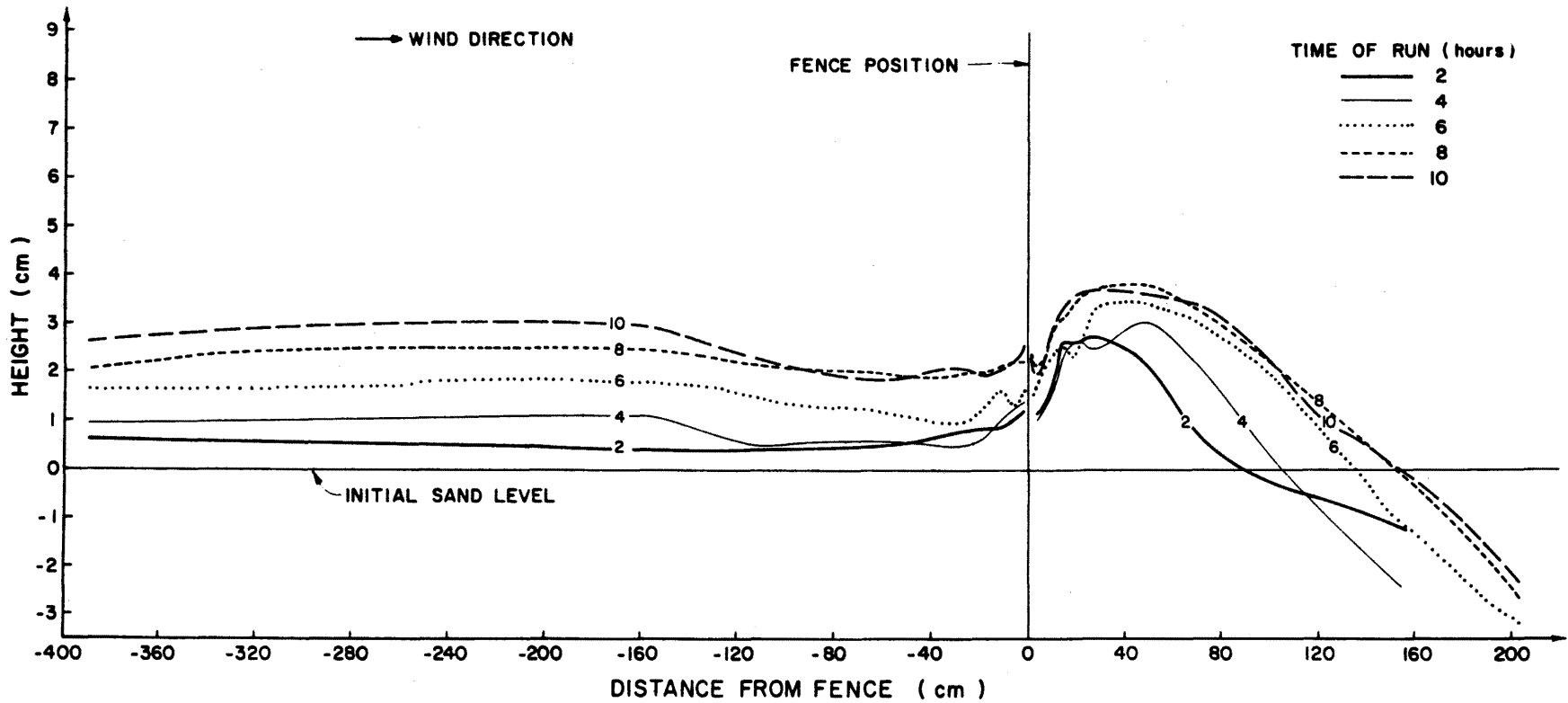
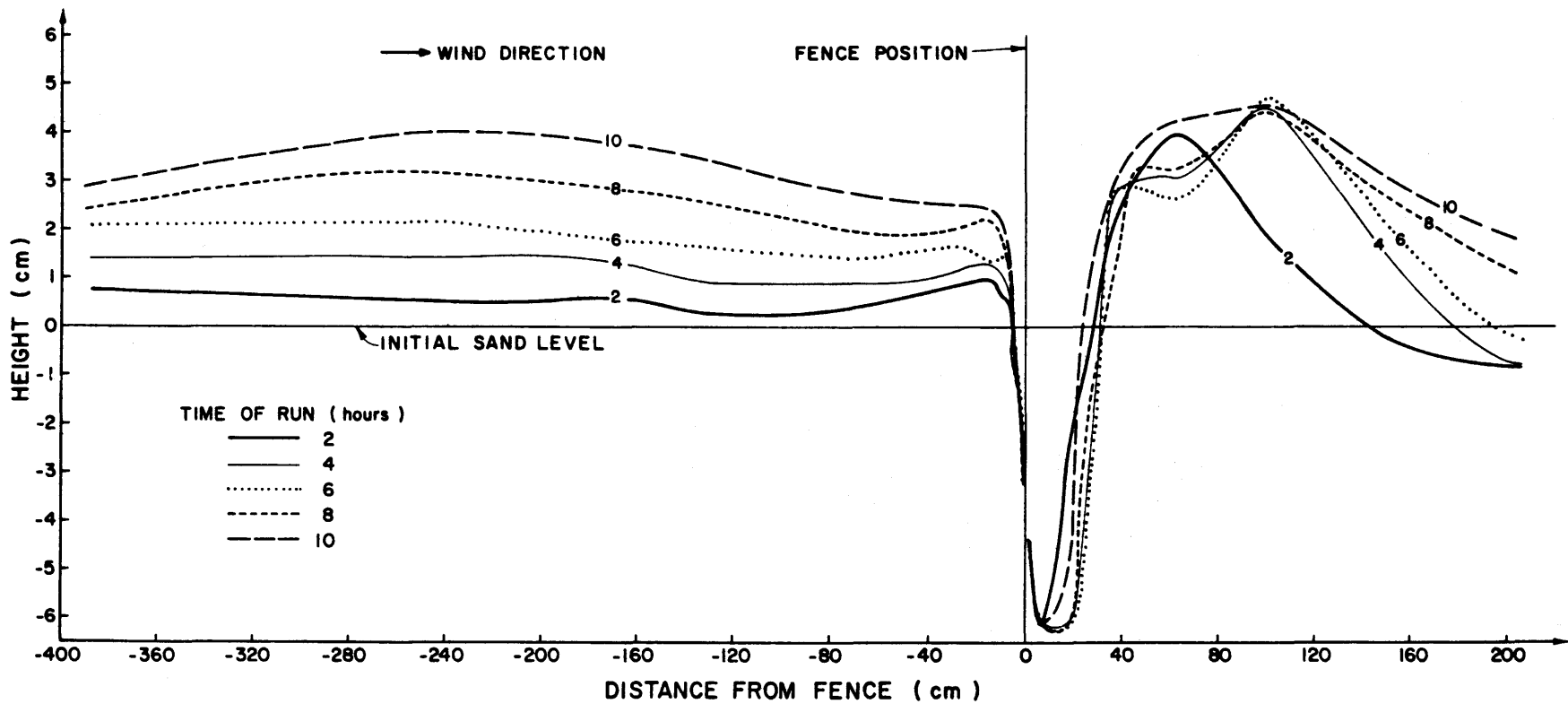


Figure 42 Sand Accumulation Profiles for Special Spire Fence with 80% Porosity and a Subsurface Barrier Installed (Run 9)



1/8 inch = 0.3175 cm

Figure 43. Sand Accumulation Profiles for a 1/8 inch Horizontal Slat Fence with 33% Uniform Porosity (Run 10)

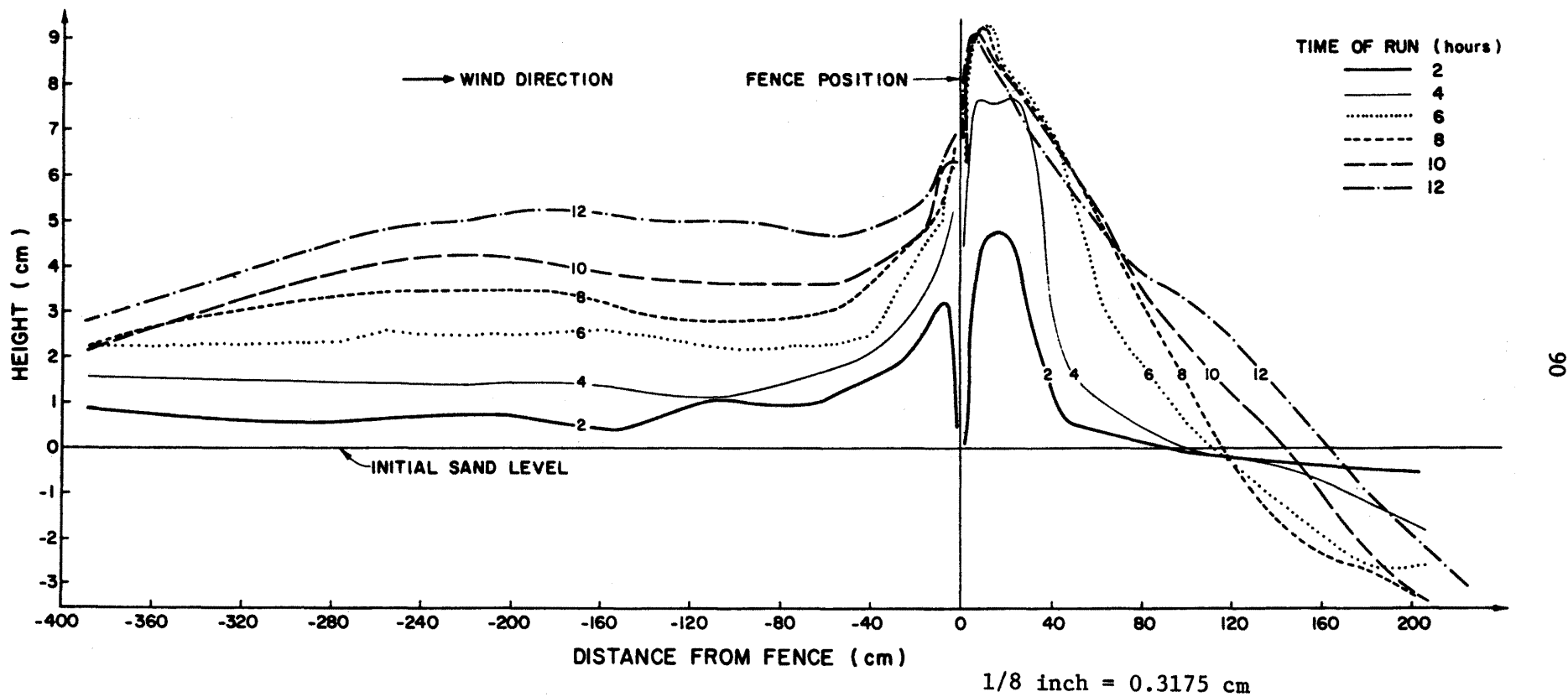


Figure 44. Sand Accumulation Profiles for a 1/8 inch Horizontal Slat Fence with 33% Uniform Porosity and a Subsurface Barrier Installed (Run 11)

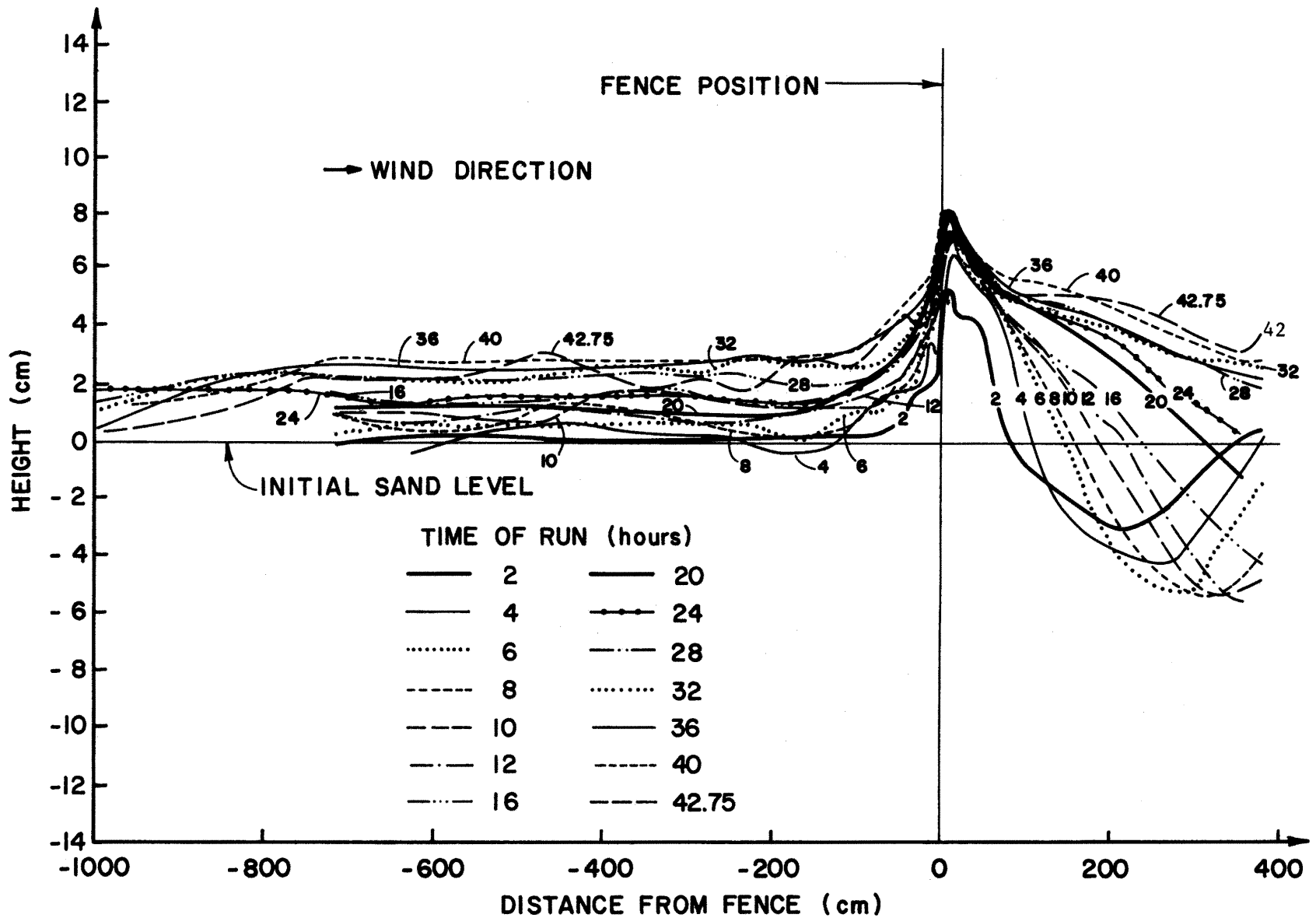


Figure 45. Sand Accumulation Profiles for 1/8 inch Vertical Slat Fence with 60% Uniform Porosity and a Subsurface Barrier Installed (Run 12) (1/8 inch = 0.3175 cm)

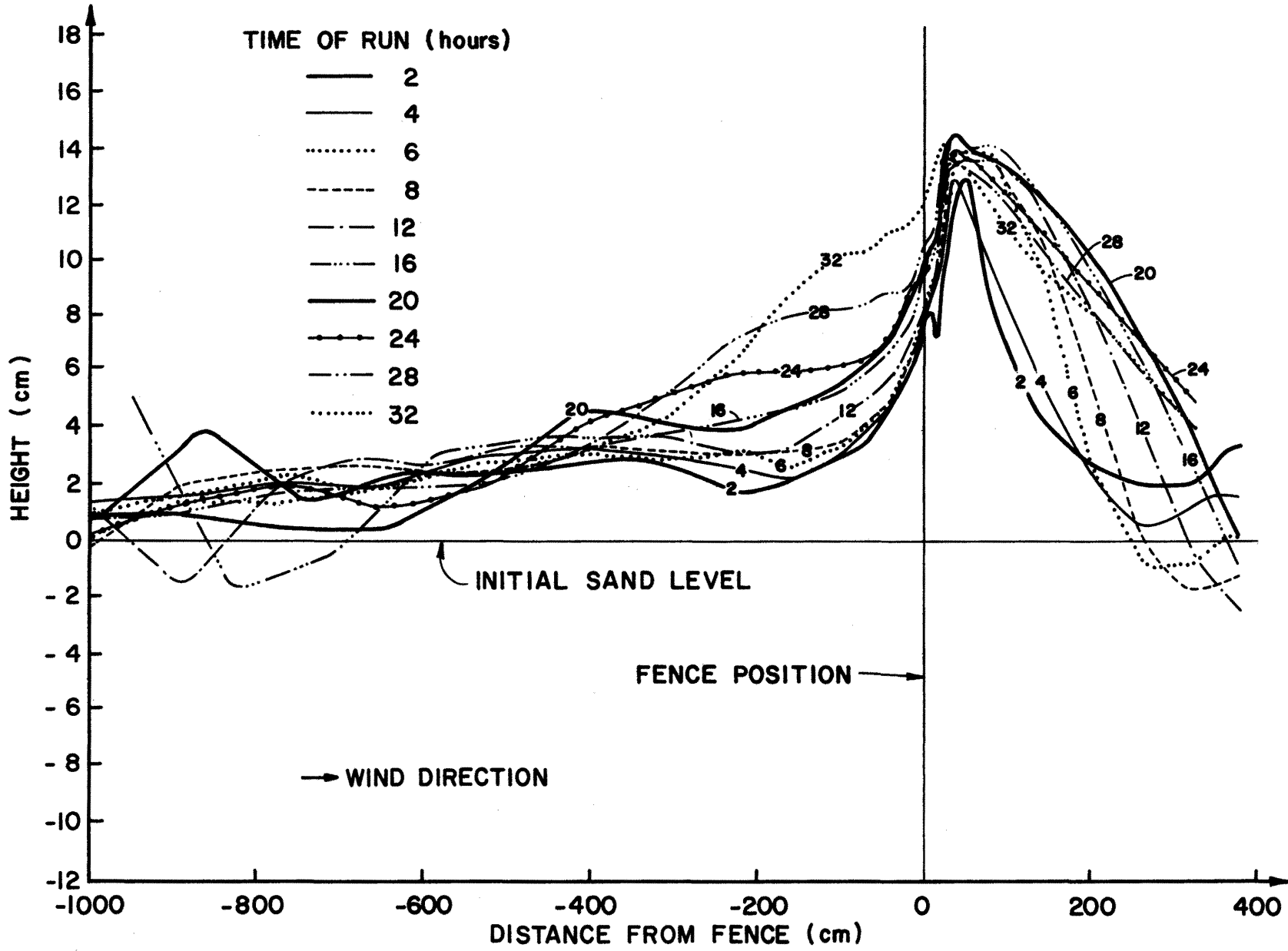


Figure 46. A Sand Fence was Installed at the Top of a Dune which was 10.16 cm Downstream from the First Fence

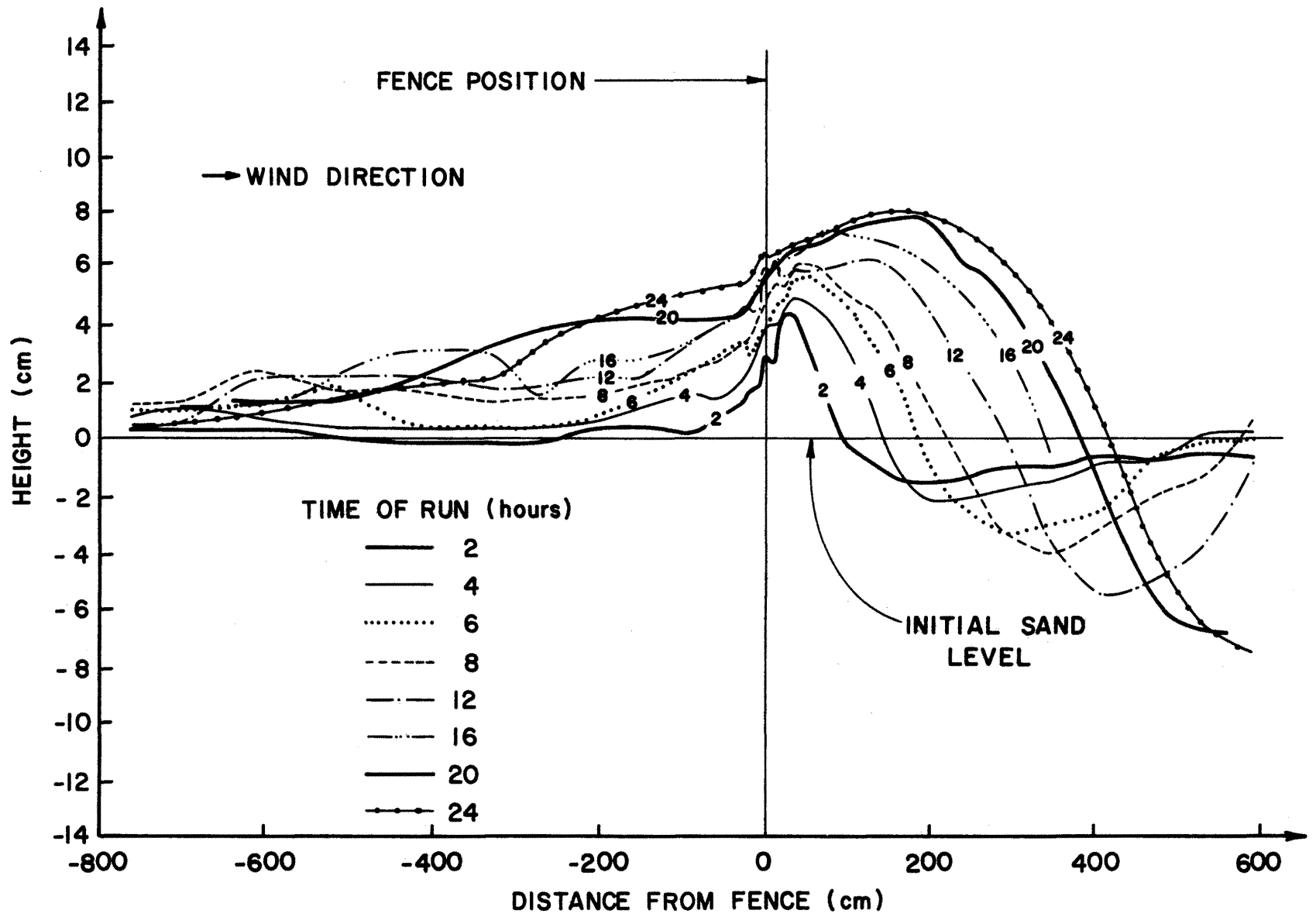


Figure 47. Vertical Spires II with 60% Uniform Porosity with Subsurface Barrier (Run 14)

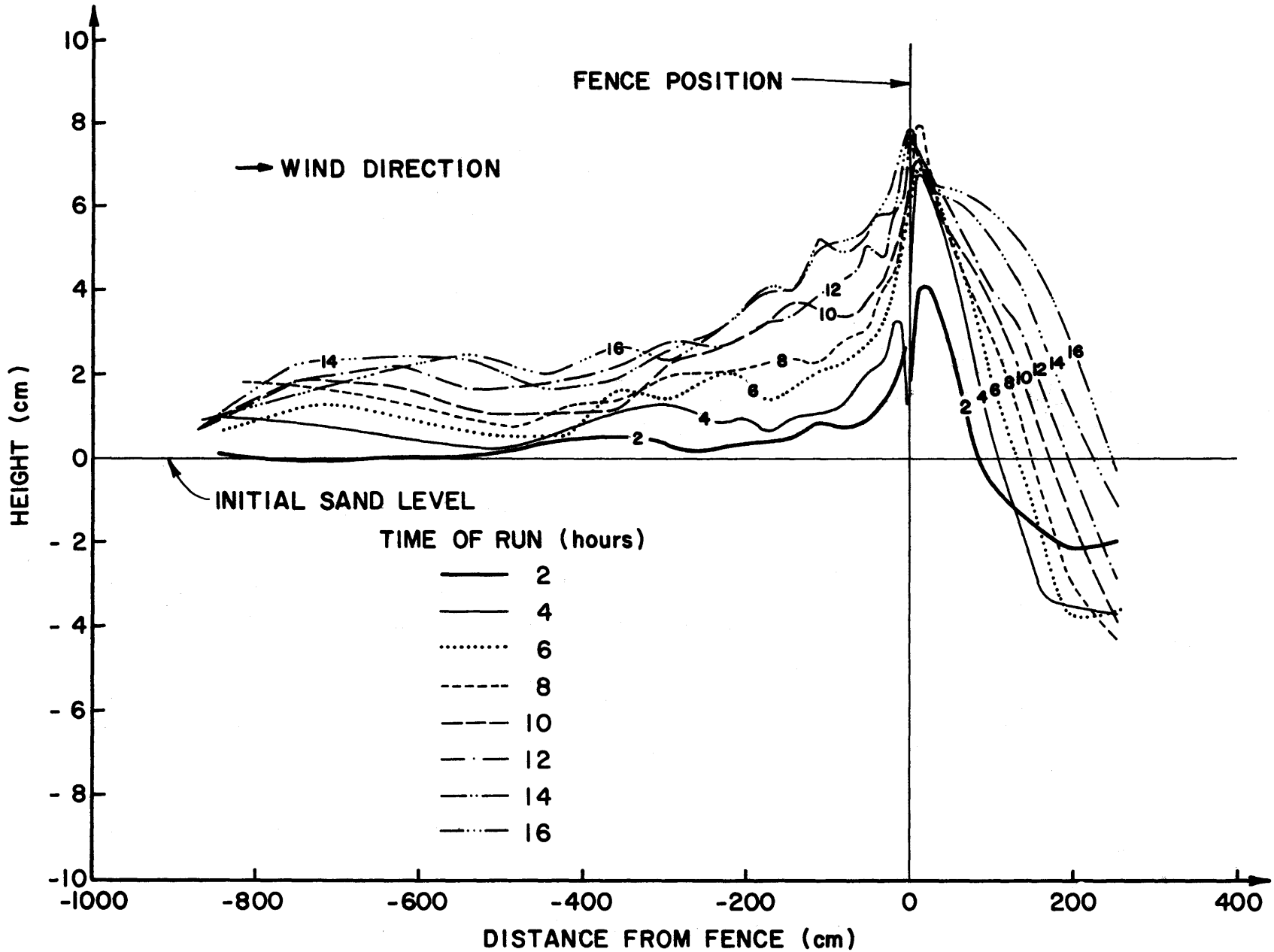


Figure 48. Sand Accumulation Profile with 60% Uniform Porosity and a Subsurface Barrier Installed (Run 15) (30° fence)

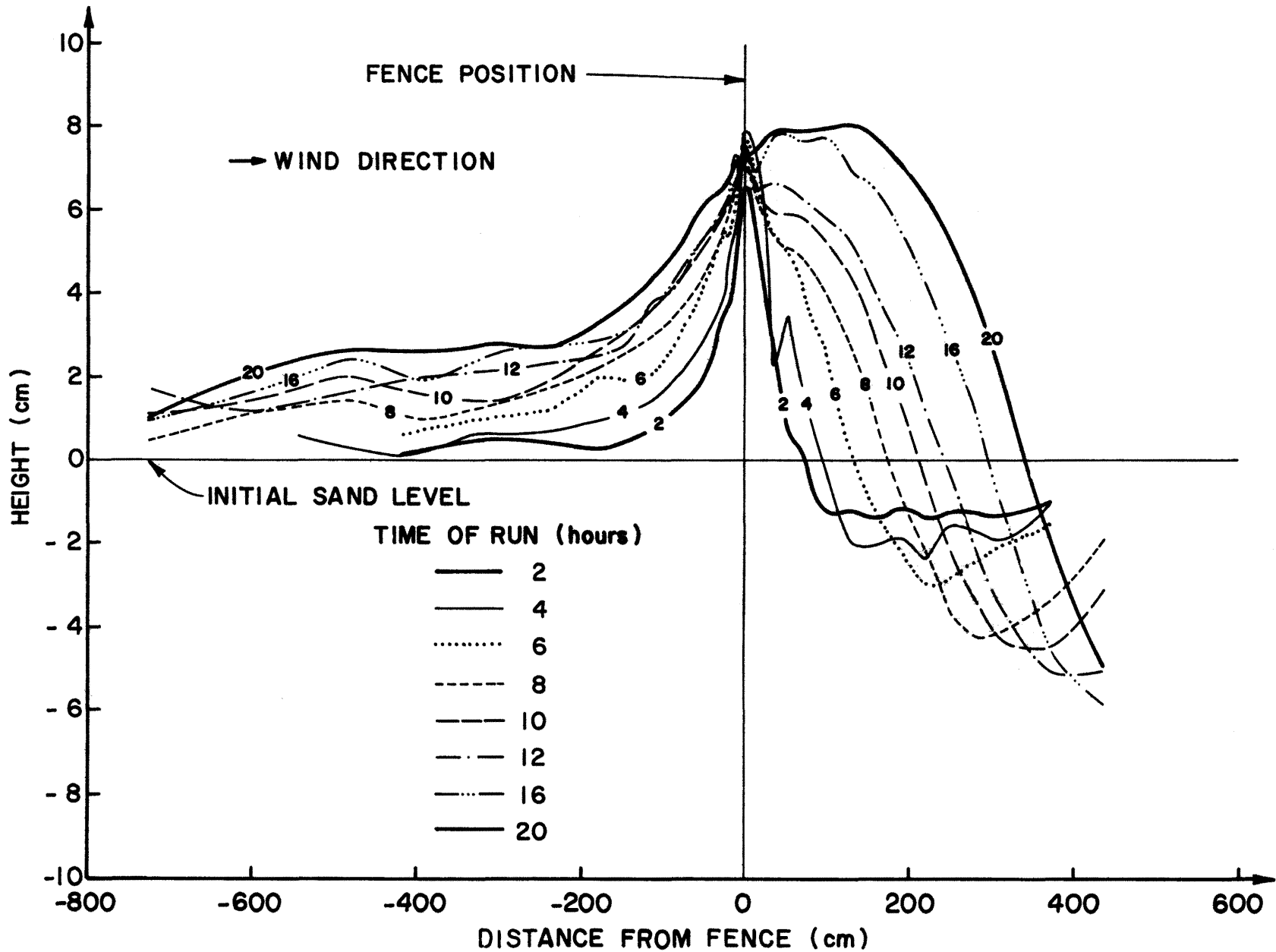


Figure 49. Sand Accumulation Profile with 60% Uniform Porosity and a Subsurface Barrier Installed (Run 16) (60° fence)

As shown in Figure 33, Run 1, with horizontal slats of 1/16 inch, 50 percent porosity and a free stream flow velocity of 8 m/sec and sand accumulation rates in both the upstream and downstream sides of the fence were nearly uniform. Finally, as shown in Figure 50, the center fence was covered with sand.

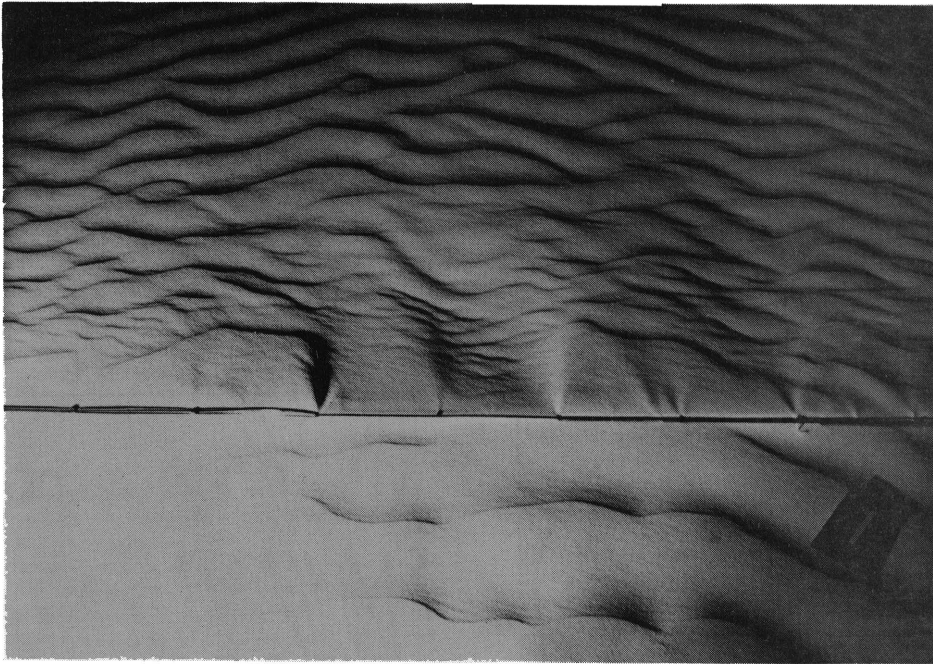


Figure 50. Sand Accumulation Reaching Top of Fence

Run 2 was conducted with horizontal slat of 1/8 inch width, with 50 percent porosity and an extra 20 percent opening at the bottom of the fence. Figure 51 shows the clear danger of allowing a scour hole to develop at the bottom of the fence. Assuming in Figure 51 sand accumulation reached a stable shape downstream from the fence after about 12 hours, the total sand accumulation is much smaller in Run 2 than in Run 1.

The shape of sand accumulation for Runs 1 and 3 is quite similar. Run 3 is for horizontal slat fences with an opening of 20 percent (opening height of 1.55 cm). Figure 35 shows the sand accumulation for this run.

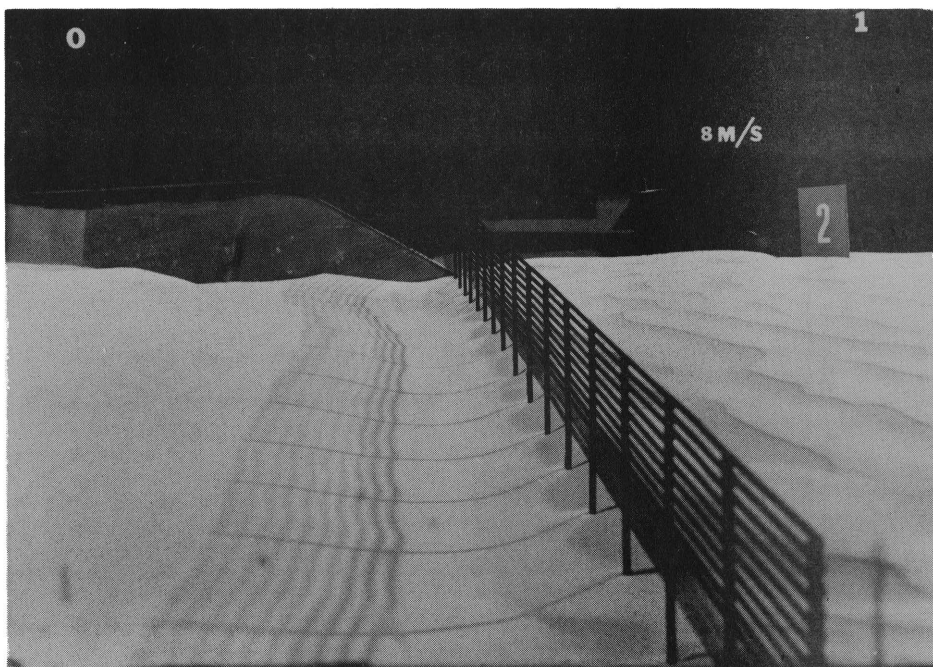


Figure 51. Scour Hole Downstream from Fence in Run 2

A comparison of sand accumulation between Runs 1 and 3 for a total duration of 14 hours is given in Figure 52. The horizontal fence with a bottom opening is more effective than that without the opening.

Figure 53 gives a comparison between Runs 2 and 4. Run 4, without a scour hole, had much less accumulation than Run 2. Although both runs were made with the same horizontal fence, a horizontal barrier was placed underneath the fence in Run 4 to reduce scour.

Runs 5 and 5A were with the same vertical fence, except Run 5A had a barrier to prevent scour. It was interesting to note that a scour hole did initially develop for Run 5, but later was filled. As shown in Figure 54 after 14 hours, the total sand accumulation for both fences was nearly the same, although a scour hole did first appear for Run 5.

Run 6 was made with a solid panel. As shown in Figure 52, the sand accumulated was much less than that for Runs 1 and 3. Figure 55 presents the comparison for sand accumulation between Run 5 (1/8 inch vertical slats)

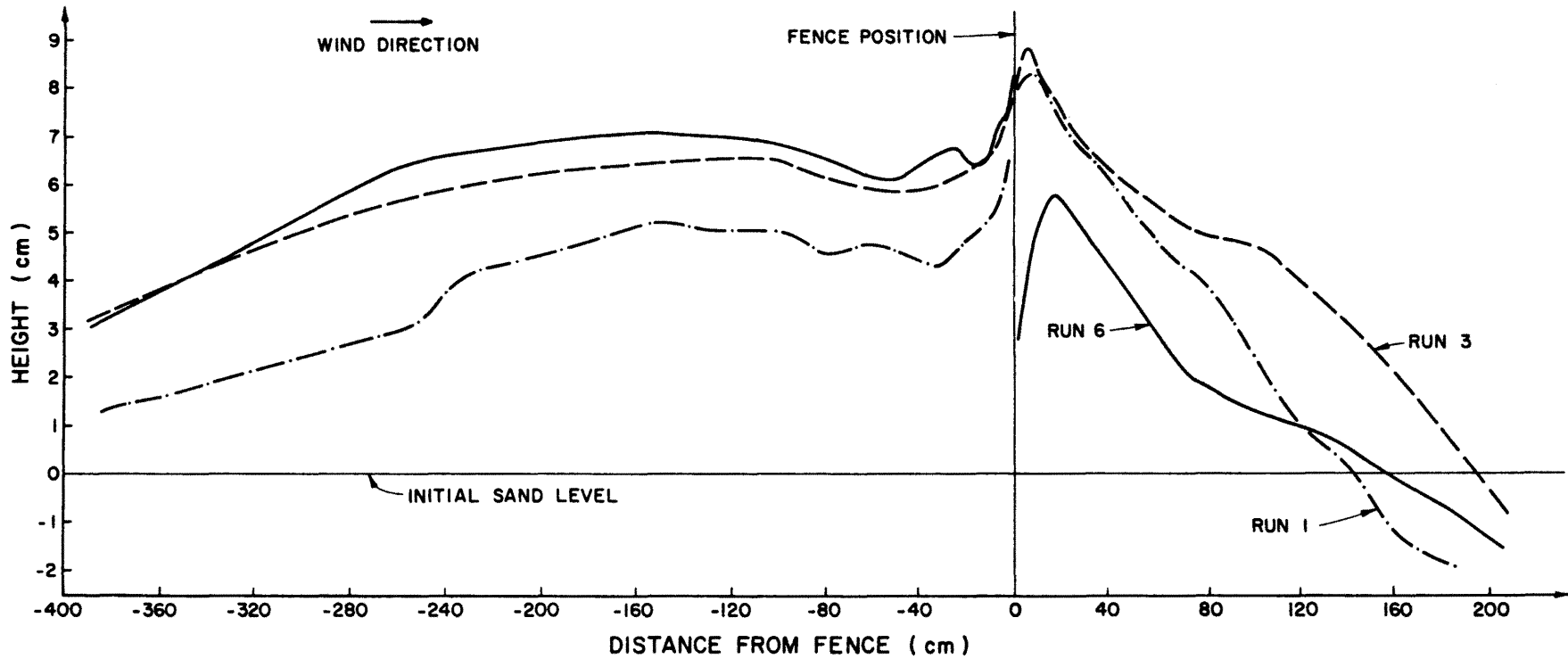


Figure 52. Comparison of Sand Accumulation Profiles to Determine the Effect of an Opening between the Fence and Surface (Runs 1, 3, and 6 at 16 hours)

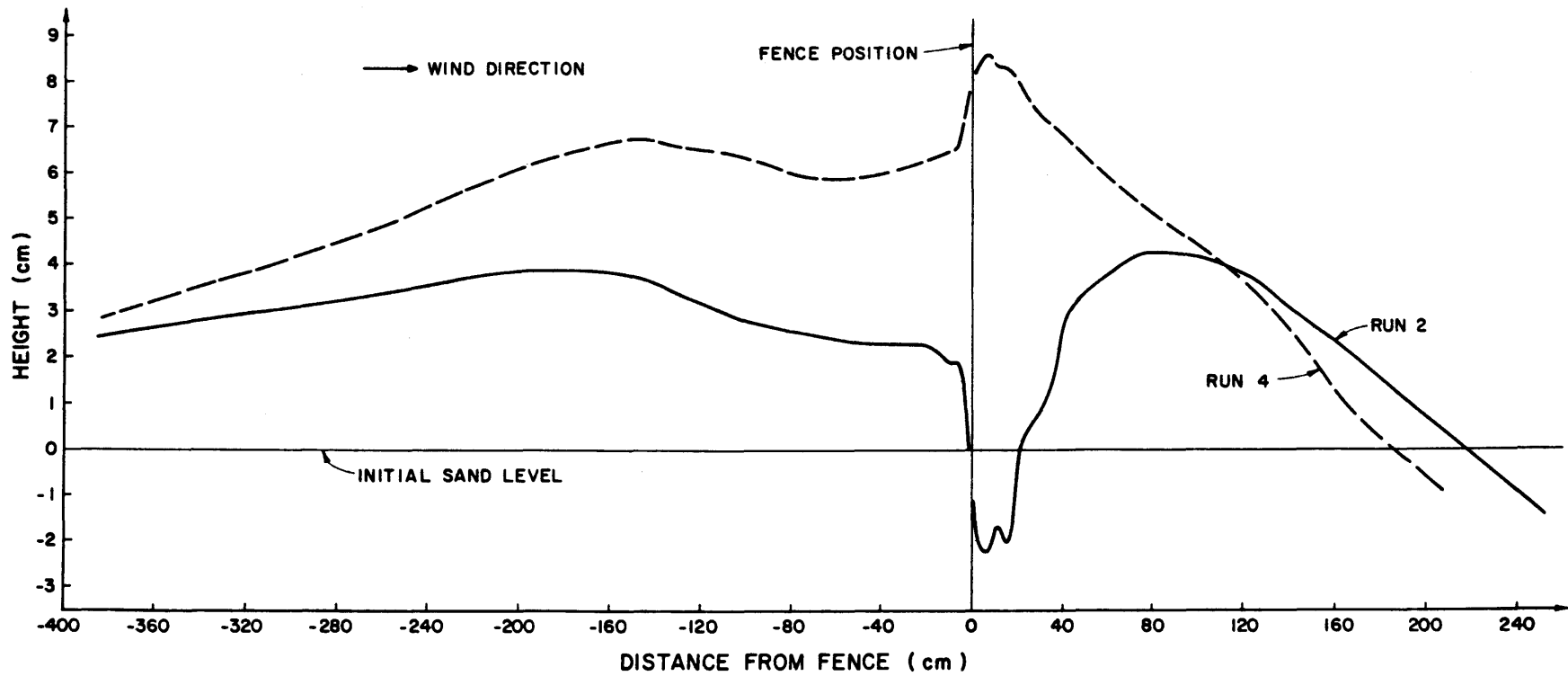


Figure 53. Comparison of Sand Accumulation Profiles to Determine the Effect of a Subsurface Barrier on a Horizontal Slat Fence with 20% Opening at the Bottom (Runs 2 and 4 at 14 hours)

and Run 7 (1/16 inch vertical slats). The width of slats did not yield a different result.

Figure 56 shows that an initial scour hole did develop for Run 7 after 2 hours; however, after 16 hours, the scour hole was almost filled. Figure 57 indicates that there was little difference in sand accumulation between Run 8 with 60 percent porosity and Run 11 with 33 percent porosity for 1/8 inch horizontal slats.

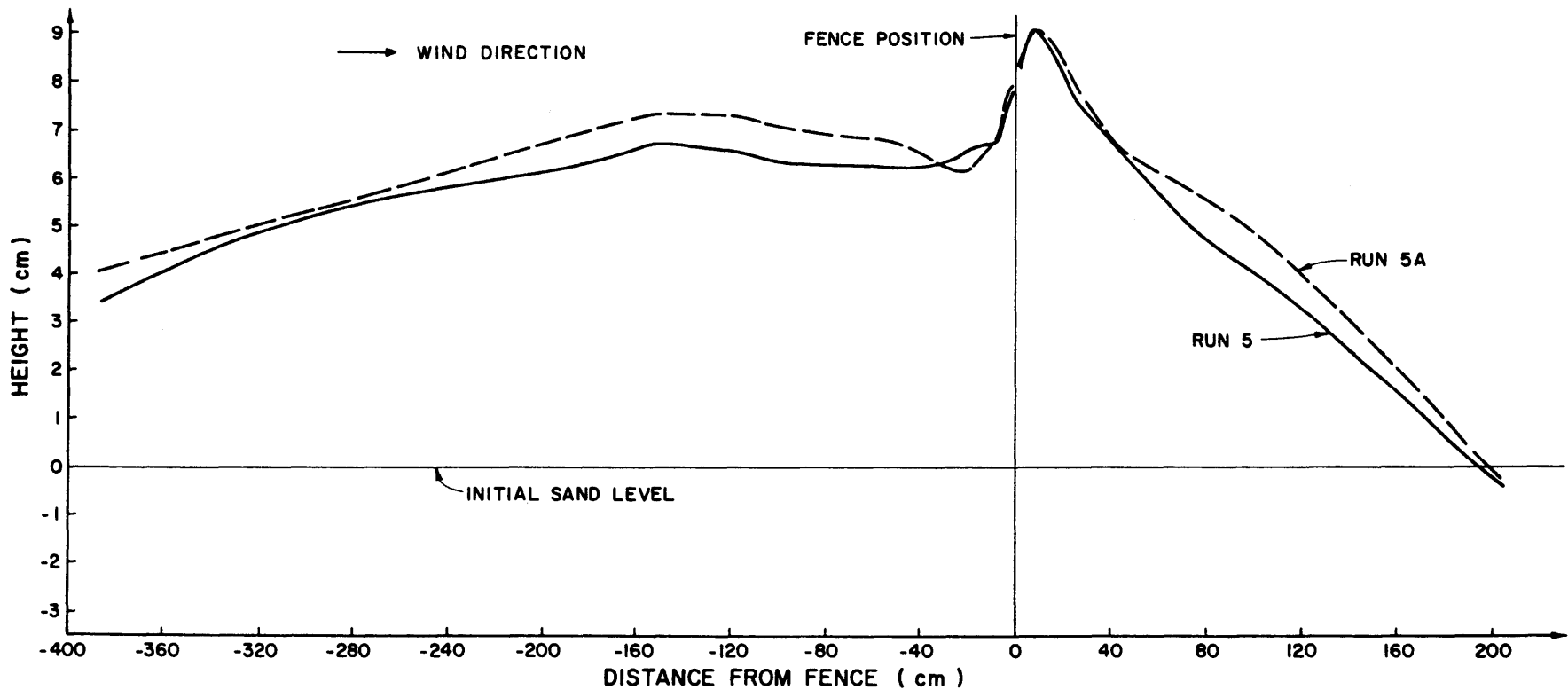


Figure 54. Comparison of Sand Accumulation Profiles to Determine the Effect of a Subsurface Barrier on a Vertical Slat Fence with 50% Uniform Porosity (Runs 5 and 5A at 16 hours)

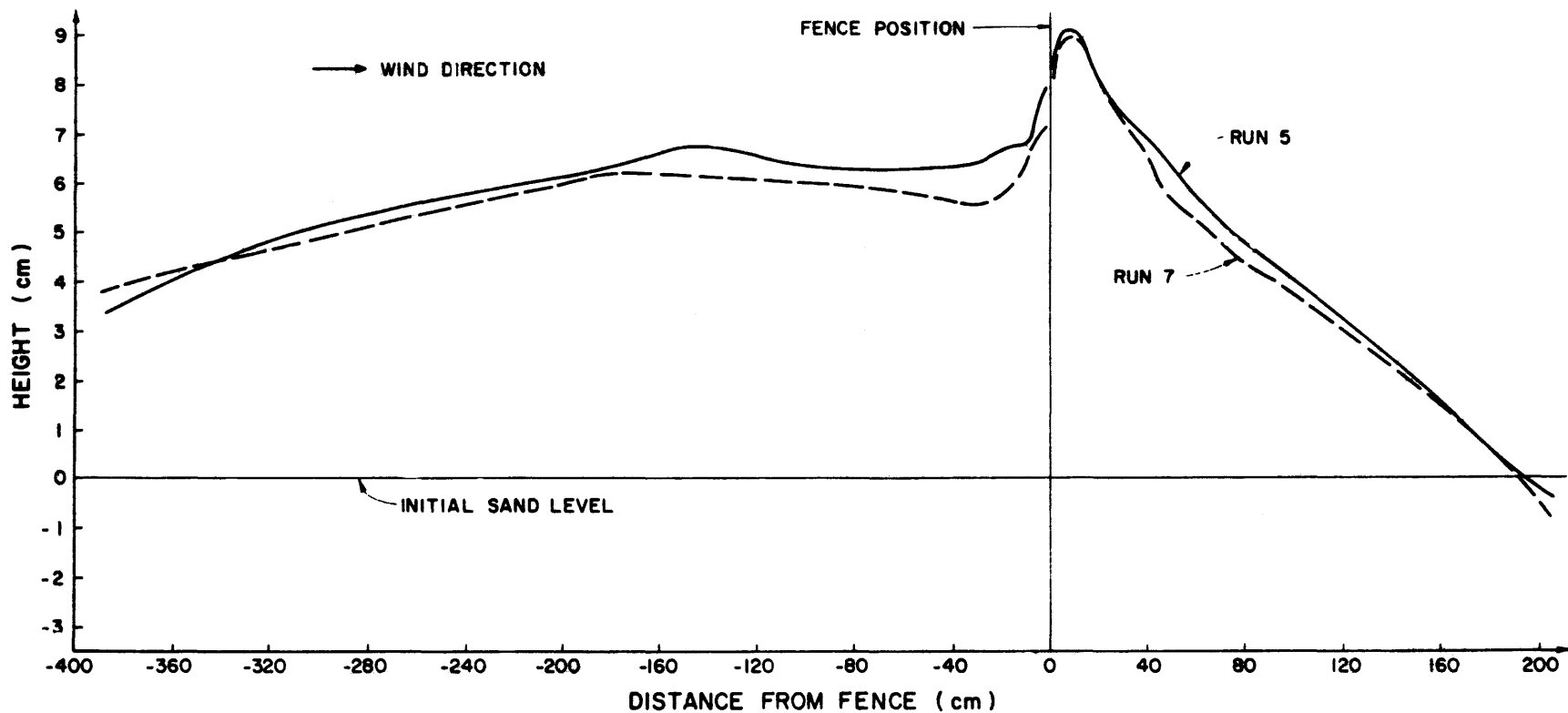


Figure 55. Comparison of Profiles to Illustrate the Effect of a Slat Width on Sand Accumulation (Runs 5 and 7 at 16 hours)

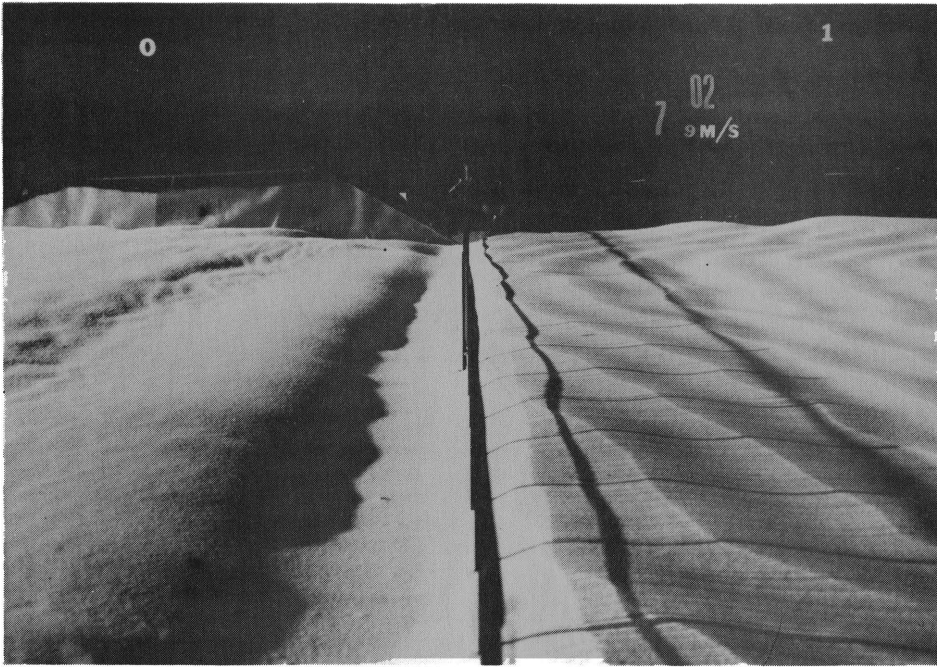


Figure 56a. Run 7 after 2 Hours

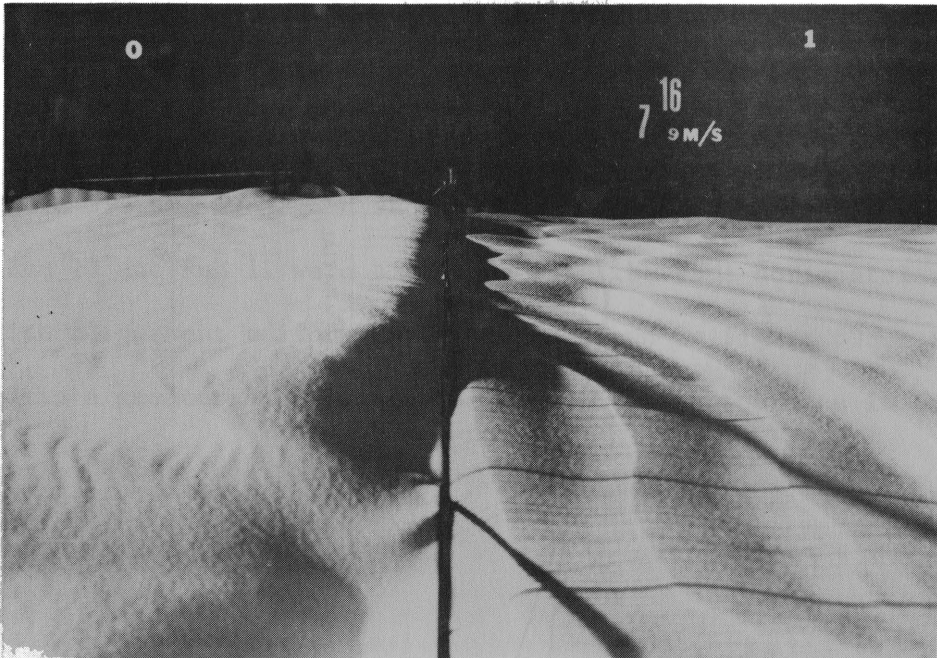


Figure 56b. Run 7 after 16 Hours

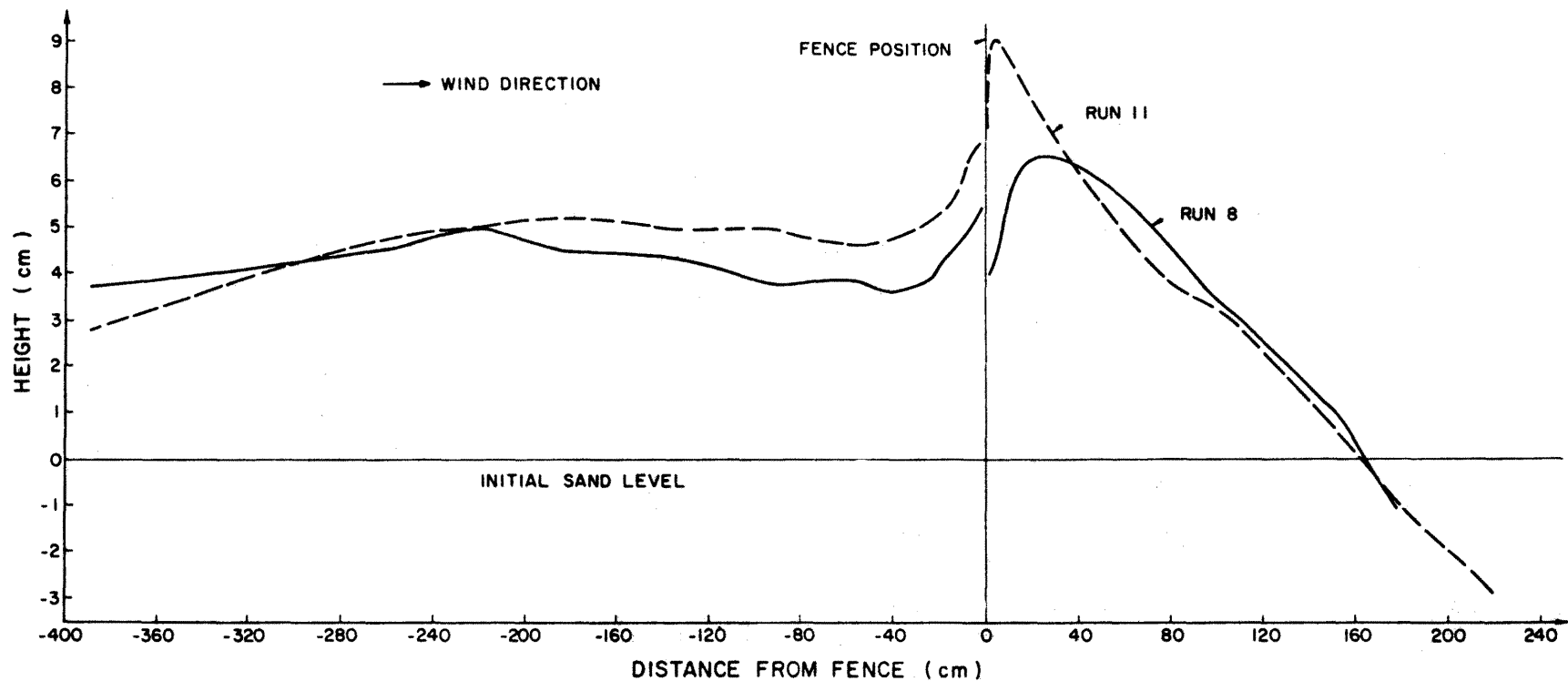


Figure 57. Comparison of Profiles to Illustrate the Effect of Porosity and Sand Accumulation (Runs 8 and 11 at 12 hours)

The vertical spires with 80 percent porosity in Run 9 gave rather poor results. A photograph of Run 9 is shown in Figure 58.

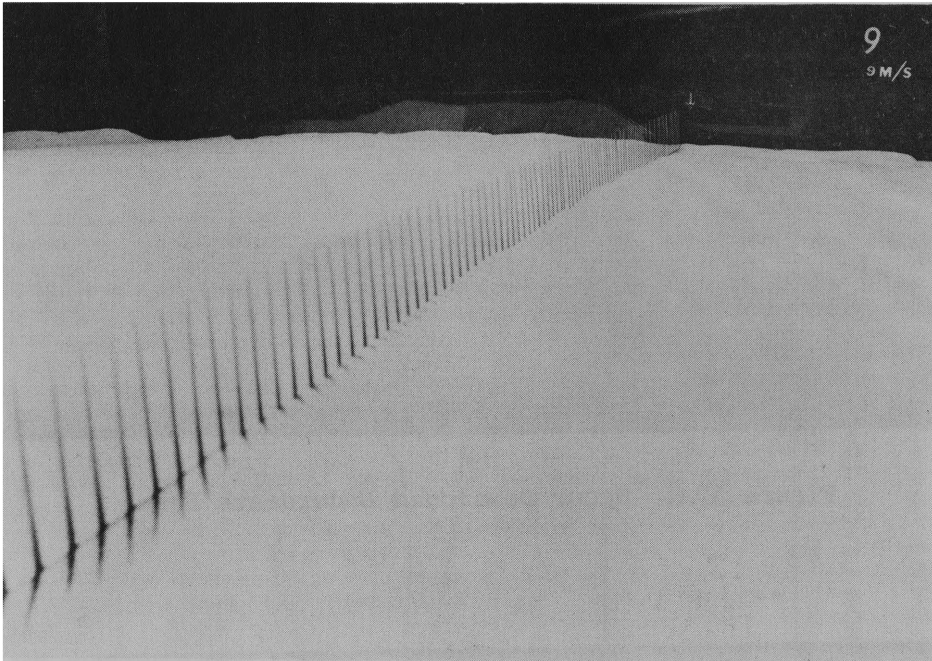


Figure 58. Run 9 with Vertical Spires

Figure 59a and 59b again show the importance of preventing scour hole. Run 10 and Run 11 were both made with the same horizontal slat fence with 33 percent uniform porosity, as shown in Figure 59c. Run 11 resulted in a greater accumulation of sand. The photographs in Figure 59 illustrate these results.

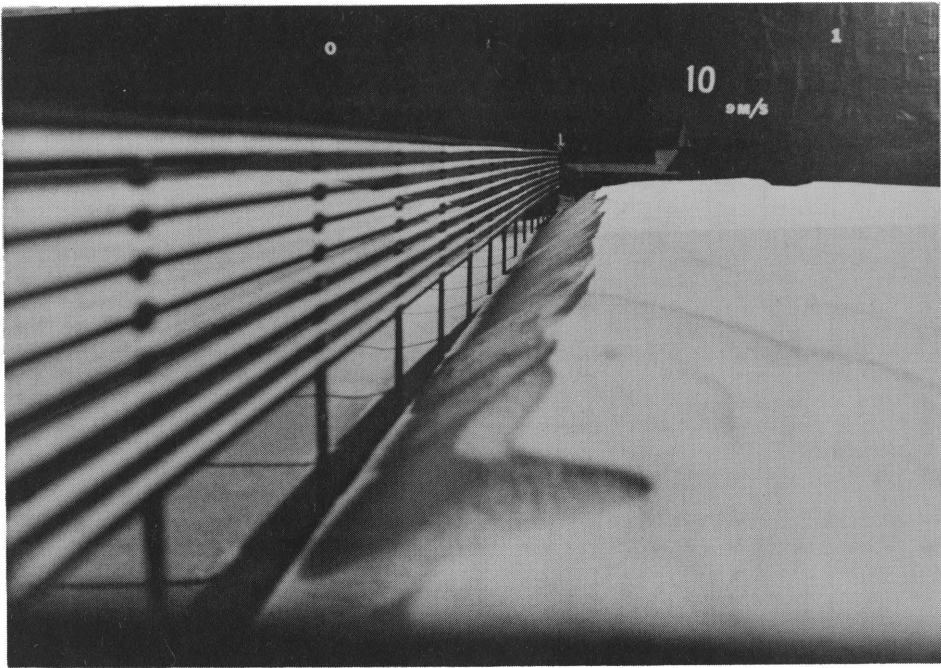


Figure 59a. Scour Developed Underneath Fence

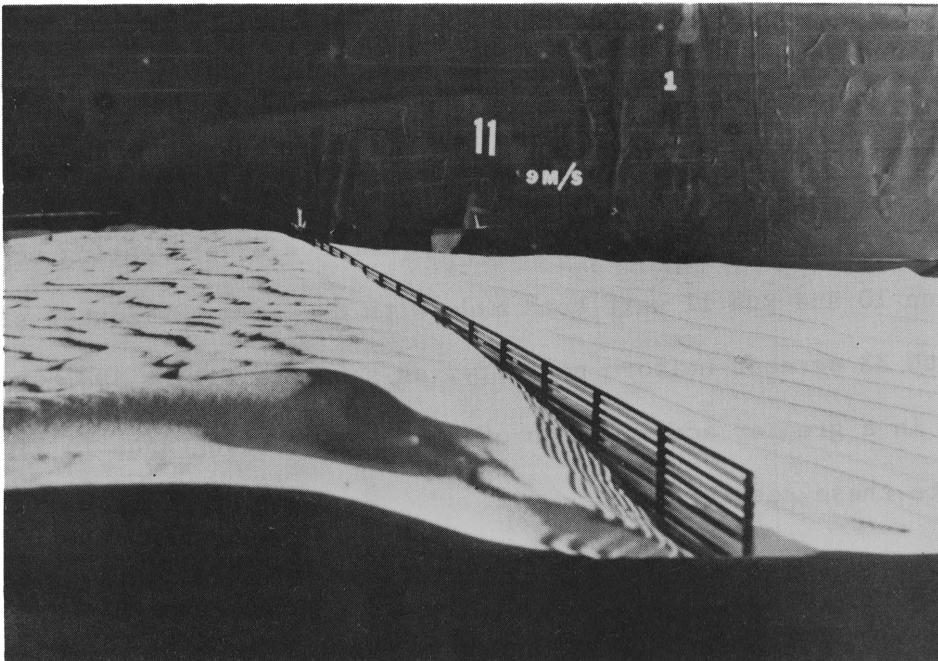


Figure 59b. Sand Accumulation around Fence with Subsurface Barrier to Reduce Scour

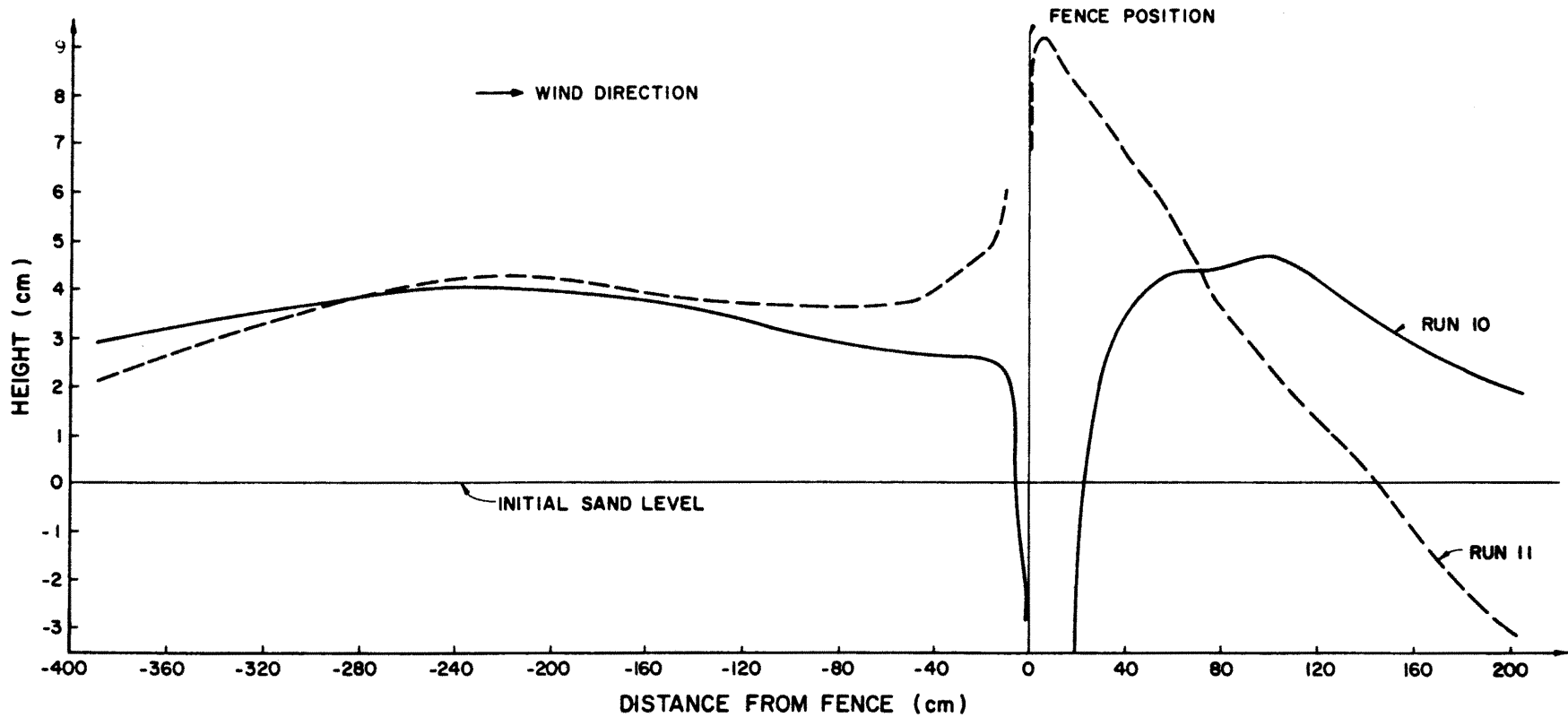


Figure 59c. Comparison of Sand Accumulation Profiles to Determine the Effect of a Subsurface Barrier on a Horizontal Slat Fence with 33% Uniform Porosity (Runs 10 and 11 at 10 hours)

Table 10 shows the total amount of sand accumulation for all 16 runs. For the first twelve runs the porosity, which varied between 33 and 66 percent, did not seem to have a strong influence on the amount of sand accumulation around the fences. Fences with vertical slats provide nearly the same results as fences with horizontal slats with the same uniform porosity. The solid fence and the fence with a porosity of 80 percent gave poor results. It was decided then to use the 60 percent porosity, vertical slat fence for further testing of multiple rows. Runs 12 through 16 were made in the last series of testing during July and August, 1982. Since the vertical slat fence with 60 percent porosity was selected for further testing, a rather long duration of 42 hours run was made with this single row of fences. It was determined that the sand accumulation profile reached an equilibrium shape after 36 hours. Further testing between 36 to 42 hours did not further increase the accumulation of sand.

The following series of preliminary tests were made to provide information on future studies. These were not included in the original proposal. Run 13 was made to conduct a preliminary test on the effect of installing a second fence on top of the first fence. As shown in Figures 46a through 46j, the sand accumulation for a second fence did increase significantly. It is speculated that if the shape of sand accumulation remains similar, a fence of double height may accumulate four times the amount of sand as the fence of regular height. This point should be investigated further.

Run 14 was made to conduct a preliminary test for a special Spire Shape II. Table 10 shows that the sand accumulation around this fence was rather large, and this fence does show great promise. However, the cost of constructing this type of fence may be rather high. Again, this shape should be investigated further.

Table 10. Volume of Sand Deposition in  $\text{cm}^{-3}$  along the Centerline per Unit Centimeter Width for 9 meters/sec Freestream Flow Velocity

| Time of Run (hrs) | Run # 4 | 5       | 5A      | 6       | 7       | 8       | 9       | 10      | 11      | 12      | 13 | 14      | 15      | 16   |
|-------------------|---------|---------|---------|---------|---------|---------|---------|---------|---------|---------|----|---------|---------|------|
| 2                 | 603.27  | 396.67  | 363.62  | 363.62  | 363.62  | 355.35  | 338.82  | 371.88  | 322.30  | 474     |    | 462     | 504.7   | 600  |
| 6                 | 826.40  | 694.18  |         | 785.08  | 1148.70 | 1082.58 | 785.08  | 1090.85 | 1264.39 | 1084    |    | 1297    | 1384.46 | 1372 |
| 10                | 2123.85 | 1661.06 | 1801.55 | 942.93  | 1148.7  | 1479.26 | 1156.96 | 1429.67 | 1743.70 | 1509.99 |    | 2148    | 1942    | 2158 |
| 16                | 2495.73 | 2446.14 | 2718.86 | 2132.11 | 2348.98 | 2289.13 |         |         |         | 1833.7  |    | 3400    | 2864    | 3132 |
| 20                | 2784.97 |         |         |         |         | 2611.42 |         |         |         | 2003.95 |    |         |         | 3794 |
| 24                |         |         |         |         |         |         |         |         |         | 2327    |    | 4339.74 |         |      |
| 28                |         |         |         |         |         |         |         |         |         | 2865    |    |         |         |      |
| 32                |         |         |         |         |         |         |         |         |         | 3083    |    |         |         |      |
| 36                |         |         |         |         |         |         |         |         |         | 3168    |    |         |         |      |
| 40                |         |         |         |         |         |         |         |         |         | 3486    |    |         |         |      |
| 42                |         |         |         |         |         |         |         |         |         | 3222    |    |         |         |      |

Runs 15 and 16 were made to conduct preliminary tests for fences set at an angle from the flow directions. It was difficult to determine the effects of these inclined angles with the sand accumulations around fences.

#### G. Conclusions

##### Sand Fences, Single Rows

- 1). It is important that formation of scour holes beneath the sand fences be prevented;
- 2). A horizontal slat fence with a bottom opening of 1.55 cm which is about half the moving sand layer depth is the most effective, although a scour hole can be easily created by the bottom opening;
- 3). The porosity variation with 33 percent to 66 percent did not seem to have a strong influence on the amount of sand accumulation around the fences. Thus, a vertical slat with 60 percent porosity is chosen for the testing of multiple rows of fences;
- 4). Fences with vertical slats provide nearly the same results as fences with horizontal slats with the same uniform porosity;
- 5). The vertical spire fence with a porosity of 80 percent gave poor results;
- 6). The solid fence gave rather poor results;
- 7). The vertical spiral fence II with 50 percent porosity showed promising results, and this fence should be investigated further;
- 8). One fence on top of another increased sand accumulation significantly. Further testing is necessary to investigate the benefit of having taller fences or multiple rows of fences.
- 9). Two preliminary tests for sand accumulation around fences set at an angle from the flow direction did not provide sufficient data for analysis.

## VI. MULTIPLE ROWS OF FENCES

### A. Brief Description of Previous Studies

Savage (1963) studied the sand accumulations for different types of fences for single row and multiple rows for a period of one year. Unfortunately, this time period of one year was too short to draw definite conclusions about the performances of double fences to trap sand. The following Table 11 gives the sand accumulations for different types of fences. The sand accumulation around double and triple rows of fences did not improve significantly over the sand accumulation around single fences, as shown in Table 8. Perhaps this can be better shown with the following two typical sand accumulation profiles, shown in Figures 60 and 61. Most of the sand particles accumulated around the first row of fences and a very insignificant amount of sand particles were trapped by the second row of fences. Straight brush fences, zigzag brush fences, and zigzag snow fences appear to perform the best of the double fences. Brush fences with 25 percent porosity appeared to perform the best of the single row fences.

Manohar and Brunn (1970) found that double rows of fences with a distance of  $4H$  between the two rows of fences are a rather effective method to trap sand.  $H$  is the height of each fence. The actual amount of sand accumulations behind the fences at velocity between 11 to 13 meters per second were greater than the sand accumulations for lower flow velocity; this was particularly true with more than two rows of fences. They also found excessive scour between the rows of fences.

Tabler (1973) stated that multiple rows of fences should be spaced at least  $35H$  apart. Gandemer (1981) found that two screens with porosities of 50 percent, lengths of 120 meters, and heights of 5 meters with spacing of 5 meters give maximum protection as wind breakers.

Table 11. Sand Accumulation around Fences, Multiple Rows, after Savage (1963)

---

| <u>Double Fence Sections</u> |                                      |             |
|------------------------------|--------------------------------------|-------------|
| H.                           | Straight Brush 50-ft. spacing        | 2.96        |
| I.                           | Straight Snow 25-ft. spacing         | 2.43        |
| G.                           | Straight Snow 50-ft. spacing         | 2.86        |
| J.                           | Straight Brush 25-ft spacing         | 2.23        |
| O.                           | Zigzag Brush 50-ft. spacing          | 3.25        |
| N.                           | Zigzag Snow 50-ft. spacing           | <u>3.12</u> |
|                              | Average of all double fence sections | 2.81        |
| <u>Triple Fence Sections</u> |                                      |             |
| M.                           | Straight Snow 50-ft. spacing         | 2.80        |

---

25 feet = 7.62 m; 50 feet = 15.24 m.

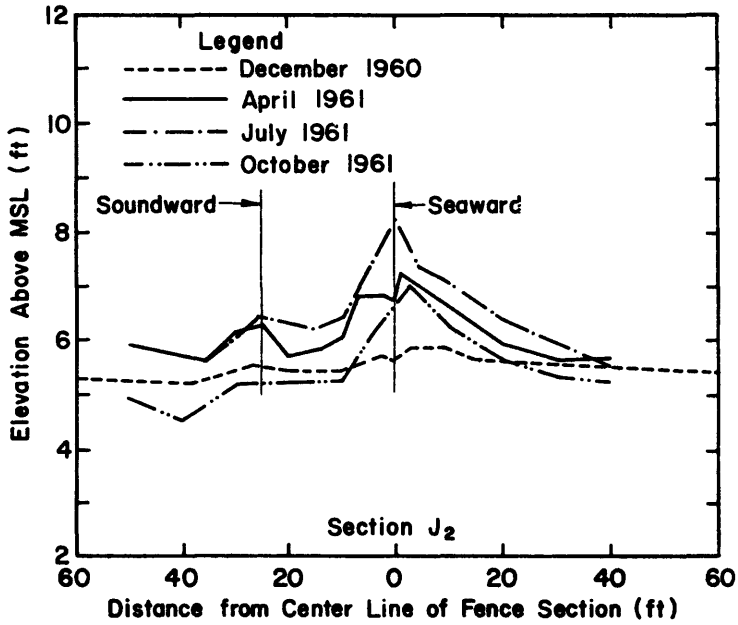


Figure 60. Typical Sand Accumulation Profiles, Double Fence Section, 25-foot Spacing

1 foot=30.48 cm  
 25 feet= 7.62 m  
 50 feet=15.24 m

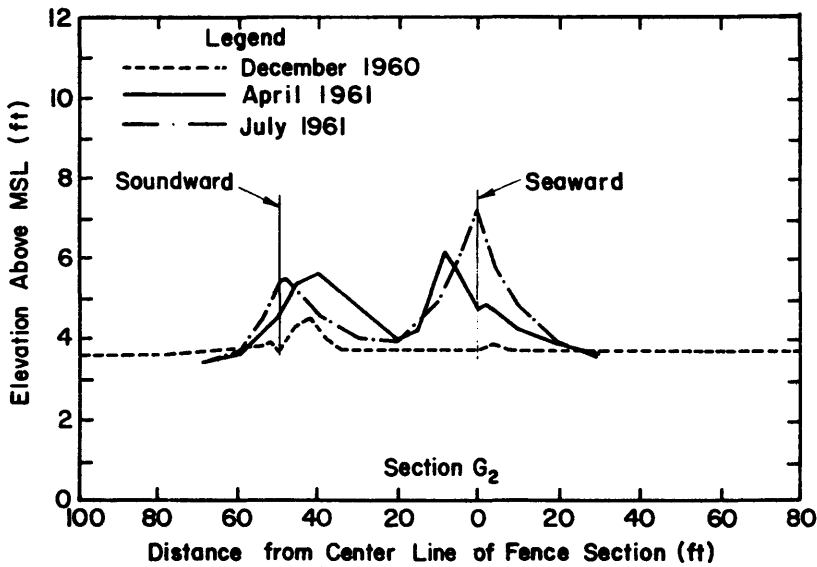


Figure 61. Typical Sand Accumulation Profiles, Double Fence Section, 50-foot Spacing

## B. Testing Program

The following three cases are considered.

Case 1). If two rows of fences are placed very far apart, each row of fence will behave independently from the other row, as shown in the following sketch.

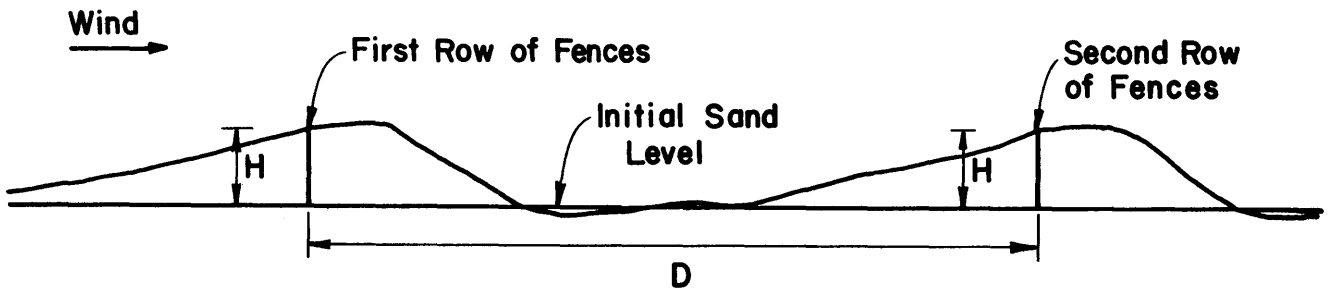


Figure 62. Sand Accumulation for Two Fences, Acting as Two Individual Rows

From examination of the sand accumulation around a single row of fence,  $D/H$  value should be around 80.

Case 2). If two rows of fences are placed too close together, the total accumulation around the two fences will be less than Case 1 (see Figure 63).

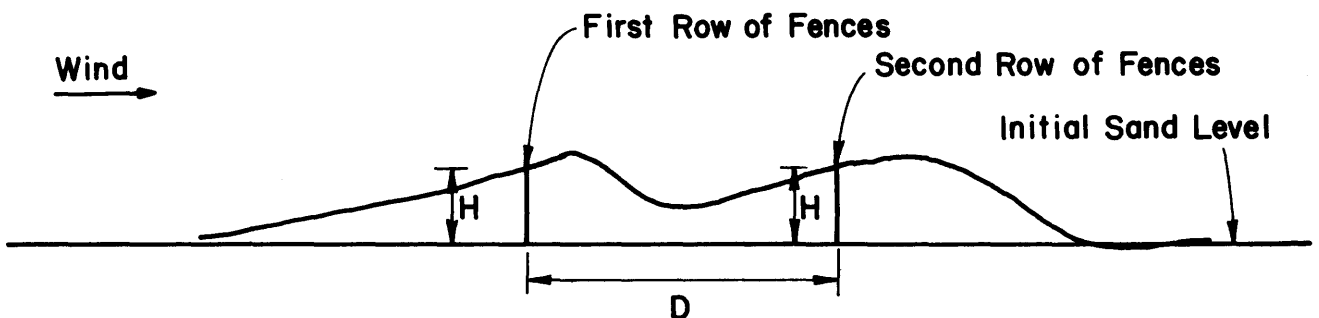


Figure 63. Sand Accumulation for Two Rows of Fences Acting Together

Case 3). The optimum spacing between the two rows of fences will probably be the maximum  $D/H$  distance so that the two rows of fences will still assist one another to trap sand. Fences with vertical slats and 60 percent porosity were selected for all testing since they behaved approximately as efficiently as the other shapes and are less expensive to construct.

### C. Experimental Results

Nine runs, 21 through 29, were made for these multiple fences. In the first six runs, the  $D/H$  values between the two rows of fences were 4, 8, 12, 20, 40, and 80. Runs 27 and 28 were for three rows of fences with the distances between any two rows of fences set at  $20H$  and  $40H$ , respectively. In all the above eight runs, the rows of fences were placed across the entire tunnel width. Run 29 was conducted with two rows of fences with the centerline of the first row of fence remaining open, as shown below.

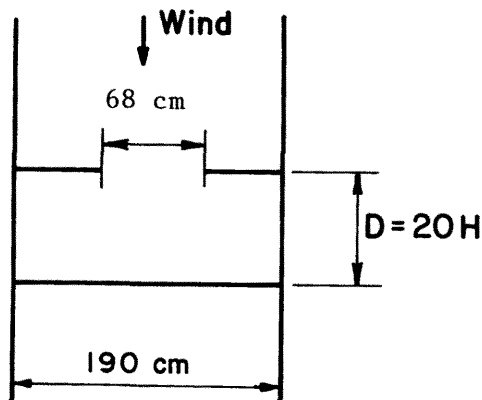


Figure 64. Schematic Diagram for Top View of Staggered Fence

Results of all sand accumulation for multiple fences are shown in Table 12. Run 25 for  $D/H = 40$  for both double and triple rows of fences seemed to provide the best results.

Thus, Run 25 was conducted over the longest duration. At about 46 to 50 hours, the equilibrium sand deposition shape reached a constant profile. Further testing did not further increase sand accumulation.

It was not clear why the staggered fences pattern as performed in Run 29 resulted in such a large amount of accumulation. This point should be investigated further.

#### D. Analysis and Conclusions

##### Multiple Rows:

1). It is quite clear from our testing that the spacing between any two rows of fences should be in the neighborhood of 40 fence heights. If the two fences are set more than this spacing, the two fences will act independently. If the fences are set too close together, a smaller amount of sand will be trapped.

2). For the first two hours, more than 90 percent of the sand particles were trapped by the double fences. The trap efficiency decreased to about 50 percent after 14 hours for double fences with  $D/H = 40$ , where  $D$  is the spacing between fences and  $H$  is the fence height. The total amount of sand moved during the first 14 hours was  $4,312 \text{ cm}^3/\text{unit}$  centimeter width. The total amount of sand trapped for this period of 14 hours for double fences with  $D/H = 4, 12, 20, 40, \text{ and } 80$  were respectively 38%, 44%, 51%, 59%, and 29%.

3). For a duration of about 50 hours, the total sand trapped for double fences with  $D/H = 40$  was  $6,433 \text{ cm}^3/\text{unit}$  cm width. This was about 42% of the total sand movements toward the fences.

Table 12. Sand Accumulation for Different Fence Spacings in Cubic Centimeters per Unit of Width along the Centerline of the Wind Tunnel (multiple rows)

| Time (hrs) | Run #21<br>D/H=4 | Run #22<br>D/H=8 | Run #23<br>D/H=12 | Run #24<br>D/H=20 | Run #25<br>D/H=40 | Run #26<br>D/H=80 | Run #27<br>TRIPLE 20H | Run #28<br>TRIPLE 40H | Run #29<br>STAGGERED | Estimated total<br>sand transport |
|------------|------------------|------------------|-------------------|-------------------|-------------------|-------------------|-----------------------|-----------------------|----------------------|-----------------------------------|
| 2          | 536.79           | 423.2            | 563.82            | 571.34            | 655.15            | 574.97            | 493.23                | 384.92                | 460.04               | 616                               |
| 4          | 780.69           | 767.99           | 1128.69           | 1081.44           | 1171.12           | 942.69            | 1084.52               | 903.43                | 920.72               | 1232                              |
| 6          | 950.34           | 1073.74          | 1334.88           | 1424.18           | 1508.61           | 1328.07           | 1749.77               | 1549.28               | 1286.34              | 1848                              |
| 8          | 1150.4           | 1271.44          | 1508.34           | 1694.66           | 1917.36           | 1473.94           | 2469.01               | 2015.06               | 1640.04              | 2464                              |
| 10         | 1228.76          | 1373.48          | 1748.96           | 1985.8            | 2687.22           | 1603.95           | 2990.48               | 2523.95               | 1905.92              | 3080                              |
| 12         | 1454.6           |                  | 1736.84           | 2101.5            | 2645.59           | 1721.24           | 3402.73               | 3087.44               | 2270.97              | 3696                              |
| 14         | 1659.25          |                  | 1879.08           | 2186.73           | 2536              | 1239.55           |                       |                       | 2911.93              | 4312                              |
| 16         | 1733.99          |                  |                   |                   | 3275.64           | 1792.08           | 3786.9                | 3835.41               |                      | 4928                              |
| 18         | 1743.94          |                  |                   |                   | 3713.97           | 1950.14           |                       |                       |                      | 5544                              |
| 20         |                  |                  |                   |                   | 3902.13           |                   | 4521.06               | 4695.71               |                      | 6160                              |
| 22         |                  |                  |                   |                   | 3946.77           |                   |                       |                       |                      | 6776                              |
| 24         |                  |                  |                   |                   |                   |                   |                       | 5390.85               |                      | 7392                              |
| 26         |                  |                  |                   |                   | 4113.97           |                   |                       |                       |                      | 8008                              |
| 28         |                  |                  |                   |                   |                   |                   |                       | 5987.82               |                      | 8624                              |
| 30         |                  |                  |                   |                   | 4568.96           |                   |                       |                       |                      | 9240                              |
| 32         |                  |                  |                   |                   |                   |                   |                       | 7747.17               |                      | 9856                              |
| 34         |                  |                  |                   |                   | 4911.49           |                   |                       |                       |                      | 10472                             |
| 36         |                  |                  |                   |                   |                   |                   |                       |                       |                      | 11088                             |
| 38         |                  |                  |                   |                   | 5456.71           |                   |                       |                       |                      | 11704                             |
| 40         |                  |                  |                   |                   |                   |                   |                       |                       |                      | 12320                             |
| 42         |                  |                  |                   |                   | 6120.39           |                   |                       |                       |                      | 12936                             |
| 46         |                  |                  |                   |                   | 6339.27           |                   |                       |                       |                      | 14168                             |
| 50         |                  |                  |                   |                   | 6433.51           |                   |                       |                       |                      | 15400                             |
| 54         |                  |                  |                   |                   | 5742.48           |                   |                       |                       |                      | 16632                             |
| 58         |                  |                  |                   |                   | 5929.36           |                   |                       |                       |                      | 17864                             |
| 62         |                  |                  |                   |                   | 6278.26           |                   |                       |                       |                      | 19096                             |

4). For a duration of 32 hours, the total sand trapped for double rows of fences ( $D/H = 40$ ) was about  $4,700 \text{ cm}^3/\text{cm}$  and the total sand trapped by triple rows of fences, with a spacing of  $D/H = 40$ , was  $7,747 \text{ cm}^3/\text{cm}$ . These values were 48 percent and 79 percent of the total amount of sand transported toward the fences during this 32 hours. According to these values, it is not sufficient to build just two or three rows of fences because a significant amount of sand still would escape from these fences.

5). Eight rows of fences at  $D/H = 40$  apart would reduce the amount of sand downstream from last fences to about 6.5 percent of the original amount that move toward the first row of fences. Six rows of fences at  $D/H = 40$  apart would reduce the amount of sand downstream from last fences to about 12.5 percent of the original amount that move toward the first row of fences.

6). Although we never tested the effect of dune movements on sand accumulations near fences, it appeared that this effect is rather significant and should definitely be studied if this situation may occur in the field.

## VII. APPLICATION OF WIND-TUNNEL TEST RESULTS TO THE PROTECTION OF THE AIRFIELD

The correct approach to derive the prototype-modeling similitude ratios is i) first to conduct a comprehensive series of wind-tunnel tests, ii) next, to perform a thorough theoretical analysis, and iii) then, to verify theoretical analysis with field data. Iversen (1981) attempted to derive drifting-snow similitude based on glass spheres and shells with different model scales. He used a rather complicated dimensionless number of parameters to define the drift area.

Actually, the useful life of a fence in the field may be estimated from the following procedure:

Assumption 1:  $q$ , the sand transport rate per unit width varies with either the third power of the  $U_*$  shear velocity of the flow or the free stream velocity.

$$q_m = k_{1m} U_{*m}^3 \quad (10)$$

or

$$q_m = k_{2m} U_{100m}^3 \quad (11)$$

and

$$q_p = k_{1p} U_{*p}^3 \quad (12)$$

$$q_p = k_{2p} U_{300p}^3 \quad (13)$$

The subscripts  $m$  and  $p$  refer to the model and the prototype, respectively.

Assumption 2: the equilibrium sand accumulation shape remains the same for field and laboratory. In other words, the ratio of  $V$ , total sand accumulation per unit width is:

$$\frac{V_p}{V_m} \propto \left(\frac{H_p}{H_m}\right)^2 \quad (14)$$

where  $H$  is the height of the fence.

According to the above two assumptions,

$$q_m t_m = V_m \quad (15)$$

$$q_p t_p = V_p \quad (16)$$

$$\frac{t_p}{t_m} = \frac{V_p/q_p}{V_m/q_m} \propto \left(\frac{H_p}{H_m}\right)^2 \frac{k_{2m} U_{100}^3}{k_{2p} U_{300}^3} \quad (17)$$

For the same flow velocity, sand characteristics and sand fences,

$$\frac{t_p}{t_m} = \left(\frac{H_p}{H_m}\right)^2 \quad (18)$$

For a prototype-model ratio of 31:1 as we used, the time scale between prototype and model should be,

$$t_p = 31^2 t_m = 961 t_m \text{ or } 1,000 t_m \quad (19)$$

Of course, this time scale factor must be verified by field tests. At this point, one must emphasize the importance of collecting reliable field samples. One should also compare field data with laboratory data. The basic two assumptions used to derive the time scale factors could be modified by field data and thus Equation (17) is subject to change.

## VIII. FUTURE RESEARCH NEEDS

### A. Roadway

A critical problem is the applicability of laboratory testing data to field conditions. The correct approach is to examine all available literature and data for the determination of the proper prototype model scale ratio.

This task should be made as soon as possible. In the meantime, a rough estimate for a rule of thumb must be determined now. The following unproven procedure might be adopted. The basic principle is to use the thickness of the moving sand layer above the bed as a scale factor; the reasoning behind this is that the moving sand layer results from a combination of the flow, sand characteristics, and ripple forms. The ratio of the thickness of the moving sand layer to the height of the roadway should be a useful governing factor to study the migration of sand particles over the roadway. Preliminary measurements of the vertical sand distribution in our wind tunnel have indicated that most of the sand particles were moving within a layer of approximately 20 millimeters from the bed surface for a wind speed of 12 meters per second. (Most of the model tests were conducted at this speed.) If this thickness of sand layer is used, the ratio between the model roadway heights and the sand layer varies between 10 and 1. Dr. D. Anton once informed us that during extremely high winds, sand drifts can reach a height of 2 meters above the ground. If this is the case, our model results should be applicable to field conditions. At the earliest possible date, one should develop a reliable field sampler to measure the vertical distribution of sand in the field.

If a great deal of roadway construction is anticipated and if the construction cost is high, a much more comprehensive series of laboratory tests should be conducted to provide proper design criteria. For instance, one should measure i) the wind velocity distribution over the roadway, ii) the vertical sand distribution over the roadway, and iii) the migration of sand particles over the roadway for unsteady flow conditions. There may be an optimal shape of a roadway for a given range of wind speeds so that extremely high wind and sand drifts would not occur near or up to the level of traffic.

## B. Fences

Single fences constructed of vertical slats to give a porosity of about 60 percent have been established through this research to be efficient sand control devices that are relatively economical and easy to install compared to other fence types. Multi-row fence systems are required in practice to improve deposition efficiency, increase system life and to provide control over large areas. Design of such systems is hampered by lack of information on optimum (for efficiency and economy) fence spacings and number of fences for a parallel-row fence grouping and the spacing in arrays of fence groups. Exploratory investigations reported herein indicate that spacing of parallel straight fences should be about 40 fence heights; however, the optimum number of fences in a group and the optimum spacing of groups in an extensive array must be determined by future research. Wind-tunnel studies in which the spacing variables are varied systematically are needed. These studies, in order to minimize tunnel wall interference, must be made in a wide (5-10 m) boundary-layer wind tunnel.

Group and group arrays of fences aligned perpendicular to the predominant strong-wind direction are installed to deposit wind transported sand upon areas covered by the fences. Another sand control strategy is to divert airborne sand transverse to the prevailing wind direction into a region that will permit bypass of the area targeted for protection. Optimum angle of fences with respect to wind direction and alignment of fences to form a long line of fences has not been established. Again systematic research in a "wide" boundary-layer wind tunnel is essential in order to obtain adequate information for design.

Deflation of sand under a fence is a common cause of fence blow-down. Application of stabilizers to a strip along the fence base has been found to reduce the risk of this type of failure. Research is needed to determine the pattern of stabilization surrounding fence supports that will provide adequate protection at minimum cost.

#### C. Vegetated Strips

Vegetation, such as the tamarisk, can provide effective sand control by inducing deposition. More information is needed to determine planting patterns and spacings for the most efficient and economical barriers. Valuable data can be obtained by laboratory studies of models in a boundary-layer wind tunnel.

#### D. Aeolian Sand Deposition and Deflation near Building Groups

Definition and control of aeolian sand through a building complex or around industrial sites has been studied only for local site specific problems. Planning and development of new cities and industrial sites should include consideration of building patterns and spacing that will result in minimization of sand drifting and deflation problems. Much useful information can be obtained by wind-tunnel studies in which systematic variation of spacings and arrangements of idealized building shapes are subjected to aeolian sand.

## REFERENCES

1. "Stabilization of Sand," Report to Abu Dhabi Emirate, Al Ain International Airport-Preliminary Design Report, September 1980.
2. Bagnold, R. A., "The Physics of Blown Sand and Desert Dunes," Methuen Co. Ltd., London, 1954.
3. Castro, I. P., "Wake Characteristics of Two-Dimensional Perforated Plates Normal to an Air-Stream," Journal of Fluid Mechanics, Volume 46, Part 3, 1971, pp. 599-609.
4. Cermak, J. E., "Laboratory Simulation of Atmospheric Boundary Layer," AIAA Journal, Vol. 9, No. 9, September 1971, pp. 1746-1754.
5. Cermak, J. E., "Simulation of the Natural Wind," Preprint 82-518, ASCE Convention and Exhibit, New Orleans, Louisiana, 25-29 October 1982.
6. Cermak, Jack E., "Wind Tunnel Design for Physical Modeling of Atmospheric Boundary Layer," Journal of the Engineering Mechanics Division, ASCE, Vol. 107, No. EM3, Proc. Paper 16340, June 1981, pp. 623-642.
7. Chang, "Flow Around a Solid Fence," Thesis, Colorado State University, 1966, unpublished.
8. Gandemer, J., "The Aerodynamic Characteristics of Windbreaks, Resulting in Empirical Design Rules," Journal of Wind Engineering and Industrial Aerodynamics, 7, 1981, pp. 15-36.
9. Horikawa, K. and Shen, H. W., "Sand Movement by Wind Action," Technical Memorandum No. 119, Beach Erosion Board-Corps of Eng., 1961.
10. Ishihara, T. and Iwagaki, Y., "On the Effects of Sand Storm in Controlling the Mouth of the Kiku River," Bulletin of the Disaster Prevention Research Inst., Kyoto University, No. 2, 1952.
11. Iversen, J. E., "Comparison of Wind Tunnel Model and Full Scale Snow Fence Drifts," Journal of Wind Engineering and Industrial Aerodynamics, No. 8, 1981, pp. 231-249.
12. Iversen, J. D., "Drifting Snow Similitude-Transport Rate and Roughness Modeling," Journal of Glaciology, Vol. 26, No. 94, 1980, pp. 393-403.
13. Kawamura, R., "Study on Sand Movement by Wind," Report of the 1st of Science and Technology, University of Tokyo, Vol. 5, No. 3/4, October 1951 (in Japanese).
14. Kawata, S., "On the Break-Wind," Journal of the Japan Society of Civil Engineering, Vol. 33, No. 3, 1948 (in Japanese).

15. Kind, R. J., "A Critical Examination of the Requirements for Model Simulation of Wind Induced Erosion/Deposition Phenomena such as Snow Drifting," *Atm. Environ.*, No. 10, pp. 219-227.
16. Manohar, M. and Brunn, P., "Mechanics of Dune Growth by Sand Fences," *Dock and Harbour Authority*, Vol. 51, October 1970.
17. O'Brien, M. P. and Rindlaub, B. D., "The Transportation of Sand by Wind," *Civil Engineering*, May 1936.
18. Plate, J., "The Aerodynamics of Shelter Belts," *Agr. Meteorology*, No. 8, 1971, pp. 203-222.
19. Raine, J. K. and Stevenson, D. C., "Wind Protection by Model Fences in a Simulated Atmospheric Boundary Layer," *Journal of Industrial Aerodynamics*, No. 2, 1977, pp. 159-180.
20. Savage, R. P., "Experimental Study of Dune Building with Sand Fences," *Coastal Engineering*, 1963, pp. 380-396.
21. Schlichting, H., "Boundary Layer Theory," McGraw-Hill, 1968.
22. Tabler, R. D., "New Engineering Criteria for Snow Fence Systems," *Transp. Res. Rec. 506*, NAS-NRC, Washington, D.C., pp. 65-78.
23. Tabler, R. D., "Geometry and Density of Drifts Formed by Snow Fences," *Journal of Glaciology*, Vol. 26, No. 94, 1980, pp. 405-419.
24. Tabler, R. D., "Predicting Profiles of Snowdrifts in Topographic Catchments," *West. Snow Conf., Proc. 43*, 1975, pp. 87-97.
25. Tabler, R. D., "New Snow Fence Design," *Amer. Transp. Eng. Conf., Proc. 46*, 1973, pp. 16-27.
26. Trossel, C. J., "Eolian Sand Control in Saudi Arabia as Experienced by Aromoco," *Dhahran*, April 1981.

## APPENDIX A

## WIND-TUNNEL FACILITY AND TEST CONFIGURATIONS

The FDDL Meteorological Wind Tunnel (see Figure A-1) was utilized for all phases of the sand study project. The wind tunnel was operated in the auxiliary mode during all tests. Outside air was drawn through an auxiliary intake and returned to the outside through an auxiliary exhaust after passing through the tunnel test section. The MWT operation is described in detail by Cermak (1981).

An atmospheric surface layer was simulated by positioning wooden spires 1.83 m tall and a brick trip 0.18 m in height across the MWT at the test-section entrance (see Figure A-2). The four spires were spaced at 43 cm intervals, while the trip was continuous. Simulation of atmospheric boundary layers in wind-tunnel flows is discussed in papers by Cermak (1971,1982).

The test-section floor was covered with a 7 cm layer of sand from a point 3.3 m downwind from the spires to a trap and barrier arrangement. The sand collection trap was installed in combination with a louvered barrier at the extreme downwind end of the test section (see Figure A-3).

Location of the pitot tube used to monitor the reference velocity is also shown in Figure A-3. Measurements for velocity and turbulence profiles were obtained at four positions downwind from selected fences. The measurement locations, representing multiples of the model fence height,  $H$ , are indicated on Figure A-4.

The position 6.34 m upwind from the sand collection trap, indicated on Figure A-4, was the approximate location for all single fences tested. Multiple/special fences were positioned in the tunnel, as indicated in

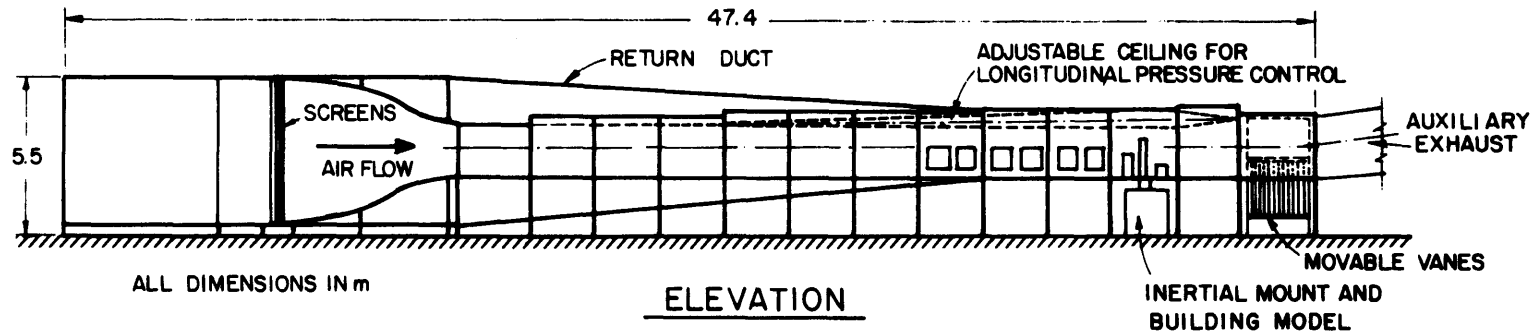
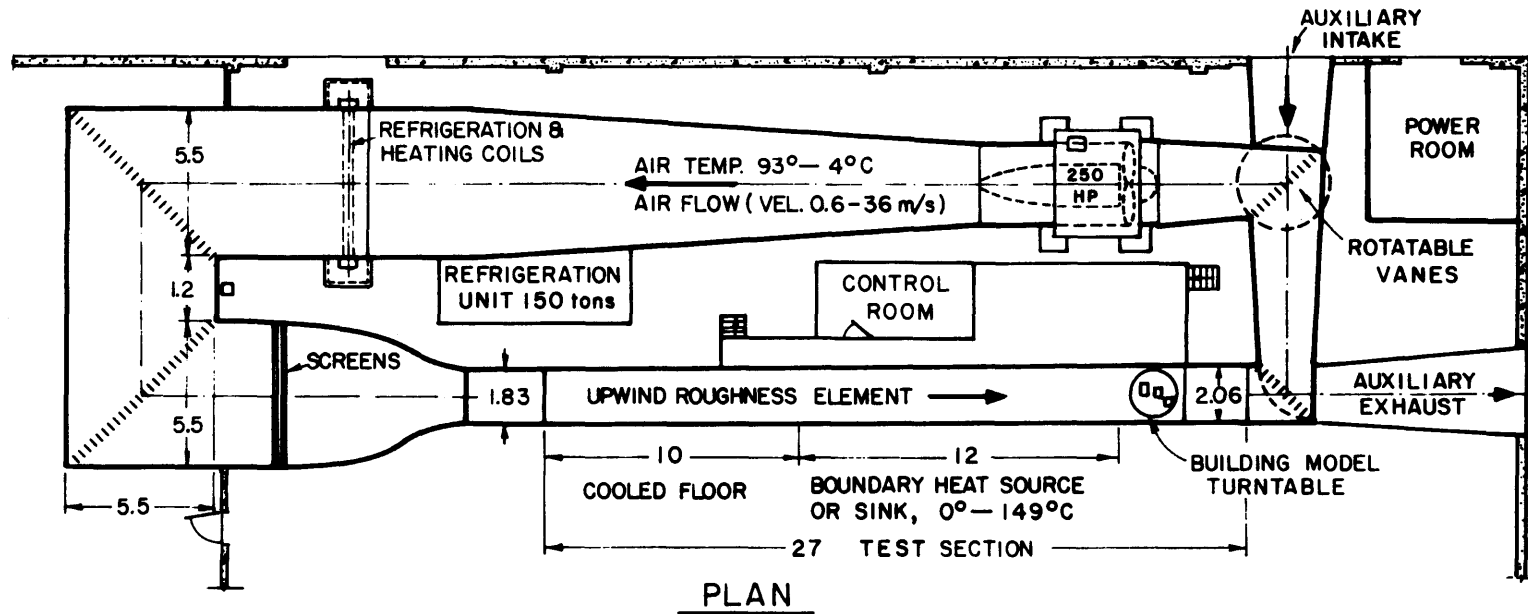


Figure A-1. Meteorological Wind Tunnel  
 Fluid Dynamics and Diffusion Laboratory  
 Colorado State University

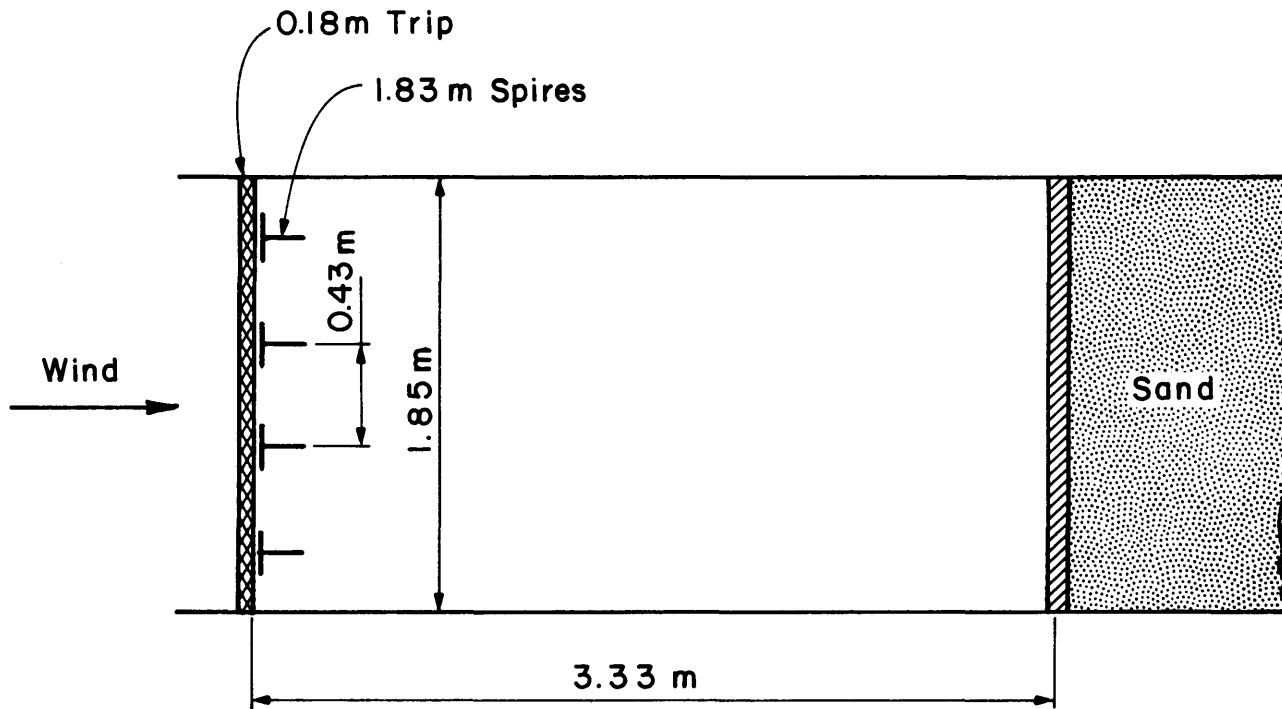


Figure A-2. Plan View of Entrance to MWT Test Section

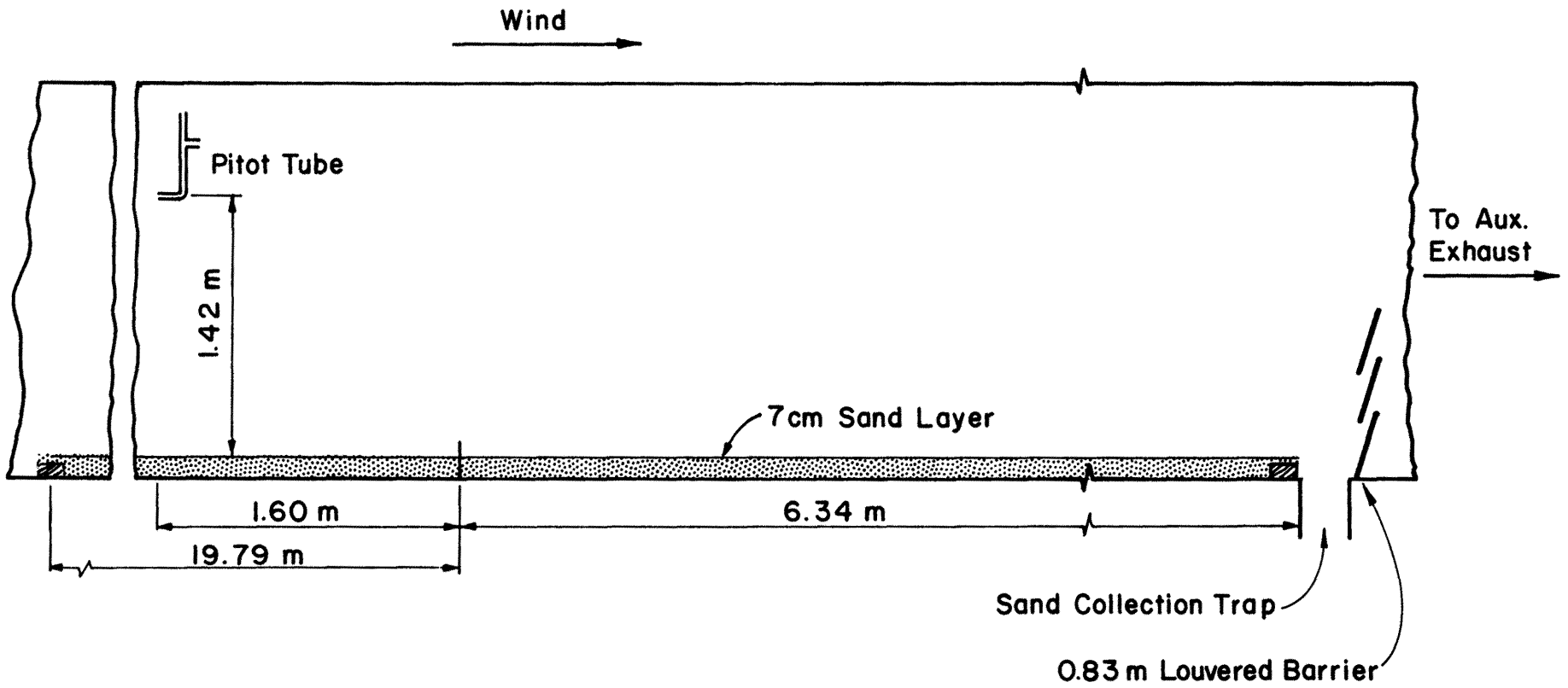


Figure A-3. Elevation View of Downwind Portion of MWT Test Section

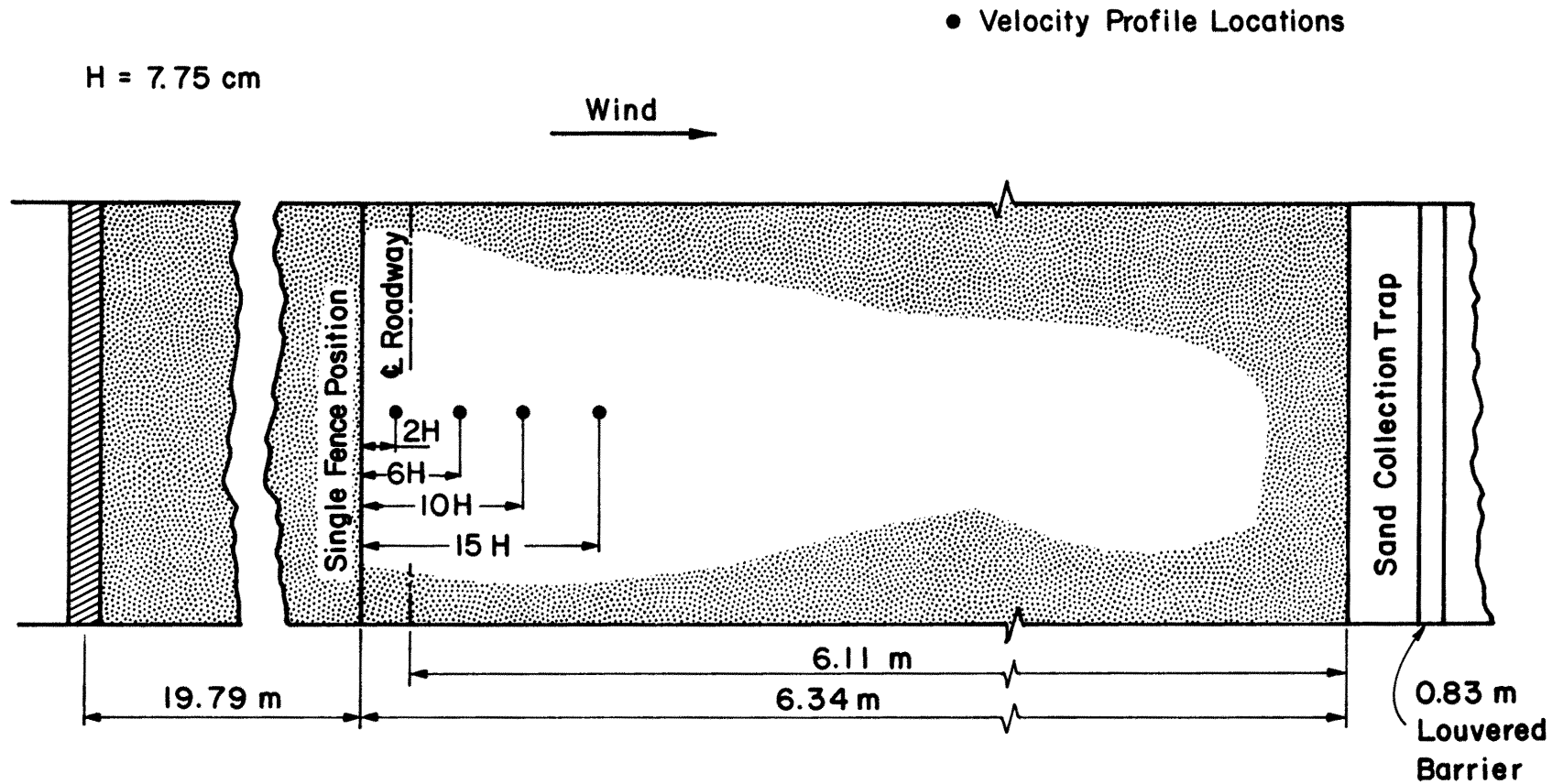


Figure A-4. Plan View of Downwind Portion of MWT Test Section

Table A-1, using the single fence position as a reference. All roadway tests were performed with the median centerline 6.11 m upwind from the referenced trap.

Table A-1. Location of Multiple/Special Fences in MWT

| Fence Description    | D/H | Fence 3 (cm) | Fence 2 (cm) | Fence 1 (cm) |
|----------------------|-----|--------------|--------------|--------------|
| Double               | 4   | -            | + 0.6        | - 31.1       |
| Double               | 8   | -            | - 0.6        | - 62.2       |
| Double               | 12  | -            | 0.0          | - 93.3       |
| Double               | 20  | -            | 0.0          | -154.9       |
| Double               | 40  | -            | - 0.6        | -310.5       |
| Double               | 80  | -            | +236.9       | -395.6       |
| Stacked Fences       | -   | -            | + 16.5       | 0            |
| Special Spire        | -   | -            | -            | -276.9       |
| Triple               | 20  | - 1.2        | -163.8       | -317.5       |
| Triple               | 40  | +67.3        | -242.6       | -552.5       |
| --                   | 20  | -            | 0            | -154.9       |
| Single (30% to Wind) | -   | -            | - 11.4       | to -448.3    |
| Single (60% to Wind) | -   | -            | - 57.2       | to -158.8    |

- Upstream from reference (single-fence location)

+ Downstream from reference (single-fence location)

Appendix B  
INSTRUMENTATION

A. VELOCITY MEASUREMENTS

In making velocity measurements in the sand cloud, a compromise was necessary in selecting a sensor rugged enough to withstand the particle impacts and dust adhesion without significant change in its response characteristics, but still have a small enough thermal mass to provide good frequency response for making turbulence measurements.

In preliminary trials, an ordinary unprotected hot-film sensor of 20 microns diameter was tried. After exposure to the sand cloud, the voltage versus velocity response characteristic of this film had changed significantly, yielding velocity errors greater than 10 percent.

Two shielded sensors were obtained for the series of tests reported herein. One of these was a hot-film sensor of the ordinary type, but of a larger than usual diameter (60 microns) and with a thin protective inert film deposited over the metallic sensor film. This could be expected to have a good frequency response up to at least a few hundred Hertz.

The other sensor was very rugged, the sensing element completely embedded in a protective metal sheath and consequently, had a large thermal time constant and relatively low frequency response.

The 60 micron sensor was the best suited to the conditions of this series of tests, even though it exhibited some change of characteristics (a few percent) after exposure to the sand cloud, but it was not used because problems of instability and electrical interference were not overcome before the completion of the tests. This sensor, Model 1240AK-60W, made by TSI Incorporated, will probably be used in future tests.

Nearly all velocity measurements were made with a Model 1610 Velocity Transducer, manufactured by TSI Incorporated. This is a rugged sensor in which a heated platinum sensor wire is encapsulated inside a nickel tube.

The time constant of this sensor was approximately 0.1 second, so that all turbulence frequency components above 10 Hertz were not sensed. Therefore, the accuracy of turbulence measurements is questionable in the areas where higher frequency components are expected to account for a fraction of the turbulent energy, such as very near the surface or immediately behind a fence.

The wind-tunnel reference velocity was set according to a pitot/static tube located 142 cm above the sand bed, 100 cm upstream of the fence position. The pressure differential was measured by an "Equibar Pressure Meter, Model 120, made by Trans-Sonics, Inc.

Velocities obtained from the pitot tube were checked periodically against a calibrated hot-film sensor at the same location.

#### B. SAND ACCUMULATION MEASUREMENTS

Sand heights were measured with a depth "point gauge" mounted on a movable platform which rolled on rails above the sand bed. The gauge vernier could be read to a resolution of 0.03 cm. The best repeatability of measurements was within about 0.06 or 0.09 cm. The greatest errors in sand heights measurements arose from selecting a point, on a rippled surface, which would represent the mean height of the surface in that vicinity. Errors from this source are estimated to be within  $\pm 0.2$  cm.

### C. SAND CONCENTRATION MEASUREMENTS

The concentrations of airborne sand were sampled with an aspirating probe set at variable heights above the sand bed. The mouth of the probe was a brass tube with an inside diameter of 6.35 millimeters and a wall thickness of 0.19 millimeters. Air was drawn into the probe at a rate which was adjusted to provide an entry velocity equal to the velocity of the surrounding air. This isokinetic sampling rate is necessary to avoid selective separation of lighter and heavier particles in the sampling process. The open port of the aspirator faced directly into the wind, the circular opening being in a plane normal to the air flow.

As shown in Figure B-1, the aspirated sample was drawn downward through a metal tube projecting through the sand bed and the floor of the wind tunnel, then through flexible plastic tubing which allowed for vertical movement of the probe and then into a sand trap. The sand trap consisted of a glass flask with a free entry for the sample through the stoppered neck and a screened exit for the now sand-free air. This separation technique proved to be quite effective, with even the finest particles rising only a few centimeters into the neck of the flask. The exit screen and filter were actually unnecessary at the drawing rates employed.

The drawing rates were adjusted by means of a needle valve and instrumented with a float-type flowmeter, which was calibrated in-line under operating condition, but with sand-free air.

An air pump, surge tank and vacuum regulator provided a constant underpressure for operation of the system.

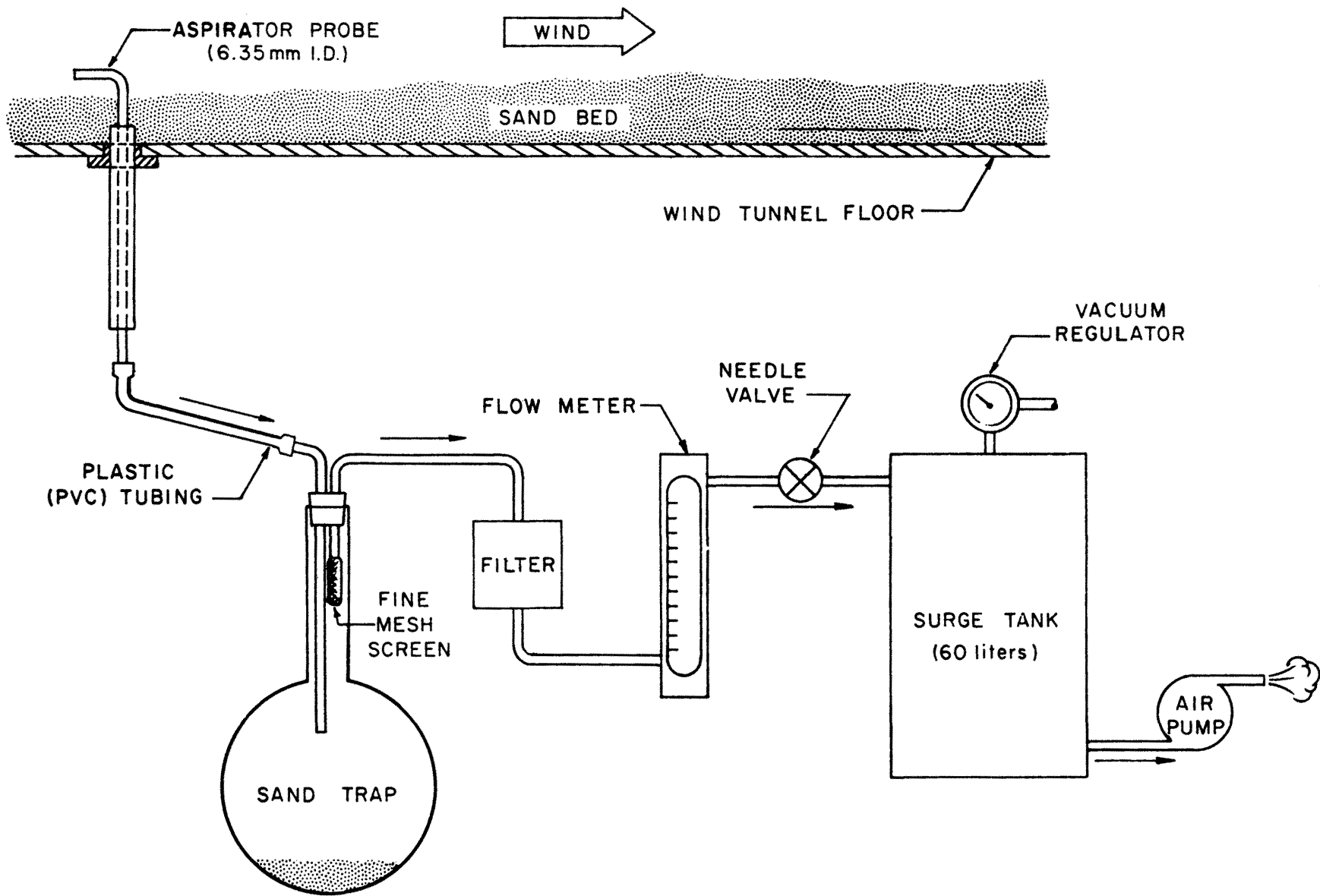


Figure B-1. Isokinetic Sand-Sampling Aspirator